`dmscatter` User Manual

Oliver Gorton

September 18, 2022

Abstract

Recent work [FHK$^+$13, AFH14], using an effective field theory framework, have shown the number of possible couplings between nucleons and the dark-matter-candidate Weakly Interacting Massive Particles (WIMPs) is larger than previously thought. Inspired by an existing Mathematica script that computes the target response [AFH14], we have developed a fast modern Fortran code, including optional OpenMP parallelization, along with a user-friendly Python wrapper, to swiftly and efficiently explore many scenarios, with output aligned with practices of current dark matter searches. A library of most of the important target nuclides is included; users may also import their own nuclear structure data, in the form of reduced one-body density matrices. This framework is designed to produce the differential event rate needed to model detector responses, although intermediate results such as nuclear form factors can also be easily accessed.

Contents

1 Introduction

Substantial experimental effort has been and continues to be expended to directly detect 'dark matter,' some as-yet unidentified nonbaryonic particles which astrophysical and cosmological evidence suggests may make up a substantial fraction (roughly a quarter) of the universe's mass-energy [BFPR84, BH18]. Because dark matter interacts with baryonic matter weakly and may be very massive compared to baryonic particles– WIMPs or *weakly interacting massive particles*–these experiments attempt to measure the recoil of nuclei from unseen and (mostly) elastic collisions [PSS88, Fen10].

Originally it was assumed that dark matter particles would simply couple either to the scalar or spin densities of nucleons [GW85, Sad99]. But a few years ago Fitzpatrick *et al.* used effective field theory (EFT) calculations assuming Galilean invariance to identify upwards of 15 possible independent couplings between nonrelativistic dark matter and nucleons [FHK$^+$13, AFH14, VKM$^+$15, HMS20].

The enlargement of the possible couplings motivates a variety of nuclear targets. More targets better constrain the actual coupling, but also complicate simulations of detector responses. To aid such simulations, Anand, Fitzpatrick, and Haxton made available a script written in Mathematica computing the dark matter event rate spectra [AFH14]; this script, `dmformfactor`, embodied the nuclear structure in a shell model framework and the user could choose the coupling to the EFT-derived operators. An updated Mathematica script has been developed and applied [Hax, XAC$^+$19, HJM22].

Not only did the EFT framework break new ground in the planning and analysis of dark matter direct detection experiments, the Mathematica script made the new framework widely accessible. Like many scripts in interpreted languages, however, `dmformfactor` is not fast, and scanning through a large set of parameters, such as exploring the effects of mixing two or more couplings or carrying out uncertainty quantification [FJP20], ends up being time-consuming.

Inspired by the Mathematica script `dmformfactor`, we present here a fast modern Fortran code, `dmscatter`, for computing WIMP-nucleus scattering event rates using the previously proposed theoretical framework. The output is designed to align with practices of current dark matter searches. Intermediate results such as nuclear form factors can be easily accessed. With advanced algorithmic and numerical implementation, including the ability to take advantage of multi-core CPUs, our code opens up new areas of research: to rapidly explore the EFT parameter space including interference terms, and to conduct sensitivity studies to address the uncertainty introduced by the underlying nuclear physics models. Furthermore, we enhance the accessibility by including Python wrapper and example scripts and which can be used to call the Fortran code from within a Python environment.

2 Theoretical Background

Although the formalism is fully developed and presented in the original papers [FHK$^+$13, AFH14, VKM$^+$15, HMS20], for completeness and convenience we summarize the main ideas here.

2.1 Differential event rate

The key product of the code is the differential event rate for WIMP-nucleus scattering events in number of events per MeV. This is obtained by integrating the differential WIMP-nucleus cross section over the velocity distribution of the WIMP-halo in the galactic frame:

$$\frac{dR}{dE_r}(E_r) = N_T n_\chi \int \frac{d\sigma}{dE_r}(v, E_r)\ \tilde{f}(\vec{v})\ v\ d^3v, \tag{1}$$

where E_r is the recoil energy of the WIMP-nucleus scattering event, N_T is the number of target nuclei, $n_\chi = \rho_\chi / m_\chi$ is the local dark matter number density, σ is the WIMP-nucleus cross section. The dark matter velocity distribution in the lab frame, $\tilde{f}(\vec{v})$, is obtained by boosting the Galactic-frame distribution $f(\vec{v})$: $\tilde{f}(\vec{v}) = f(\vec{v} + \vec{v}_{earth})$, where $\vec{v}_{earth}$ is the velocity of the earth in the galactic rest frame.

2.2 Halo model

There are many models for the dark matter distributions of galaxies. We provide the Simple Halo Model (SHM) with smoothing, a truncated three-dimensional Maxwell-Boltzmann distribution:

$$f(\vec{v}) = \frac{\Theta(v_{esc} - |\vec{v}|)}{N_{esc}\pi^{3/2}v_0^3} \left\{ \exp\left[-(\vec{v}/v_0)^2\right] - \exp\left[-(v_{esc}/v_0)^2\right] \right\}, \tag{2}$$

where v_0 is some scaling factor (typically taken to be around 220 km/s), and N_{esc} re-normalizes due to the cutoff [DFS86, FFG88]. Halo distributions are not the focus of this paper, and we leave the implementation of more sophisticated halo models, such as SMH++ [EOM18], to future work. The integral in equation (1) is evaluated numerically. Details can be found in 2.12.

2.3 Differential cross section

The differential scattering cross section is directly related to the scattering transition probabilities $T(v, q(E_r))$:

$$\frac{d\sigma}{dE_r}(v, E_r) = 2m_t \frac{d\sigma}{dq^2}(v, q) = \frac{2m_T}{4\pi v^2} T(v, q). \tag{3}$$

The momentum transfer q is directly related to the recoil energy by $q^2 = 2m_t E_r$, where m_t is the mass of the target nucleus in GeV/c^2.

2.4 Transition probability

The WIMP-nucleus scattering event probabilities are computed as a sum of squared nuclear-matrix-elements:

$$T(v, q) = \frac{1}{2j_\chi + 1} \frac{1}{2j_T + 1} \sum_{M_i M_f} \left| \langle j_T M_f \,|\, \mathcal{H} \,|\, j_T M_i \rangle \right|^2 \tag{4}$$

$$= \frac{1}{2j_\chi + 1} \frac{1}{2j_T + 1} \left| \langle j_T \,\|\, \mathcal{H} \,\|\, j_T \rangle \right|^2 \tag{5}$$

which we have rewritten in terms of reduced (via the Wigner-Eckart theorem) matrix elements [Edm96], as denoted by the double bars $||$. Here v is the speed of the WIMP in the lab frame, q is the momentum transferred in the collision, and j_χ and j_T are the intrinsic spins of the WIMP and target nucleus, respectively. $\mathcal{H}$ is the WIMP-nucleus interaction.

2.5 WIMP-nucleus interaction

The WIMP-nucleus interaction $\mathcal{H}$ is defined in terms of the effective field theory Lagrangian constructed from all leading order combinations of the following operators:

$$i\frac{\vec{q}}{m_N},\ \vec{v}^{\perp},\ \vec{S}_\chi,\ \vec{S}_N. \tag{6}$$

$\vec{v}^{\perp}$ is the relative WIMP-target velocity and $\vec{S}_\chi, \vec{S}_N$ are the WIMP and nucleon spins, respectively. There are fifteen such combinations, listed in 2.10, and $\mathcal{H}$ is specified implicitly by corresponding coupling constants c_i^x, (for $i = 1, ..., 15$), where $x = p, n$ for coupling to protons or neutrons individually:

$$\mathcal{H} = \sum_{x=p,n} \sum_{i=1,15} c_i^x \mathcal{O}_i^x \tag{7}$$

2.6 Coupling coefficients

The EFT coefficients c_i^x can be expressed in terms of proton and neutron couplings $x = p, n$, or, equivalently, isospin and isovector couplings $\tau = 0, 1$. The relationship between the two is:

$$c_i^{\tau=0} = \frac{1}{2}(c^{x=p} + c_i^{x=n}) \tag{8}$$

$$c_i^{\tau=1} = \frac{1}{2}(c^{x=p} - c_i^{x=n}). \tag{9}$$

Our code accepts either specification and automatically converts between the two. (Note: while [AFH14] specifies this same relationship, the Mathematica script distributed in Supplementary Material, `dmformfactor-prc.m`, also `dmformfactor-V6.m`, actually uses a different transformation, namely that $c_i^{\tau=0,1} = c_i^{x=p} \pm c_i^{x=n}$. Later versions [Hax, XAC+19, HJM22] however, are consistent with the above relationship.)

2.7 Response functions

The summand of equation (4) is ultimately factorized into two factors: one containing the EFT content, labeled $R_i^{x,x'}$, and another containing the nuclear response functions, labeled $W_i^{x,x'}$ for each of the $i = 1, ..., 8$ allowed combinations of electro-weak-theory, discussed in the next section. The former are listed in 2.11.

There are eight nuclear response functions $W_i^{x,x'}$ considered here. The first six nuclear response functions have the following form:

$$W_X^{x,x'} = \sum_J \langle\Psi|\,|X_J^x|\,|\Psi\rangle \langle\Psi|\,|X_J^{x'}|\,|\Psi\rangle\,, \tag{10}$$

with X selecting one of the six electroweak operators:

$$X_J = M_J, \Delta_J, \Sigma'_J, \Sigma''_J, \tilde{\Phi}'_J, \Phi''_J. \tag{11}$$

(further described in section 2.8) and Ψ being the nuclear wave function for the ground state of the target nucleus. The sum over operators spins J is restricted to even or odd values of J, depending on restrictions from conservation of parity and charge conjugation parity (CP) symmetry.

As a check of normalization, the $J = 0$ contribution to $W_M^{xx'}$ is just the square of the Fourier transform of the rotationally invariant density. (For even-even targets, this is the only contribution to ground state densities.) This means, at momentum transfer $q = 0$, the $J = 0$ contribution to $W_M^{pp} = Z^2/4\pi$, $W_M^{nn} = N^2/4\pi$, and for isospin-format form factors, the $J = 0$ contribution to $W_M^{00} = \frac{1}{4\pi}\left(\frac{A}{2}\right)^2$. Such limits are useful when comparing to other calculations, to ensure agreement in normalizations.

Two additional response functions add interference-terms:

$$W_{M\Phi''}^{x,x'} = \sum_J \langle\Psi|\,|M_J^x|\,|\Psi\rangle \langle\Psi|\,|\Phi''^{x'}_J|\,|\Psi\rangle\,, \tag{12}$$

$$W_{\Delta\Sigma'}^{x,x'} = \sum_J \langle\Psi|\,|\Sigma'^x_J|\,|\Psi\rangle\,\langle\Psi|\,|\Delta^{x'}_J|\,|\Psi\rangle\,. \tag{13}$$

The transition probability is thus [FHK+13, AFH14]:

$$T(v,q) = \frac{4\pi}{2j_T+1}\sum_{x=p,n}\sum_{x'=p,n}\sum_{i=1}^{8} R_i^{x,x'}(v^2,q^2)W_i^{x,x'}(q), \tag{14}$$

where $i \to X$ for $i = 1,..,6$, and $i = 7 \to M\Phi''$, $i = 8 \to \Delta\Sigma'$.

2.8 Nuclear operators

There are six basic operators, $M_J, \Delta_J, \Sigma'_J, \Sigma''_J, \tilde{\Phi}'_J, \Phi''_J$, describing the electro-weak coupling of the WIMPs to the nucleon degrees of freedom. These are constructed from Bessel spherical and vector harmonics [DH79]:

$$M_{JM}(q\vec{x}) \equiv j_J(qx)Y_{JM}(\Omega_x) \tag{15}$$

$$\vec{M}_{JML}(q\vec{x}) \equiv j_L(qx)\vec{Y}_{JLM}(\Omega_x), \tag{16}$$

where, using unit vectors $\vec{e}_{\lambda=-1,0,+1}$,

$$Y_{JLM}(\Omega_x) = \sum_{m\lambda}\langle Lm1\lambda|\,|(L1)JM_J\rangle\, Y_{Lm}(\Omega_x)\vec{e}_\lambda. \tag{17}$$

The six multipole operators are defined as:

$$M_{JM} \tag{18}$$

$$\Delta_{JM} \equiv \vec{M}_{JJM}\cdot\frac{1}{q}\vec{\nabla} \tag{19}$$

$$\Sigma'_{JM} \equiv -\,i\left\{\frac{1}{q}\vec{\nabla}\times\vec{M}_{JJM}\right\}\cdot\vec{\sigma} \tag{20}$$

$$\Sigma''_{JM} \equiv \left\{\frac{1}{q}\vec{\nabla}M_{JM}\right\}\cdot\vec{\sigma} \tag{21}$$

$$\tilde{\Phi}'_{JM} \equiv \left(\frac{1}{q}\vec{\nabla}\times\vec{M}_{JJM}\right)\cdot\left(\vec{\sigma}\times\frac{1}{q}\vec{\nabla}\right) + \frac{1}{2}\vec{M}_{JJM}\cdot\vec{\sigma} \tag{22}$$

$$\Phi''_{JM} \equiv i\left(\frac{1}{q}\vec{\nabla}M_{JM}\right)\cdot\left(\vec{\sigma}\times\frac{1}{q}\vec{\nabla}\right) \tag{23}$$

The matrix elements of these operators can be calculated for standard wave functions from second-quantized shell model calculations:

$$\langle\Psi_f|\,|X_J|\,|\Psi_i\rangle = \sum_{a,b}\langle a|\,|X_J|\,|b\rangle\,\rho_J^{fi}(ab), \tag{24}$$

where single-particle orbital labels a imply shell model quantum number n_a, l_a, j_a, and the double-bar $||$ indicates reduced matrix elements [Edm96]. For elastic collisions, only the ground state is involved, i.e. $\Psi_f = \Psi_i = \Psi_{g.s.}$.

2.9 Nuclear structure

We assume a harmonic oscillator single-particle basis, with the important convention that the radial nodal quantum number n_a starts at 0, that is, we label the orbitals as $0s, 0p, 1s0d$, etc.., and *not* starting with $1s, 1p$, etc. By default, the harmonic oscillator basis length $b = \sqrt{\hbar/(m\omega)}$ is set to the Blomqvist and Molinari prescription [BM68]:

$$b^2 = 41.467/(45A^{-1/3} - 25A^{-2/3})\ \text{fm}^2. \tag{25}$$

Other values can be set using the control words `hofrequency` or `hoparameter` (see 7). Then, the one-body matrix elements for operators $\langle a|\,|X_J^{(f)}|\,|b\rangle$, built from spherical Bessel functions and vector spherical harmonics, have closed-form expressions in terms of confluent hypergeometric functions [DH79].

The nuclear structure input is in the form of one-body density matrices between many-body eigenstates,

$$\rho_J^{fi}(ab) = \frac{1}{\sqrt{2J+1}}\langle\Psi_f||[\hat{c}_a^\dagger \otimes \tilde{c}_b]_J||\Psi_i\rangle, \tag{26}$$

where $\hat{c}_a^\dagger$ is the fermion creation operator (with good angular momentum quantum numbers), $\tilde{c}_b$ is the time-reversed [Edm96] fermion destruction operator. Here the matrix element is reduced in angular momentum but not isospin, and so are in proton-neutron format. These density matrices are the product of a many-body code, in our case BIGSTICK [JOK13, JOMS18], although one could use one-body density matrices, appropriately formatted (see 6), from any many-body code.

The theoretical formalism for computing the WIMP-nucleus form factors is largely the same as in [FHK$^+$13, AFH14]. In this paper we will therefore only provide the basic formalism which is necessary to understand the differences in our numerical and algorithmic approaches to the implementation.

2.10 Effective field theory

The WIMP-nucleus interaction is defined by the user in terms of an effective field theory Lagrangian, specified implicitly by fifteen operator coupling constants c_i^x, (for $i = 1, ..., 15$), where $x = p, n$ for coupling to protons or neutrons individually. The code uses the EFT coefficients in explicit proton-neutron couplings, i.e. the interaction is defined by:

$$\mathcal{H} = \sum_{x=p,n}\sum_{i=1,15} c_i^x \mathcal{O}_i \tag{27}$$

and the 15 momentum-dependent operators are:

$$\mathcal{O}_1 = 1_\chi 1_N \tag{28}$$
$$\mathcal{O}_2 = (v^\perp)^2 \tag{29}$$
$$\mathcal{O}_3 = i\vec{S}_N \cdot \left(\frac{\vec{q}}{m_N} \times \vec{v}^\perp\right) \tag{30}$$
$$\mathcal{O}_4 = \vec{S}_\chi \cdot \vec{S}_N \tag{31}$$
$$\mathcal{O}_5 = i\vec{S}_\chi \cdot \left(\frac{\vec{q}}{m_N} \times \vec{v}^\perp\right) \tag{32}$$
$$\mathcal{O}_6 = \left(\vec{S}_\chi \cdot \frac{\vec{q}}{m_N}\right)\left(\vec{S}_N \cdot \frac{\vec{q}}{m_N}\right) \tag{33}$$
$$\mathcal{O}_7 = \vec{S}_N \cdot \vec{v}^\perp \tag{34}$$
$$\mathcal{O}_8 = \vec{S}_\chi \cdot \vec{v}^\perp \tag{35}$$
$$\mathcal{O}_9 = i\vec{S}_\chi \cdot \left(\vec{S}_N \times \frac{\vec{q}}{m_N}\right) \tag{36}$$
$$\mathcal{O}_{10} = i\vec{S}_N \cdot \frac{\vec{q}}{m_N} \tag{37}$$
$$\mathcal{O}_{11} = i\vec{S}_\chi \cdot \frac{\vec{q}}{m_N} \tag{38}$$
$$\mathcal{O}_{12} = \vec{S}_\chi \cdot \left(\vec{S}_N \times \vec{v}^\perp\right) \tag{39}$$
$$\mathcal{O}_{13} = i\left(\vec{S}_\chi \cdot \vec{v}^\perp\right)\left(\vec{S}_N \cdot \frac{\vec{q}}{m_N}\right) \tag{40}$$
$$\mathcal{O}_{14} = i\left(\vec{S}_\chi \cdot \frac{\vec{q}}{m_N}\right)\left(\vec{S}_N \cdot \vec{v}^\perp\right) \tag{41}$$

$$\mathcal{O}_{15} = -\left(\vec{S}_\chi \cdot \frac{\vec{q}}{m_N}\right)\left(\left(\vec{S}_N \times \vec{v}^{\perp}\right) \cdot \frac{\vec{q}}{m_N}\right) \tag{42}$$

Operator 2 is generally discarded because it is not a leading order non-relativistic reduction of a manifestly relativistic operator [AFH14]. Operators 1 and 4 correspond to the naive density- and spin-coupling, respectively.

2.11 WIMP response functions

In the following, the EFT coefficients c_i^x are grouped according to how they couple to each of the eight nuclear responses $W_i^{x,x'}$. As a shorthand, $cl(j) \equiv 4j(j+1)/3$, and $v^{\perp 2} \equiv v^2 - (q/2\mu_t)^2$.

$$R_M^{xx'}(v,q) = \frac{1}{4} cl(j_\chi)[v^{\perp 2}(c_5^x c_5^{x'} q^2 + c_8^x c_8^{x'}) + c_{11}^x c_{11}^{x'} q^2] \tag{43}$$

$$+(c_1^x + c_2^x v^{\perp 2})(c_1^{x'} + c_2^{x'} v^{\perp 2}) \tag{44}$$

$$R_{\Sigma''}^{xx'}(v,q) = \frac{1}{16} cl(j_\chi)[c_6^x c_6^{x'} q^4 + (c_{13}^x c_{13}^{x'} q^2 + c_{12}^x c_{12}^{x'}) v^{\perp 2} \tag{45}$$

$$+2c_4^x c_6^{x'} q^2 + c_4^x c_4^{x'}] + \frac{1}{4} c_{10}^x c_{10}^{x'} q^2 \tag{46}$$

$$R_{\Sigma'}^{xx'}(v,q) = \frac{1}{32} cl(j_\chi)[2c_9^x c_9^{x'} q^2 + (c_{15}^x c_{15}^{x'} q^4 + c_{14}^x c_{14}^{x'} q^2 \tag{47}$$

$$-2c_{12}^x c_{15}^{x'} q^2 + c_{12}^x c_{12}^{x'}) v^{\perp 2} + 2c_4^x c_4^{x'}] \tag{48}$$

$$+\frac{1}{8}(c_3^x c_3^{x'} q^2 + c_7^x c_7^{x'}) v^{\perp 2} \tag{49}$$

$$R_{\Phi''}^{xx'}(v,q) = \frac{q^2}{16 m_N^2} cl(j_\chi)(c_{12}^x - c_{15}^x q^2)(c_{12}^{x'} - c_{15}^{x'} q^2) \tag{50}$$

$$+\frac{q^4}{4m_N^2} c_3^x c_3^{x'} \tag{51}$$

$$R_{\tilde{\Phi}'}^{xx'}(v,q) = \frac{q^2}{16 m_N^2} cl(j_\chi)(c_{13}^x c_{13}^{x'} q^2 + c_{12}^x c_{12}^{x'}) \tag{52}$$

$$R_{\Delta}^{xx'}(v,q) = \frac{q^2}{4m_N^2} cl(j_\chi)(c_5^x c_5^{x'} q^2 + c_8^x c_8^{x'}) \tag{53}$$

$$+2\frac{q^2}{m_N^2} c_2^x c_2^{x'} v^{\perp 2} \tag{54}$$

$$R_{\Sigma'\Delta}^{xx'}(v,q) = \frac{q^2}{4m_N} cl(j_\chi)(c_4^x c_5^{x'} - c_8^x c_9^{x'}) - \frac{q^2}{m_N} c_2^x c_3^{x'} v^{\perp 2} \tag{55}$$

$$R_{M\Phi''}^{xx'}(v,q) = \frac{q^2}{4m_N} cl(j_\chi) c_{11}^x (c_{12}^{x'} - c_{15}^{x'} q^2) \tag{56}$$

$$+\frac{q^2}{m_N} c_3^{x'}(c_1^x + c_2^x v^{\perp 2}) \tag{57}$$

It should be noted that the last two dark matter responses are composed entirely of interference terms, which is to say, they do not come into play unless certain combinations of EFT coefficients are simultaneously active. These are the coefficient pairs listed in Section 8. For example, c_4 and c_5 together will activate $R_{\Sigma'\Delta}$, but not alone.

2.12 Integrals

We use numerical quadrature evaluate the integral in equation (1) for the velocity distribution (2). While there are analytic solutions [LS96, FZ10, McC10] for specific forms for the cross section, namely with v^0 and v^2 dependence, we derive a general equation that can be used for any isotropic dark matter halo model, which to our knowledge has not been presented in publication. The integral has the form:

$$I = \int_\Omega d^3v \frac{d\sigma(v,q)}{dq^2}\ v\ f(\vec{v}+\vec{v}_E), \tag{58}$$

where the constraint Ω is that $v_{min}^2 < (\vec{v}+\vec{v}_E)^2 < v_{esc}^2$ and $f(\vec{v})$ is equation (2). Here we present only the result; the full derivation can be found in the manual. Switching to spherical coordinates and taking special care for the constraint Ω, one obtains:

$$I = \frac{1}{N}\int_{v_{min}}^{v_{esc}+v_E} dv\ \frac{d\sigma(v,q)}{dq^2} v^2 (I_{MB} - I_S), \tag{59}$$

where,

$$I_{MB} = \frac{\pi v_0^2}{v_E}\begin{cases} g(v-v_E) - g(v+v_E), & v < v_{low} \\ g(v-v_E) - g(v_{esc}), & otherwise \end{cases}, \tag{60}$$

$$I_S = 2\pi g(v_{esc})\begin{cases} 2v, & v < v_{low} \\ [v_{esc}^2 - (v-v_E)^2]/(2v_E), & otherwise \end{cases}. \tag{61}$$

with $v_{low} = v_{esc} - v_E$. $g(x)$ is a one-dimensional Gaussian form:

$$g(v) = e^{-v^2/v_0^2}. \tag{62}$$

The normalization factor is the same as previously derived [LS96, FZ10, McC10]:

$$N_{sesc} = \pi^{3/2} v_0^3 \left[\mathrm{erf}(z) - \frac{2}{\sqrt{\pi}} z \left(1 + \frac{2}{3}z^2\right) e^{-z^2}\right], \tag{63}$$

with $z = v_{esc}/v_0$. I is a one-dimensional definite integral. We evaluate it with Gauss-Legendre quadrature.

The limits of the integral have physical constraints. The minimum speed is defined by the minimum recoil energy of a WIMP-nucleus collision at a momentum transfer q: $v_{min} = q/(2\mu_T)$, where μ_T is the reduced mass of the WIMP-nucleus system. In some approximations the upper limit is simply set to infinity. (Numerically, we approximate $\infty \approx 12 \times v_0$.) One can do slightly better by taking the maximum speed to be the galactic escape velocity: $v_{max} = v_{escape} \approx 550$ km/s.

2.13 Integrals in more detail

We provide the simplest model, a three-dimensional Maxwell-Boltzmann distribution,

$$f(\vec{v}) \propto e^{-\vec{v}^2/v_0^2}, \tag{64}$$

where v_0 is some scaling factor (typically taken to be around 220 km/s). This is called the Simple Halo Model (SHM) when a maximum value of the speed, due to the galactic escape velocity v_{escape}, is taken into account [DFS86, FFG88]:

$$f_{SHM}(\vec{v}) = \frac{\Theta(v_{esc} - |\vec{v}|)}{\pi^{3/2} v_0^3 N_{esc}} e^{-(\vec{v}/v_0)^2}, \tag{65}$$

where N_{esc} renormalizes due to the cutoff:

$$N_{esc} = erf(v_{esc}/v_0) - \frac{2v_{esc}}{\sqrt{\pi}v_0} \exp\{-(v_{esc}/v_0)^2\}. \tag{66}$$

With this distribution, the integral in the differential event-rate has the form:

$$I_{MB} = \int_{\Omega} d^3v \frac{d\sigma(v,q)}{dq^2}\ v\ e^{-(\vec{v}+\vec{v}_E)^2/v_0^2}, \tag{67}$$

where the constraint Ω is that $v_{min}^2 < (\vec{v}+\vec{v}_E)^2 < v_{esc}^2$.

To reduce to a one-dimensional integral, we make the conversion to spherical coordinates. Special care has to be taken to properly handle the truncated domain. Noting that $(\vec{v}+\vec{v}_{earth})^2 = \vec{v}^2+\vec{v}_{earth}^2+2vv_{earth}\cos(\theta)$, with θ defining the angle between the two vectors, we make the substitution $d^3v = d\phi d(\cos\theta)v^2dv$.

Now we follow the geometrical argument: Imagine constructing $\vec{v}_E+\vec{v}$. There are three cases to consider depending on the size of $\vec{v}$, and the implications for the allowed angles θ between $\vec{v}_E$ and $\vec{v}$ that satisfy the constraint $(\vec{v}_E+\vec{v})^2 < v_{esc}^2$.

Case 1: "Small v", which we define as $v < v_{esc} - v_E$. Here there are no restrictions on θ since by construction the magnitudes together cannot exceed v_{esc}, so $\cos\theta$ is limited only by -1 and $+1$.

Case 2: 11Medium v", in which now $v > v_{esc} - v_E$, so not all angles are allowed. To keep the sum from exceeding v_{esc}, the angle must be restricted such that $\cos\theta < (v_{esc}^2 - v_E^2 - v^2)/2vv_E$. Case 2 also requires that $v < v_{esc} + v_E$ because we reach...

Case 3: "Big v": It becomes impossible to satisfy the restriction once $v > v_{esc} + v_E$.

It follows that

$$\int_{(\vec{v}+\vec{v}_E)^2<v_{esc}^2} d^3v = \int_0^{2\pi} d\phi \Big[\int_0^{v_{esc}-v_E} v^2dv \int_{-1}^{+1} d\cos\theta \tag{68}$$

$$+ \int_{v_{esc}-v_E}^{v_{esc}+v_E} v^2dv \int_{-1}^{(v_{esc}^2-v_E^2-v^2)/2vv_E} d\cos\theta \Big]. \tag{69}$$

Making the physically justified assumption that $v_{esc} - v_E > v_{min}$, we can simply shift the limit on the first integral from 0 to v_{min}. Along the way we will need to work out the angular integrals:

$$\int_{-1}^{+1} d\cos\theta e^{-2vv_E\cos\theta/v_0^2} = -\frac{v_0^2}{2vv_E}\left(e^{-2vv_E/v_0^2} - e^{2vv_E/v_0^2}\right); \tag{70}$$

$$\int_{-1}^{(v_{esc}^2-v_E^2-v^2)/2vv_E} d\cos\theta e^{-2vv_E\cos\theta/v_0^2} = -\frac{v_0^2}{2vv_E}\left(e^{-(v_{esc}^2-v^2-v_E^2)/v_0^2} - e^{2vv_e/v_0^2}\right). \tag{71}$$

Combining all of this together, and simplifying, we obtain a one-dimensional integral which we can evaluate with quadrature:

$$I_{MB} = \int_{v_{min}}^{v_{esc}+v_E} dv\ \frac{d\sigma(v,q)}{dq^2} v^2 \frac{\pi v_0^2}{v_e} \tag{72}$$

$$\{\Theta_{v<v_{esc}-v_e}\left[g(v-v_E) - g(v+v_E)\right] + \Theta_{v>v_{esc}-v_E}\left[g(v-v_E) - g(v_{esc})\right]\}, \tag{73}$$

where

$$g(v) = \exp\left(-v^2/v_0^2\right). \tag{74}$$

We then use Gauss-Legendre quadrature to evaluate I[1]. While there are analytic solutions for specific velocity-dependences of the cross section [LS96, FZ10, McC10], our implementation favors a model-independent framework without the need to lock-in a particular form for the WIMP-nucleus cross section.

[1]While there are analytic solutions for this integral in the form of error functions; we use quadrature since it makes easy to later modify the velocity distribution. For example, adding a velocity cut-off is as easy as changing the limit on the quadrature, with no need to write a whole new subroutine.

The limits of the integral, v_{min} and v_{esc}, have physical constraints. The minimum speed is defined by the minimum recoil energy of a WIMP-nucleus collision at a momentum transfer q:

$$v_{min} = q/(2\mu_T), \tag{75}$$

where $\mu_T = m_T m_\chi/(m_T+m_\chi)$ is the reduced mass of the WIMP-nucleus system. To use the simple Maxwell-Bolztmann distribution approximation, the maximum speed is taken to be $\infty \approx 12 \times v_0$. Otherwise, the maximum speed is taken to be the galactic escape velocity: $v_{esc} \approx 550$ km/s.

Note that as a function of momentum q, the integral is guarenteed to go to zero above some maximum momentum q_{max}. This happens when $v_{min} = v_{max} + v_{earth}$, which corresponds to:

$$q_{max} = 2\mu_T(v_{max} + v_{earth}), \tag{76}$$

$$E_{R,max} = q_{max}^2/2m_T = 2\mu_T^2 v_{max}^2/m_T. \tag{77}$$

With 150 GeV WIMPs and ^{29}Si, for example, $\mu_T = 23.031916$ GeV, $m_T = 27.209888$ GeV, $v_{max} = 550$ km/s $= 0.001834602$ GeV/c: $E_{R,max} = 265.2987$ keV.

2.14 Electroweak matrix elements

To compute the matrix elements of the electroweak operators in a harmonic oscillator basis, we use the derivations from[DH79]. Namely, aligns (1a) - (1f) and (3a) - (3d), which express the necessary geometric matrix elements in terms of matrix elements of the spherical Bessel functions. Here, we write out the remaining explicit formulas for obtaining matrix elements of the Bessel functions $j_L(y)$ in a harmonic oscillator basis in terms of the confluent hypergeometric function:

$${}_1F_1(a,b,z) = \sum_{n=0}^{\infty} \frac{a^{(n)} z^n}{b^{(n)} n!}, \tag{78}$$

which makes use of the rising factorial function:

$$m^{(n)} = \frac{(m+n-1)!}{(m-1)!}. \tag{79}$$

The first additional relation is computed in `dmscatter` by the function 'BesselElement':

$$\langle n'l'j'|\, j_L(y)\, |nlj\rangle = \frac{2^L}{(2L+1)!!} y^{L/2} e^{-y} \sqrt{(n'-1)!(n-1)!}\sqrt{\Gamma(n'+l'+1/2)\Gamma(n+l+1/2)} \tag{80}$$

$$\times \sum_{m=0}^{n-1}\sum_{m'=0}^{n'-1} \frac{(-1)^{m+m'}}{m!m'!(n-m-1)!(n'-m'-1)!} \tag{81}$$

$$\times \frac{\Gamma[(l+l'+L+2m+2m'+3)/2]}{\Gamma(l+m+3/2)\Gamma(l'+m'+3/2)}\ {}_1F_1[(L-l'-l-2m'-2m)/2; L+3/2; y]. \tag{82}$$

The two additional relations are needed. As computed by 'BesselElementMinus':

$$\langle n'l'j'|\, j_L(y)(\frac{d}{dy} - \frac{l}{y})\, |nlj\rangle = \frac{2^(L-1)}{(2L+1)!!} y^{(L-1)/2} e^{-y} \sqrt{(n'-1)!(n-1)!}\sqrt{\Gamma(n'+l'+1/2)\Gamma(n+l+1/2)} \tag{83}$$

$$\times \sum_{m=0}^{n-1}\sum_{m'=0}^{n'-1} \frac{(-1)^{m+m'}}{m!m'!(n-m-1)!(n'-m'-1)!} \frac{\Gamma[(l+l'+L+2m+2m'+2)/2]}{\Gamma(l+m+3/2)\Gamma(l'+m'+3/2)} \tag{84}$$

$$\times \Big\{ -\frac{1}{2}(l+l'+L+2m+2m'+2)\ {}_1F_1[(L-l'-l-2m'-2m-1)/2; L+3/2; y] \tag{85}$$

$$+2m\ {}_1F_1[(L-l'-l-2m'-2m+1)/2; L+3/2; y]\Big\}. \tag{86}$$

As computed by 'BesselElementPlus':

$$\langle n'l'j'|\, j_L(y)(\frac{d}{dy}+\frac{l}{y})\,|nlj\rangle = \frac{2^(L-1)}{(2L+1)!!}y^{(L-1)/2}e^{-y}\sqrt{(n'-1)!(n-1)!}\sqrt{\Gamma(n'+l'+1/2)\Gamma(n+l+1/2)} \tag{87}$$

$$\times\sum_{m=0}^{n-1}\sum_{m'=0}^{n'-1}\frac{(-1)^{m+m'}}{m!m'!(n-m-1)!(n'-m'-1)!}\frac{\Gamma[(l+l'+L+2m+2m'+2)/2]}{\Gamma(l+m+3/2)\Gamma(l'+m'+3/2)} \tag{88}$$

$$\times\Big\{-\frac{1}{2}(l+l'+L+2m+2m'+2)\ {}_1F_1[(L-l'-l-2m'-2m-1)/2; L+3/2; y] \tag{89}$$

$$+(2l+2m+1)\ {}_1F_1[(L-l'-l-2m'-2m+1)/2; L+3/2; y]\Big\}. \tag{90}$$

All remaining electroweak matrix elements can be computed in terms of these Bessel elements, combined with vector coupling coefficients, etc., as set forth in the aforementioned reference.

2.15 Vector coupling functions

We implement a standard set of functions and subroutines for computing the vector-coupling 3-j, 6-j, and 9-j symbols using the Racah alebraic expressions [Edm96]. We distribute the Fortran library for these functions in their own Github repository (https://github.com/ogorton/wigner) as well.

One method we use to improve compute time is to cache Wigner 3-j and 6-j symbols [Edm96] (used to evaluate electro-weak matrix elements) in memory at the start of run-time. As a side effect, our tests show that this adds a constant compute time to any given calculation of roughly 0.3 seconds in serial execution and uses roughly 39 MB of memory (for the default table size). As a point of comparison, the ^{131}Xe example with all-nonzero EFT coefficients has a run-time of 30 seconds in parallel execution. If we disable the table caching, the run-time is roughly 150 seconds, 5 times longer. The size of the table stored in memory can be controlled via the control file with the keywords 'sj2tablemin' and 'sj2tablemax'.

For the 3-j symbol, we use the relation to the Clebsh-Gordon vector-coupling coefficients:

$$\begin{pmatrix} j_1 & j_2 & J \\ m_1 & m_1 & M \end{pmatrix} = (-1)^{j_1-j_2-M}(2J+1)^{-1/2}(j_1 j_2 m_1 m_2|j_1 j_2; J, -M). \tag{91}$$

The vector coupling coefficients are computed as:

$$(j_1 j_2 m_1 m_2|j_1 j_2; J, M) = \delta(m_1+m_1, m)(2J+1)^{1/2}\Delta(j_1 j_2 J) \tag{92}$$

$$\times[(j_1+m_1)(j_1-m_1)(j_2+m_2)(j_2-m_2)(J+M)(J-M)]^{1/2}\sum_z(-1)^z\frac{1}{f(z)}, \tag{93}$$

where

$$f(z) = z!(j_1+j_2-J-z)!(j_1-m_2-z)! \tag{94}$$

$$(j_2+m_2-z)!(J-j_2+m_1+z)!(J-m_1-m_2+z)!, \tag{95}$$

and

$$\Delta(abc) = \left[\frac{(a+b-c)!(a-b+c)!(-a+b+c)!}{(a+b+c+1)!}\right]^{1/2}. \tag{96}$$

The sum over z is over all integers such that the factorials are well-defined (non-negative-integer arguments).

Similarly, for the 6-j symbols:

$$\begin{Bmatrix} j_1 & j_2 & j_3 \\ m_1 & m_1 & m_3 \end{Bmatrix} = \Delta(j_1 j_2 j_3)\Delta(j_1 m_2 m_3)\Delta(m_1 j_2 m_3)\Delta(m_1 m_2 j_3) \sum_z (-1)^z \frac{(z+1)!}{g(z)}, \tag{97}$$

with $g(z) = (\alpha - z)!(\beta - z)!(\gamma - z)!(z - \delta)!(z - \epsilon)!(z - \zeta)!(z - \eta)!$ and

$$\alpha = j_1 + j_1 + m_1 + m_2 \qquad \beta = j_2 + j_3 + m_2 + m_3 \tag{98}$$

$$\gamma = j_3 + j_1 + m_3 + m_1 \tag{99}$$

$$\delta = j_1 + j_2 + j_3 \qquad \epsilon = j_1 + m_2 + m_3 \tag{100}$$

$$\zeta = m_1 + j_2 + m_3 \qquad \eta = m_1 + m_2 + j_3. \tag{101}$$

For the 9-j symbol, we use the relation to the 6-j symbol:

$$\begin{Bmatrix} j_1 & j_2 & j_3 \\ j_4 & j_5 & j_6 \\ j_7 & j_8 & j_9 \end{Bmatrix} = \sum_k (-1)^{2k}(2k+1) \begin{Bmatrix} j_1 & j_4 & j_7 \\ j_8 & j_9 & z \end{Bmatrix} \begin{Bmatrix} j_2 & j_5 & j_8 \\ j_4 & z & j_6 \end{Bmatrix} \begin{Bmatrix} j_3 & j_6 & j_9 \\ z & j_1 & j_2 \end{Bmatrix}. \tag{102}$$

The 6-j symbols used to calculate the 9-j symbol are first taken from any tabulated values. Otherwise, they are computed as previously described.

2.16 Note on unique couplings

Previous work has focused on setting limits on a single operator coupling at a time. But of course, multiple couplings may exist simultaneously, and in fact, some nuclear response functions are only activated with specific pairs of EFT coefficients.

To create a minimal list of inputs to validate all possible nonzero couplings, we need to test each coefficient on its own ($i = 1, ..., 15$), and also test the following 9 unique combinations: (1,2), (1,3), (2,3), (4, 5), (5,6), (8,9), (11,12), (11,15), (12,15).

Table of EFT coefficient interactions. Shows which coefficients multiply each coefficient in addition to itself.

Coefficient	Couples to
1	2, 3
2	1, 3
3	1, 2
4	5, 6
5	4
6	4
7	
8	9
9	8
10	
11	12, 15
12	11, 15
13	
14	
15	11, 12

3 Getting Started

To get started, one needs a modern Fortran compiler, the `make` tool, and, optionally, a Python interpreter (with NumPy, Matplotlib). We used the widely available GNU Fortran (`gfortran`) compiler, but we use only standard Fortran and our code should be able to be compiled by other Fortran compilers as well; the user will have to modify the makefile.

3.1 Compiling the code

To compile `dmscatter` , navigate to the `make` directory and run:

```
make dmscatter
```

This will compile the code using `gfortran`, creating the executable `dmscatter` in the `bin` directory. If you want to use a different compiler, you must edit the corresponding Makefile line to set "`FC = gfortran`" e.g., by replacing 'gfortran' with 'ifort'. To compile an OpenMP-parallel version of the code, use the option:

```
make openmp
```

Note that if you switch between and serial or parallel version, you must first run `make clean`.

3.2 Using the code

`dmscatter` is a modern Fortran code with a Python wrapper. It can be used interactively via the command line - details for this approach are found in section 4.

While the `dmscatter` executable can be run by itself, we provide Python APIs for integrating the Fortran program into Python scripts.

We also provide a generic application programming interface (API) for the Python language. This API essentially offers a prescribed and easy-to-use way to run `dmscatter` in a programmatic way. Any sufficiently experienced linux user could probably write a script to produce any possible set of inputs to our code. But our API removes the need by making it easy for anyone who can use a Python function to write their own advanced scripts allowing them to perform parameter studies and comparisons of different inputs to the theory. Details for this approach are found in section 5.

3.3 Understanding the structure of the code

The structure of the code and its inputs are outlined in Figure 1. The Fortran code replicates the capabilities of the earlier Mathematica script [AFH14]. Notably, one can compute the differential WIMP-nucleon scattering event rate for a range of recoil energies or transfer momenta, and any quantity required to determine those, such as the tabulated nuclear response functions.

The central engine, `dmscatter`, is written in standard modern Fortran and has OpenMP for an easy and optional parallel speed-up. While the distributed Makefile assumes the GNU Fortran compiler `gfortran`, the code should be able to be compiled by most recent Fortran compilers and does not require any special compilation flags, aside from standard (and optional) optimization and parallel OpenMP flags.

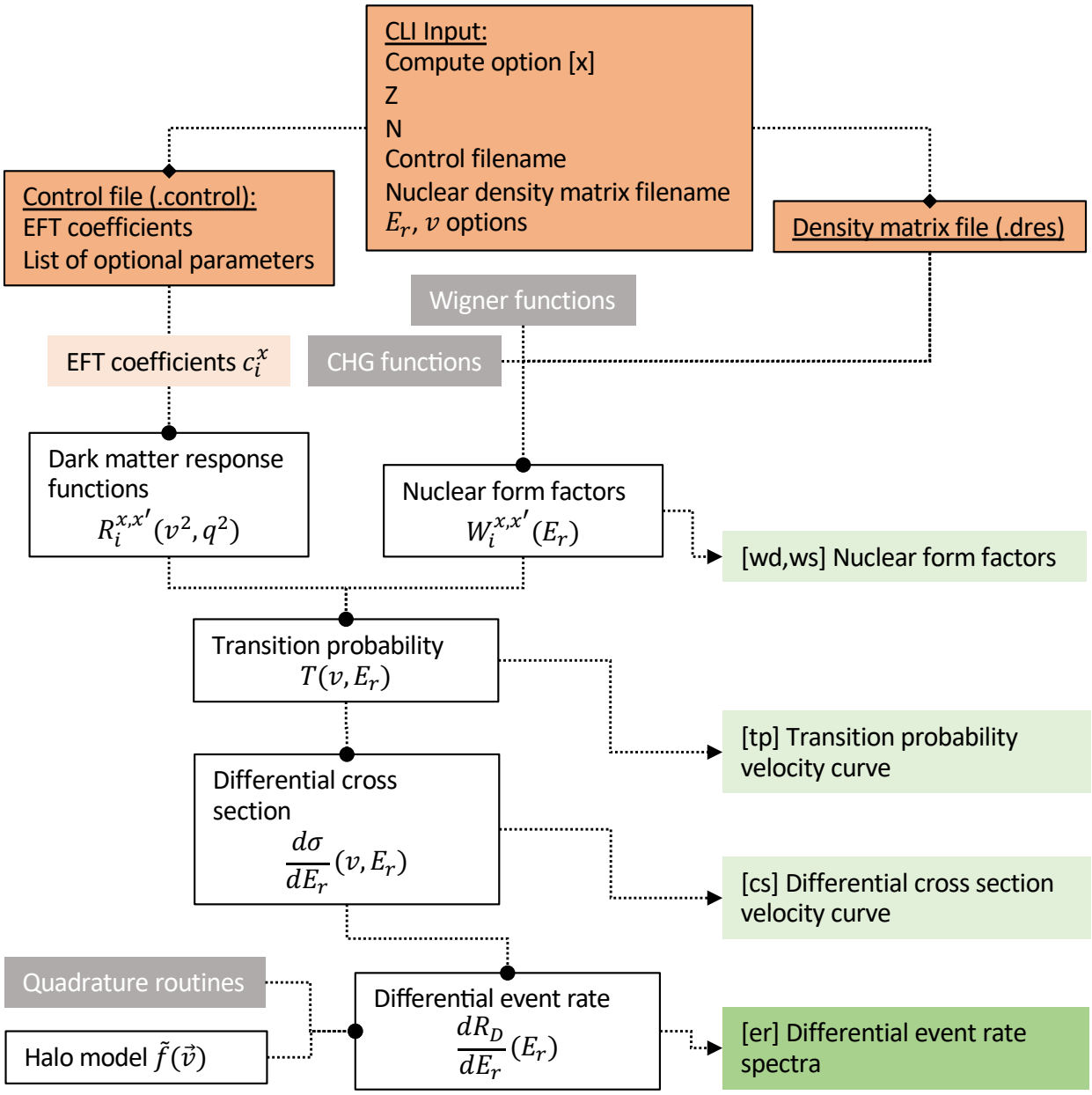

Figure 1: Flow of `dmscatter`. Information at various steps can be extracted and compared to other calculations. Orange boxes represent input files. Green boxes represent quantities the code can write to file. White boxes are important steps of interest and grey boxes are libraries built into the code. There are three groups of inputs for a WIMP-nucleus scattering event calculation. (1) The nuclear target information: target nucleus mass, spin, and one-body density matrix elements. (2) The generic, non-relativistic EFT-specification of the WIMP-nucleon interaction, in the form of coupling parameters along with the WIMP mass and spin. (3) The velocity distribution describing the relative motion of incoming WIMP particles in the laboratory frame.

4 Usage with Command Line

`dmscatter` can be used interactively from the command line, where the user is guided by prompts for a small number of datafiles and parameters. Naturally, this interactive process can be expedited by piping a pre-written input file into the command line interface (CLI).

The command line interface (CLI) to the code prompts the user for the type of calculation they wish to perform from a menu of options, then the target nucleus, given by the number of protons Z and neutrons N, two input files, and finally other CLI inputs depending on the compute-option chosen. These final inputs are typically three numbers specifying the range of recoil energies or momentum for which to compute the output. After running, the code prints the results to a plain text file in tabulated format.

The two files are:

1. Control file (.control)
2. Nuclear structure input (.dres)

The control file specifies the EFT interaction and any optional settings desired.

The nuclear structure inputs needed are one-body density matrices, defined below. We supply a library of density matrices for many of the common expected targets. The density matrix files are written in plain ASCII, using the format output by the nuclear configuration-interaction code Bigstick [JOK13, JOMS18]. The only assumption is that the single-particle basis states are harmonic oscillator states; the user must supply the harmonic oscillator single particle basis frequency Ω, typically given in MeV as $\hbar\Omega$, or the related length parameter $b = \sqrt{\hbar/M\Omega}$, where M is the nucleon mass.

If density matrices are generated in some other single-particle basis, such as those from a Woods-Saxon potential or a Hartree-Fock calculation, that basis must be expanded into harmonic oscillator states. By using harmonic oscillator basis states one can efficiently compute the matrix elements. One can use either phenomenological or ab initio model spaces and interactions; as an example, we provide density matrices for ^{12}C, both from the phenomenological Cohen-Kurath shell model interaction [CK65], and from an interaction derived from chiral effective field theory [EM03].

4.1 Running the code

The command line interface (CLI) to the code prompts the user for:

1. Type of calculation desired
2. Number of protons Z in the target nucleus
3. Number of neutrons N in the target nucleus
4. Control file name (.control)
5. Nuclear structure file name (.dres)
6. Secondary options related to the type of calculation

For details on each type of input file, see sections 7 and 6. Additionally, if the user enables the option "usenergyfile", then a file containing the input energies or momentum will also be required. The secondary options are typically three numbers specifying the range of recoil energies or momentum for which to compute the output. After running, the code writes the results to a plain text file in tabulated format.

The control file is a user-generated file specifying the EFT interaction, and any optional customizations to the settings. (See 7.) The nuclear structure inputs needed are one-body density matrix files (See 6).

An example input file can be found in the runs directory. The file `example.input` contains:

```
er
54
77
example
../targets/Xe/xe131gcn
1.0  1000.0  1.0
```

These inputs would compute a [er] differential event rate spectra; for [54] Xenon; [77] mass number 131 (54+77); [example] using the control file example.control located in the current directory; [../targets/Xe/xe131gcn] using the density matrix file xe131gcn.dres located in the `targets/Xe` directory; [1.0 1000.0 1.0] for a range of recoil energies from 1 to 1000 keV in 1 keV increments.

The corresponding control file, `example.control`, contains:

```
wimpmass     150.0
coefnonrel   1  n          0.00048
...
```

with 29 additional lines setting the remaining coefficients to equivalent values. This combination of input and control file produces the calculation in the last row of Table 3.

Assuming a user has successfully compiled the code, they can run this example from the 'examples' directory like this:

```
../bin/dmscatter < example.input
```

While the Fortran executable `dmscatter` can be run by itself, we provide Python application programming interfaces (APIs) for integrating the Fortran program into Python work flows. See section 5 for details.

4.2 Compute options

There are a handful of options available from the main menu of the code:

- er Differential event rate, for a range of recoil energies or transfer momenta
- cs Differential cross section at a fixed recoil energy over a range of speeds
- tp Transition/scattering probability at a fixed recoil energy over a range of speeds
- te Total integrated events (without producing spectra file)
- wd Nuclear response functions at a given value of $y = (qb/2)^2$
- ws Nuclear response function spectra (for a range of q or E)

The string in square brackets [x] is the compute-option. Once a compute-option is chosen, subsequent CLI inputs are the same up until the density matrix file (.dres) has been read-in. Then, the inputs depend on the compute-option chosen.

- cs Differential cross section per recoil energy. Four additional inputs:
  1. E-recoil (keV)
  2. v-start (km/s)
  3. v-stop (km/s)
  4. v-step (km/s)
- tp Scattering probability. Same as [2].
- te Total scattering events per detector (does not produce spectra data). This option uses adaptive quadrature to perform the integral of the event rate spectra with the fewest number of evaluations to reach the desired relative error. This will be much faster than the result from options [1]. Three additional inputs:
  1. E-start (keV)
  2. E-stop (keV)
  3. Desired relative error (decimal value)

wd Nuclear response function test. This compute-option allows the user to evaluate the nuclear response functions $W_i^{x,x'}(y)$ for a provided value of y. All combinations of x and x' will be printed for both isospin and proton-neutron couplings. Two additional inputs are required:

1. Function number (1 - 8)
2. Value of $y = (qb/2)^2$ (dimensionless)

ws Nuclear response function spectra. Enter a range of recoil energy or momentum values to evaluate the nuclear response funcions on. Tabulates the data to a file - one momentum per line or energy per line. Momentum/energy is written to the first column. The inputs are:

1. E-start (keV)
2. E-stop (keV)
3. E-step (keV)

The following 32 columns store the (8,2,2)-dimensional response functions $W_i^{x,x'}$:

```
q_1  W_1^00 W_2^00 ... W_8^00 W_1^10 ... W_8^11
q_2  W_1^00 W_2^00 ... W_8^00 W_1^10 ... W_8^11
...
q_m  W_1^00 W_2^00 ... W_8^00 W_1^10 ... W_8^11
```

For the event-rate spectra [er] and for the nuclear response function spectra [ws], the range of values is either over recoil energy E_r (kev) (the default) or over the transfer momentum q (Gev/c). To use q instead of E_r, use the control word `usemomentum` set to 1.

5 Usage with Python

We provide a Python interface (a wrapper) for the Fortran code and a number of example scripts demonstrating its use. The wrapper comes with two Python functions `EventrateSpectra`, and `NucFormFactor` which can be imported from `dmscatter.py` in the Python directory. Each function has three required arguments:

1. Number of protons Z in the target nucleus
2. Number of neutrons N in the target nucleus
3. Nuclear structure file name (.dres)

If no other arguments are provided, default values will be used for all of the remaining necessary parameters, including zero interaction strength. Default values are specified in the control file keyword table (see 7).

5.1 Event rate spectra

To calculate an event rate with a nonzero interaction, the user should also provide one or more of the optional EFT coupling coefficient arrays: `cp, cn, cs, cv`. These set the couplings to protons, neutrons, isoscalar, and isovector, respectively. The 0^{th} index sets the first operator coefficient: `cp[0]`$= c_1^p$, etc. Finally, the user can also pass a dictionary of valid control keywords and values to the function in order to set any of the control words defined in 7.

To compute the event-rate spectra for ^{131}Xe with a WIMP mass of 50 GeV and a $c_3^v = 0.0048$ coupling, one might call:

```
import dmscatter as dm
control_dict = {"wimpmass" : 50.0}
cv = np.zeros(15)
cv[2] = 0.0048
Erkev, ER = dm.EventrateSpectra(
            Z = 54,
            N = 77,
            dres = "../targets/Xe/xe131gcn",
            controlwords = control_dict,
            cv = cv,
            exec_path = "../bin/dmscatter")
```

This will return the differential event rate spectra for recoil energies from 1 keV to 1 MeV in 1 keV steps.

The file 'xe131gcn.dres' must be accessible at the relative or absolute path name specified (in this case '../targets/Xe/'), and contain a valid one-body density matrix for ^{131}Xe. Similarly, the `dmscatter` executable should be accessible from the user's default path - or else the path to the executable should be specified, as in the above example (`exec_path = "../bin/dmscatter"`).

5.2 Nuclear response functions

We have provided an additional option in `dmscatter` which computes these nuclear form factors from the target density-matrix and exports the results to a data file. This output may be useful for codes like WimPyDD [JKST21], which compute the WIMP-nucleus event rate spectra starting from nuclear form factors (equation (10)) from an external source.

The Python wrapper-function `NucFormFactor` runs the `dmscatter` option to export the nuclear response functions to file, and additionally creates and returns an interpolation function $W(q)$ which can be called. In the following code listing, the nuclear response function for ^{131}Xe is generated for transfer momentum from 0.001 to 10.0 GeV/c.

```
import dmscatter as dm
cwords = {"usemomentum": 1}
Wfunc = dm.NucFormFactor(
```

```
        Z = 54,
        N = 77,
        dres = "../targets/Xe/xe131gcn",
        controlwords = cwords,
        epmin = 0.001,
        epmax = 10.0,
        epstep = 0.001)
Wfunc(0.001)
```

The final line returns an (8,2,2)-shaped array with the evaluate nuclear response functions at $q = 0.001$ GeV/c. Note that, had we not set the keyword `usemomentum` to 1, the function input values would have been specified in terms of recoil energy (the default) instead of transfer momentum.

The first index runs over, in order, the 8 nuclear form factors:

$$M_J, \Phi''_J, \tilde{\Phi}'_J, \Delta_J, \Sigma'_J, \Sigma''_J, M\Phi'', \Sigma'\Delta \tag{103}$$

The second two indices are τ and τ', the isospin couplings. There is a simple relationship between the isospin and proton/neutron couplings:

$$\begin{bmatrix} 00 \\ 01 \\ 10 \\ 11 \end{bmatrix} = \frac{1}{4} \begin{bmatrix} 1 & 1 & 1 & 1 \\ 1 & -1 & 1 & -1 \\ 1 & 1 & -1 & -1 \\ 1 & -1 & -1 & 1 \end{bmatrix} \begin{bmatrix} pp \\ pn \\ np \\ nn \end{bmatrix}. \tag{104}$$

The inverse relation is simply:

$$\begin{bmatrix} pp \\ pn \\ np \\ nn \end{bmatrix} = \begin{bmatrix} 1 & 1 & 1 & 1 \\ 1 & -1 & 1 & -1 \\ 1 & 1 & -1 & -1 \\ 1 & -1 & -1 & 1 \end{bmatrix} \begin{bmatrix} 00 \\ 01 \\ 10 \\ 11 \end{bmatrix}. \tag{105}$$

6 Nuclear structure input (.dres)

Users must provide nuclear one-body density matrix elements, either in isospin format,

$$\rho^{\Psi}_{J,T}(a,b) = (2J+1)^{-1/2}(2T+1)^{-1/2}\langle\Psi|||[\hat{c}^{\dagger}_a \otimes \tilde{c}_b]_{J,T}|||\Psi\rangle, \tag{106}$$

or proton-neutron format, Users must provide nuclear one-body density matrix elements, either in isospin form,

$$\rho^{\Psi}_{J}(a,b) = (2J+1)^{-1/2}\langle\Psi|||[\hat{c}^{\dagger}_a \otimes \tilde{c}_b]_{J}||\Psi\rangle, \tag{107}$$

where Ψ is the nuclear-target wave function and $\hat{c}^{\dagger}$, $\hat{c}$ are the one-body creation, destruction operators. For proton-neutron format, the orbital indices a are distinct for protons and neutrons. The matrix elements must be stored in a file in a standard format produced by shell-model codes like BIGSTICK. The only assumption is that the single-particle basis states are harmonic oscillator states. If density matrices are generated in some other single-particle basis, such as those from a Woods-Saxon potential or a Hartree-Fock calculation, that basis must be expanded into harmonic oscillator states. By using harmonic oscillator basis states one can efficiently compute the matrix elements. One can use either phenomenological or *ab initio* model spaces and interactions; as an example, we provide density matrices for ^{12}C, both from the phenomenological Cohen-Kurath shell model interaction [CK65], and from two no-core shell model interactions [EM03, SSK$^+$16]. A detailed description of the provenance of the supplied targets can be found in the included manual, and will be updated as more density matrices become available. We also include, for purposes of validation, the 'legacy' density matrices available in the original `dmscatter` script.

6.1 List of nuclear targets

We supply a library of nuclear structure files (one-body density matrix files) for many of the common expected targets, as listed in Table 1. (We also include, for purposes of validation, some density matrices included with the original public Mathematica script [AFH14].) These density matrix files are written in plain ASCII, using the format output by the nuclear configuration-interaction code BIGSTICK [JOK13, JOMS18]. The only assumption is that the single-particle basis states are harmonic oscillator states; the user must supply the harmonic oscillator single particle basis frequency Ω, typically given in MeV as $\hbar\Omega$, or the related length parameter $b = \sqrt{\hbar/M\Omega}$, where M is the nucleon mass.

Nuclei	Isotopes	Source
He	4	[EM03, SSK$^+$16]
C	12	[CK65, EM03, SSK$^+$16]
F	19	[Wil84, BW88]*,[BR06]
Na	23	[Wil84, BW88],[BR06]
Si	28, 29	[Wil84, BW88]*,[BR06]
Ar	40	[UOB$^+$12]
Ge	70, 72, 73, 74, 76	[HOMHJ09]
I	127	[BSS$^+$05]; [GCN] used in [CMNP08, CNPS10]
Xe	128, 129, 130, 131, 132, 134, 136	[BSS$^+$05]; [GCN] used in [CMNP08, CNPS10]

Table 1: Table of nuclear data for targets we include with the program at time of publication. Each corresponds to a (.dres) density matrix file in the `targets` directory. The source indicates the nuclear Hamiltonian that was used to generate the wave function data. See the manual and GitHub repository for updates and full information on provenance. New targets may be added in future releases. * = density matrix used in original Mathematica script [AFH14]

6.2 Density matrix format

We adopt the output format from the BIGSTICK shell-model code. The output one-body densities (26) are written to a file with extension `.dres`. We provide a full specification of this plain-text-file format in the `docs` directory. Here, we show the form of the file and explain its contents.

```
<Header information>
   4   -5
  State      E        Ex         J       T
    1   -330.17116   0.00000     1.500  11.500
  Single particle state quantum numbers
ORBIT      N     L   2 x J
     1     0     2     3
     2     0     2     5
     3     1     0     1
 Initial state # 1 E = -330.17117 2xJ, 2xT = 3  23
 Final state   # 1 E = -330.17117 2xJ, 2xT = 3  23
 Jt =   0, proton      neutron
    1    1   1.55844   5.40558
```

The first line of the file is an arbitrary header. The second line of the file contains two integers: the number of protons and number of neutrons in the valence space. These numbers may be negative, in which case they represent the number of holes in a completely full valence space. In the previous example, there are 4 valence protons and 5 valence neutron holes, which translates to 27 valence neutrons.

The file is then comprised of three sections: (1) many-body state information, (2) single-particle state quantum numbers, (3) density matrix element blocks. Only the ground state is needed for inelastic WIMP-nucleus scattering calculations. The single-particle state quantum numbers specify the quantum numbers for the simple-harmonic oscillator states involved in the one-body operators.

Finally, the one-body density matrix elements are listed in nested blocks with three layers: (i) the initial and final state specification (corresponding to the many-body states listed in section (1) of the file), (ii) the angular momentum carried by the one-body density matrix operator, labeled `Jt` here, and (iii) the single-particle state labels `a`, `b` in columns 1 and 2 (corresponding to the single-particle state labels listed in section (2) of the file) and the proton and neutron (isospin-0 and isospin-1) density matrix elements in columns 3 and 4.

Both (i) and (ii) must be specified along with columns 1 and 2 of (iii) in order to fully determine a matrix element $\rho_K^{f,i}(a,b)$, where $K = J_t$. Note that the values of K are restricted by conservation of angular momentum; both between the many-body states labeled i and f, and the single-particle states labeled a and b.

6.3 Calling the library of targets

To call a nuclide from the library of targets, a mandatory command line input is the name of the `.dres` file with the nuclear structure information. See Section 4.1 above. The location is relative to the `/runs` directory. Our library of targets is located in directory `/targets`. To use your own nuclear data file, place it in the same directory or specify the directory relative to the `/runs` directory, i.e., `../MyTargets/X` will use `X.dres` in the directory `/MyTargets`, where both `/runs` and `/MyTargets` are subdirectories of the main directory, `/darkmatter`.

6.4 Filling core orbitals for phenomenological interactions

Since standard one-body density matrices in phenomenological model spaces contain only matrix elements for orbitals in the valence space, it is necessary to infer the matrix elements for the core orbitals. Our code does this by default, but the user can disable this option using the `fillnuclearcore` control word.

For phenomenological interactions one typically has a 'frozen' core of nucleons which do not participate in the two-body forces of the Hamiltonian. In such cases the single-particle space listed in the .dres file consists only of the valence orbitals and the one-body density matrices are only specified for the valence orbitals.

DMFormFactor reads the valence space orbitals from the .dres file and infers the number of core nucleons by subtracting the number of valence protons and neutrons from the number of nucleons in the target nucleus. The core orbitals are assumed to be one of the standard shell model orbital sets associated with possible cores: ^{4}He, ^{16}O, ^{40}Ca,^{56}Ni, ^{100}Sn.

The one-body density matrix elements for the core orbitals are then determined from the (full) occupation of the core orbitals. Because the orbitals are full and here we assume both proton and neutron orbitals filled, the core can contribute only to $J = 0, T = 0$ densities. Two formats are possible: proton-neutron format:

$$\rho^{\Psi}_{J,x=p,n}(a,b)_{(core)} = \delta_{a,b}\delta_{J,0}[j_a], \tag{108}$$

where $[y] \equiv \sqrt{2y+1}$ and j_a is the angular momentum of a-orbit. J is the total spin of the nuclear target state Ψ; and isospin format for a target state with good total isospin T:

$$\rho^{\Psi}_{J,T=0}(a,b)_{(core)} = \delta_{a,b}\delta_{J,0}\delta_{T,0}[1/2][j_a], \tag{109}$$

$$\rho^{\Psi}_{J,T=1}(a,b)_{(core)} = 0.0. \tag{110}$$

Internally the code expands densities in isospin format into proton and neutron densities. Note that our libraries only include isoscalar cores; if one had cores with $N > Z$ then one could also have $T = 1$ contributions.

6.5 Checking for valid densities

When a density matrix is read in, `dmscatter` performs a test to validate the number of particles in the valence orbitals matches the declared number of valence particles at the top of the density matrix file. If this test fails, the code will stop. This is an indication that the density matrices being used were not fully converged, or have some other problem. The check is that

$$n_p = \sum_a \rho_{J=0,p}(a,a)[j_a]/[J_0] \tag{111}$$

$$n_n = \sum_a \rho_{J=0,n}(a,a)[j_a]/[J_0], \tag{112}$$

where n_p is the number of valence protons, j_a is the total angular momentum of the a-th valence orbital, and J_0 is the total angular momentum of the ground state of the nucleus. Similarly for the number of neutrons n_n.

7 Control words

Each EFT parameter is written on its own line in '[mycontrolfile].control', with four values: the keyword 'coefnonrel', the operator number (integer 1..16), the coupling type ('p'=proton, 'n'=neutron, 's'=scalar, 'v'=vector), and the coefficient value. For example:

```
coefnonrel    1    s     3.1
```

would set $c_1^{\tau=0} = 3.1$. We take the isospin convention:

$$\begin{aligned} c^0 &= (c^p + c^n)/2 \\ c^1 &= (c^p - c^n)/2 \end{aligned} \tag{113}$$

Thus, the previous example is equivalent to:

```
coefnonrel    1    p     1.55
coefnonrel    1    n     1.55
```

The control file also serves a more general but optional function: to set any parameter in the program to a custom value. Simply add an entry to the control file with two values: the first should be the keyword for the parameter and the second should be the value to set that parameter to. For example, to set the velocity of the earth in the galactic frame to 240 km/s, you should add the line:

```
vearth  240.0
```

As an example, here is the complete control file used to calculate the event rate for the c_1^n coupling to ^{131}Xe shown in Table 3:

```
# Coefficient matrix (non-relativistic)
# Ommitted values are assumed to be 0.0.
# c_i^t
# i = 1,...,16
# t: p=proton n=neutron s=scaler v=vector
coefnonrel  1  n  0.00048
wimpmass 150.0
vearth 232.0
maxwellv0 220.0
dmdens 0.3
usemomentum 0
useenergyfile 0
ntscale  2500.0
printdensities 0
#vescape 550.
```

Un-commenting the last line would set the escape velocity to 550 km/s.

A complete list of control words is given below.

Keyword	Symbol	Meaning	Units	Default
dmdens	ρ_χ	Local dark matter density.	GeV/cm^3	0.3
dmspin	j_χ	Instrinsic spin of WIMP particles.	$\hbar$	$\frac{1}{2}$

fillnuclearcore		Logical flag (enter 0 for False, 1 for True) to fill the inert-core single-particle orbitals in the nuclear level densities. Phenomenological shell model calculations typically provide only the density matrices for the active valence-space orbitals, leaving it to the user to infer the core-orbital densities. This option automatically assigns these empty matrix elements assuming a totally filled core.		1 (true)
gaussorder		Order of the Gauss-Legendre quadrature to use when using Type 2 quadrature. (See quadtype.) An n-th order routine will perform n function evaluations. Naturally, a higher order will result in higher precision, but longer compute time.		12
hofrequency	$\hbar\omega$	Set the harmonic oscillator length by specifying the harmonic oscillator frequency. (b = 6.43/sqrt($\hbar\omega$)). If using an *ab initio* interaction, $\hbar\omega$ should be set to match the value used in the interaction.	MeV	See hoparameter.
hoparameter	b	Harmonic oscillator length. Determines the scale of the nuclear wavefunction interaction.	fm	See eqn. (25).
maxwellv0	v_0	Maxwell-Boltzman velocity distribution scaling factor.	km/s	220.0
mnucleon	m_N	Mass of a nucleon. It's assumed that $m_p \approx m_n$.	GeV	0.938272
ntscale	N_t	Effective number of target nuclei scaling factor. The differential event rate is multiplied by this constant in units of kilogram-days. For example, if the detector had a total effective exposure of 2500 kg days, one might enter 2500 for this value.	kg days	1.0
printdensities		Option to print the nuclear one-body density matrices to screen.		0 (false)
pnresponse		Option to print the nuclear response functions in terms of proton-neutron coupling instead of isospin coupling		0 (false)
quadrelerr		Desired relative error for the adaptive numerical quadrature routine (quadtype 1).		10^{-6}
quadtype		Option for type of numerical quadrature. (Type 1 = adaptive 8th order Gauss-Legendre quadrature. Type 2 = static n-th order Gauss-Legendre quadrature.)		1 (type 1)
sj2tablemax		Maximum value of $2 \times J$ used when caching Wigner 3-J and 6-J functions into memory.		12
sj2tablemin		Minimum value of $2 \times J$ used when caching Wigner 3-J and 6-J functions into memory.		-2
useenergyfile		Logical flag (enter 0 for False, 1 for True) to read energy grid used for calculation from a user-provided file intead of specifying a range.		0 (false)

usemomentum		Logical flag (enter 0 for False, 1 for True) to use momentum transfer intead of recoil energy as the independent variable.		0 (false)
vearth	v_{earth}	Speed of the earth in the galactic frame.	km/s	232.0
vescape	v_{escape}	Galactic escape velocity. Particles moving faster than this speed will escape the galaxy, thus setting an upper limit on the WIMP velocity distribution.	km/s	$12 \times v_{scale}$
weakmscale	m_v	Weak interaction mass scale. User defined EFT coefficients are divided by m_v^2.	GeV	246.2
wimpmass	m_χ	WIMP particle mass.	GeV	50.0

8 Validation and performance

There are two sources of error in our calculation. The first is from the model uncertainty of the nuclear wave functions. This source of error is therefore also present in `dmscatter`. While phenomenological calculations can get energies within a few hundred keV [BR06], other observables often require significant renormalization of operators to agree with experiment, see, e.g., [RMB08]. These errors in observables can have complex origins, arising both from truncations of the model space and higher-order corrections to the corresponding operators [GHH$^+$19]. Errors in the numerical methods to solve the many-body problem given a set of input parameters are, by comparison, vanishingly small. Nonetheless experience suggest that in most cases the renormalization is of order one. We have qualitative support of this fact from comparisons of event rate spectra from *ab initio* calculations with increasing model space dimension (scaling with N_{max}, the maximum excitation in an non-interacting harmonic oscillator basis, sometimes written as $N_{max}\,\hbar\omega$ excitations), and from different chiral effective-field theoretical interactions.

The second source of error is from the numerical integration. By comparison, the error from the numerical integration is expected to be many orders of magnitude smaller. Using an adaptive quadrature routine from a standard source [Dav84], the code iteratively increases the complexity of the estimator until it achieves a desired relative uncertainty.

8.1 Validation

We validated our Fortran program `dmscatter` against the Mathematica script `dmformfactor` (version 6.0). We used ^{29}Si as a validation case since we have access to the same nuclear density matrix file provided in the `dmformfactor` package. With a $J = 1/2$ ground state, ^{29}Si also has non-zero coupling to all 15 operators.

We evaluated the differential event rate for recoil energies from 1 keV to 1000 keV in 1 keV increments for each coefficient individually c_i^x; for $i = 1, 3, 4, 5, ..., 15$; for linearly independent coupling pairs $c_a \cdot c_b = 1$ for (a, b) = (1,2), (1,3), (2,3), (4, 5), (5,6), (8,9), (11,12), (11,15), (12,15), and for both $x = p, n$. An example is shown in Figure 2. In each case we reproduce the results of `dmformfactor`. Typical 'error' with respect to `dmformfactor` is shown in Figure 3. A full suite of validation plots are attached at the end of the manual.

8.2 Performance

The Fortran code has been optimized for multi-processor CPUs with shared memory architecture using OpenMP. As a result of this parallelism and the inherent efficiency of a compiled language, our program sees an extreme speedup when computing event-rate spectra compared to the Mathematica package `dmformfactor` version 6.

We provide timing data for two benchmark cases: ^{29}Si and ^{131}Xe, shown in Table 3. The compute time of our code depends primarily on two sets of factors: the first is the number of elements in the nuclear densities matrices (which depends on the complexity of the nuclear structure for a given target nucleus), and the second is the number of nonzero EFT coefficients. We include logic to skip compute cycles over zero EFT coefficients.

The timing data in Table 3 provides a general indication of the compute time for basic calculations. We also ran a more complex benchmark calculation to represent the complexity of a practical application. In this calculation, we compute the differential event rate spectra for ^{131}Xe over a range of recoil energies from 1 keV to 1000 keV, and for a range of WIMP masses from 1 GeV to 300 GeV, in 1 GeV increments. We provide the Python script `exampleMassHeatPlot.py` used to generate this plot in the `python/` directory. The result is shown in the heat plot in Figure 4. This calculation represents 300 calculations of the type in Table 3, and so we estimate that generating the data for such a plot using the Mathematica package `dmformfactor` would require roughly 70 days of CPU time. Our calculation takes only 20 minutes of CPU time with serial execution (including overhead from the Python script running the code), and with parallel execution across 4 threads the wall time is 7 minutes.

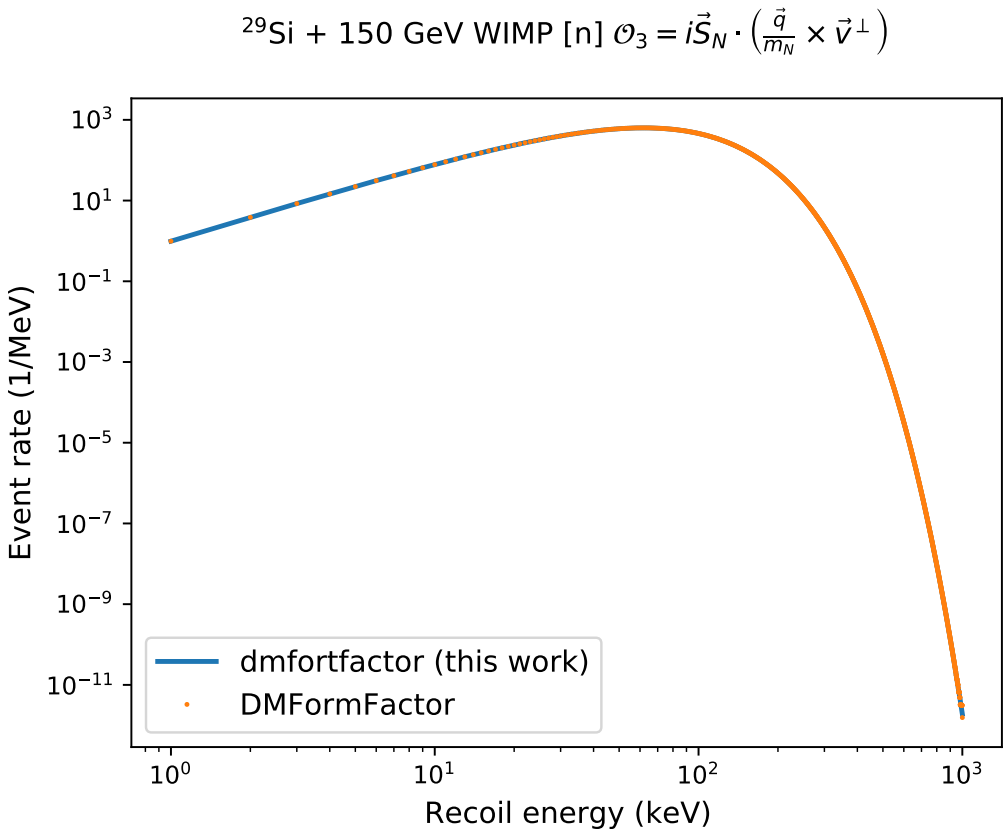

Figure 2: Example differential event rate spectra for $c_3^n = 1$ with 150 GeV WIMPS on ^{29}Si computed with `dmscatter` (solid blue line) and with `dmformfactor` (orange dots).

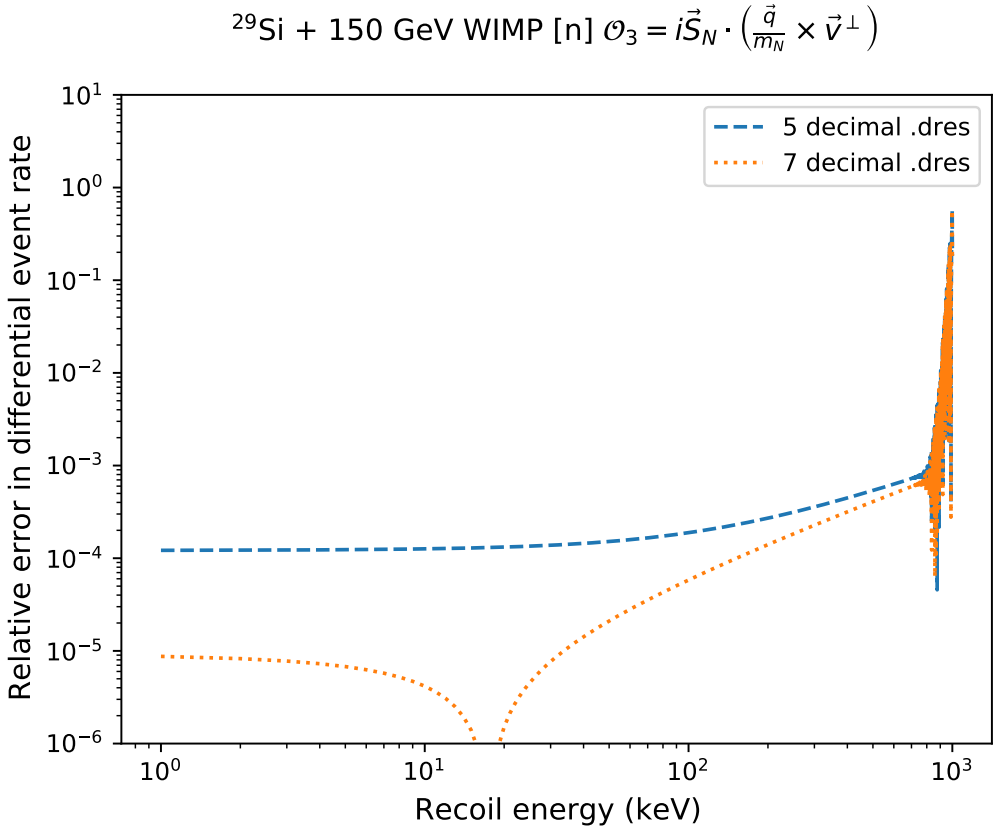

Figure 3: Relative error of `dmscatter` with respect to the Mathematica script `dmformfactor` for the same example. The spike near recoil energy 10^3 keV is due to round-off error on zero; the event rate there is nearly zero. The (blue) dashed line was calculated with the BIGSTICK-standard 5 decimals of precision in the nuclear structure input (.dres file). The (orange) dotted line has 7 decimal places of precision, matching that used in the `dmformfactor` calculation.

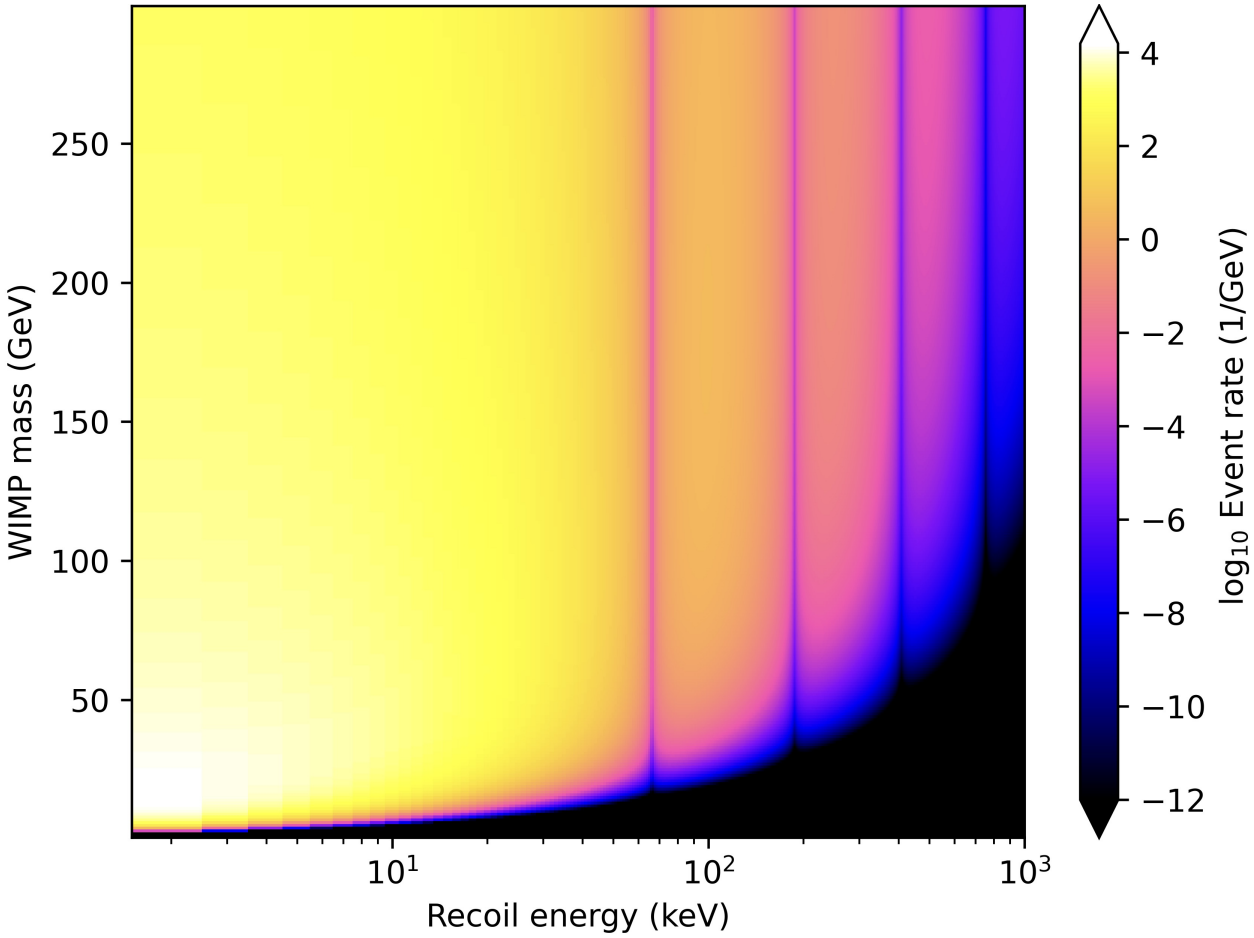

Figure 4: Event rate as a function of WIMP mass and recoil energy for ^{131}Xe. 300 masses are represented in this figure (1000 recoil energies each; a slice along the horizontal axis is analogous to the calculation shown in Figure 2). Using our code, this consumed roughly 30 minutes of CPU time. We estimate that using `dmformfactor` to generate the same figure would take at least 70 days (300 curves, 20 000 seconds each). The EFT interaction used was vector isospin-coupling to operator-1 ($c_1^{\tau=1} = 0.00048$).

Coupling	DMFormFactor	dmscatter	
		Serial	Parallel
	Nuclear target: ^{29}Si		
c_1^n	3,800	0.5	0.2
c_3^n	3,800	1.3	0.5
c_4^n	3,700	1.5	0.5
c_5^n	3,700	0.9	0.3
c_6^n	3,700	0.8	0.3
	Nuclear target: ^{131}Xe		
c_1^n	20,000	1.7	0.5
c_1^p		1.7	0.5
c_1^s	20,000	5.8	1.6
c_1^v		5.8	1.6
All nonzero	20,000	75	20

Table 3: Program execution time in seconds for a sample event-rate calculation with 1000 recoil energies with $m_\chi = 150$ GeV. The velocity distribution was taken to be Maxwellian with $v_{escape} \approx \infty$. All calculations were done on the same machine (Apple M1 processor, 2020). Multi-threaded execution was performed with 4 threads on the 8-core CPU. ^{29}Si has 23 matrix elements in its one-body density matrix, while ^{131}Xe has 67.

References

[AFH14] Nikhil Anand, A. Liam Fitzpatrick, and W. C. Haxton. Weakly interacting massive particle-nucleus elastic scattering response. *Physical Review C*, 89(6), Jun 2014.

[BFPR84] George R. Blumenthal, S.M. Faber, Joel R. Primack, and Martin J. Rees. Formation of Galaxies and Large Scale Structure with Cold Dark Matter. *Nature*, 311:517–525, 1984.

[BH18] Gianfranco Bertone and Dan Hooper. History of dark matter. *Rev. Mod. Phys.*, 90(4):045002, 2018.

[BM68] J. Blomqvist and A. Molinari. Collective 0− vibrations in even spherical nuclei with tensor forces. *Nuclear Physics A*, 106(3):545–569, 1968.

[BR06] B. Alex Brown and W. A. Richter. New "USD" hamiltonians for the *sd* shell. *Phys. Rev. C*, 74:034315, Sep 2006.

[BSS+05] B. A. Brown, N. J. Stone, J. R. Stone, I. S. Towner, and M. Hjorth-Jensen. Magnetic moments of the 2_1^+ states around ^{132}Sn. *Phys. Rev. C*, 71:044317, Apr 2005.

[BW88] B Alex Brown and BH Wildenthal. Status of the nuclear shell model. *Annual Review of Nuclear and Particle Science*, 38(1):29–66, 1988.

[CK65] S Cohen and D Kurath. Effective interactions for the 1p shell. *Nuclear Physics*, 73(1):1–24, 1965.

[CMNP08] E. Caurier, J. Menéndez, F. Nowacki, and A. Poves. Influence of pairing on the nuclear matrix elements of the neutrinoless $\beta\beta$ decays. *Phys. Rev. Lett.*, 100:052503, Feb 2008.

[CNPS10] E. Caurier, F. Nowacki, A. Poves, and K. Sieja. Collectivity in the light xenon isotopes: A shell model study. *Phys. Rev. C*, 82:064304, Dec 2010.

[Dav84] Appendix 2 - fortran programs. In Philip J. Davis and Philip Rabinowitz, editors, *Methods of Numerical Integration (Second Edition)*, pages 480–508. Academic Press, second edition edition, 1984.

[DFS86] Andrzej K. Drukier, Katherine Freese, and David N. Spergel. Detecting cold dark-matter candidates. *Phys. Rev. D*, 33:3495–3508, Jun 1986.

[DH79] T.W. Donnelly and W.C. Haxton. Multipole operators in semileptonic weak and electromagnetic interactions with nuclei: Harmonic oscillator single-particle matrix elements. *Atomic Data and Nuclear Data Tables*, 23(2):103–176, 1979.

[Edm96] Alan Robert Edmonds. *Angular momentum in quantum mechanics*. Princeton University Press, 1996.

[EM03] D. R. Entem and R. Machleidt. Accurate charge-dependent nucleon-nucleon potential at fourth order of chiral perturbation theory. *Phys. Rev. C*, 68:041001, Oct 2003.

[EOM18] N. Wyn Evans, Ciaran A. J. O'Hare, and Christopher McCabe. Shm^{++}: A refinement of the standard halo model for dark matter searches in light of the gaia sausage, 2018.

[Fen10] Jonathan L. Feng. Dark Matter Candidates from Particle Physics and Methods of Detection. *Ann. Rev. Astron. Astrophys.*, 48:495–545, 2010.

[FFG88] Katherine Freese, Joshua Frieman, and Andrew Gould. Signal modulation in cold-dark-matter detection. *Phys. Rev. D*, 37:3388–3405, Jun 1988.

[FHK+13] A. Liam Fitzpatrick, Wick Haxton, Emanuel Katz, Nicholas Lubbers, and Yiming Xu. The effective field theory of dark matter direct detection. *Journal of Cosmology and Astroparticle Physics*, 2013(02):004–004, feb 2013.

[FJP20] Jordan M. R. Fox, Calvin W. Johnson, and Rodrigo Navarro Perez. Uncertainty quantification of an empirical shell-model interaction using principal component analysis. *Phys. Rev. C*, 101:054308, May 2020.

[FZ10] A. Liam Fitzpatrick and Kathryn M. Zurek. Dark moments and the dama-cogent puzzle. *Phys. Rev. D*, 82:075004, Oct 2010.

[GCN] A Gniady, E Caurier, and F Nowacki. Unpublished.

[GHH+19] P Gysbers, Gaute Hagen, JD Holt, Gustav R Jansen, Titus D Morris, P Navrátil, T Papenbrock, S Quaglioni, A Schwenk, SR Stroberg, et al. Discrepancy between experimental and theoretical β-decay rates resolved from first principles. *Nature Physics*, 15(5):428–431, 2019.

[GW85] Mark W. Goodman and Edward Witten. Detectability of certain dark-matter candidates. *Phys. Rev. D*, 31:3059–3063, Jun 1985.

[Hax] Wick C. Haxton. unpublished.

[HJM22] Wick C. Haxton, Calvin W. Johnson, and Ken S. McElvain. to be submitted to Annual Review of Nuclear and Particle Science, 2022.

[HMS20] Martin Hoferichter, Javier Menéndez, and Achim Schwenk. Coherent elastic neutrino-nucleus scattering: EFT analysis and nuclear responses. *Phys. Rev. D*, 102:074018, 7 2020.

[HOMHJ09] M. Honma, T. Otsuka, T. Mizusaki, and M. Hjorth-Jensen. New effective interaction for f_5pg_9-shell nuclei. *Phys. Rev. C*, 80:064323, Dec 2009.

[JKST21] Injun Jeong, Sunghyun Kang, Stefano Scopel, and Gaurav Tomar. Wimpydd: an object-oriented python code for the calculation of wimp direct detection signals. *arXiv preprint arXiv:2106.06207*, 2021.

[JOK13] Calvin W. Johnson, W. Erich Ormand, and Plamen G. Krastev. Factorization in large-scale many-body calculations. *Computer Physics Communications*, 184:2761–2774, 2013.

[JOMS18] Calvin W. Johnson, W. Erich Ormand, Kenneth S. McElvain, and Hongzhang Shan. Bigstick: A flexible configuration-interaction shell-model code, 2018.

[LS96] J.D. Lewin and P.F. Smith. Review of mathematics, numerical factors, and corrections for dark matter experiments based on elastic nuclear recoil. *Astroparticle Physics*, 6(1):87–112, 1996.

[McC10] Christopher McCabe. Astrophysical uncertainties of dark matter direct detection experiments. *Phys. Rev. D*, 82:023530, Jul 2010.

[PSS88] Joel R. Primack, David Seckel, and Bernard Sadoulet. Detection of Cosmic Dark Matter. *Ann. Rev. Nucl. Part. Sci.*, 38:751–807, 1988.

[RMB08] W. A. Richter, S. Mkhize, and B. Alex Brown. *sd*-shell observables for the usda and usdb hamiltonians. *Phys. Rev. C*, 78:064302, Dec 2008.

[Sad99] Bernard Sadoulet. Deciphering the nature of dark matter. *Rev. Mod. Phys.*, 71:S197–S204, Mar 1999.

[SSK+16] AM Shirokov, IJ Shin, Y Kim, M Sosonkina, P Maris, and JP Vary. N3lo nn interaction adjusted to light nuclei in ab exitu approach. *Physics Letters B*, 761:87–91, 2016.

[UOB+12] Yutaka Utsuno, Takaharu Otsuka, B. Alex Brown, Michio Honma, Takahiro Mizusaki, and Noritaka Shimizu. Shape transitions in exotic si and s isotopes and tensor-force-driven Jahn-Teller effect. *Phys. Rev. C*, 86:051301, Nov 2012.

[VKM+15] L. Vietze, P. Klos, J. Menéndez, W.C. Haxton, and A. Schwenk. Nuclear structure aspects of spin-independent WIMP scattering off xenon. *Phys. Rev. D*, 91(4):043520, 2015.

[Wil84] BH Wildenthal. Empirical strengths of spin operators in nuclei. *Progress in particle and nuclear physics*, 11:5–51, 1984.

[XAC+19] Jingkai Xia, Abdusalam Abdukerim, Wei Chen, Xun Chen, Yunhua Chen, Xiangyi Cui, Deqing Fang, Changbo Fu, Karl Giboni, Franco Giuliani, et al. Pandax-II constraints on spin-dependent WIMP-nucleon effective interactions. *Physics Letters B*, 792:193–198, 2019.

DMFortFactor Validation Plots for ^{29}Si

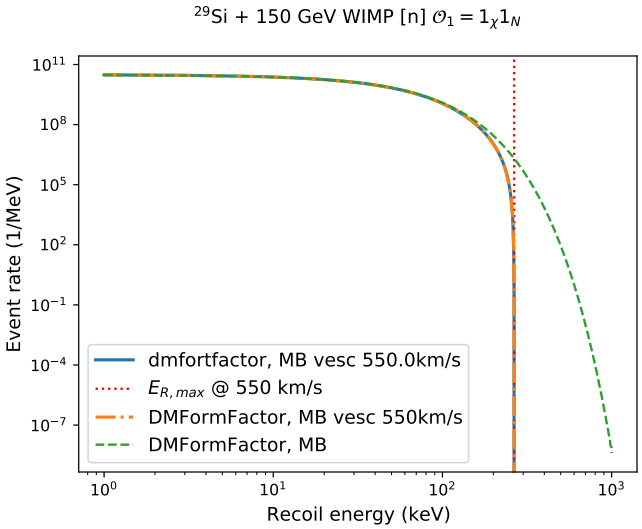

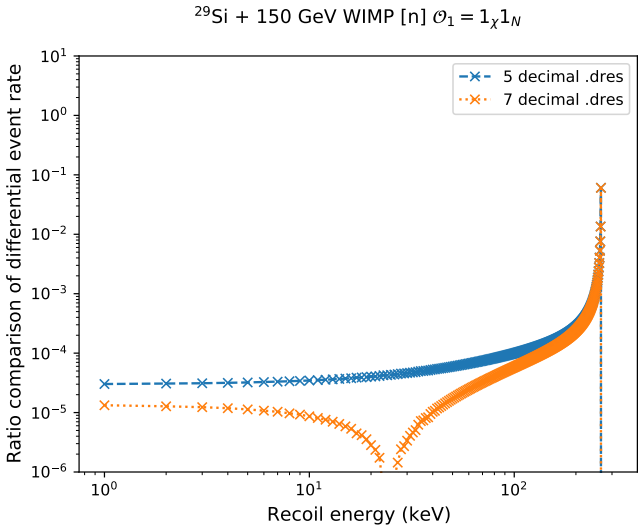

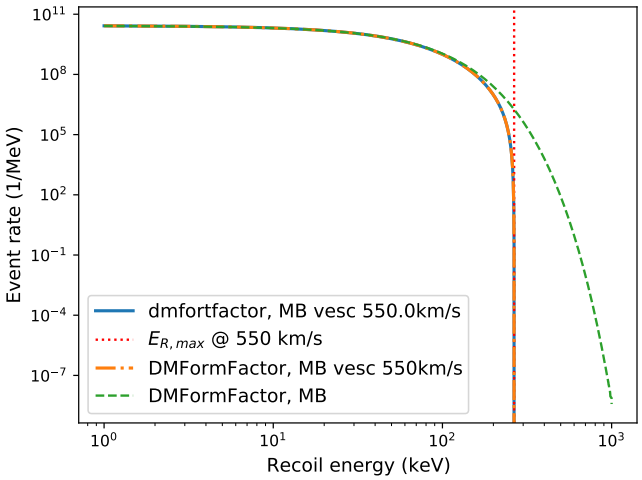

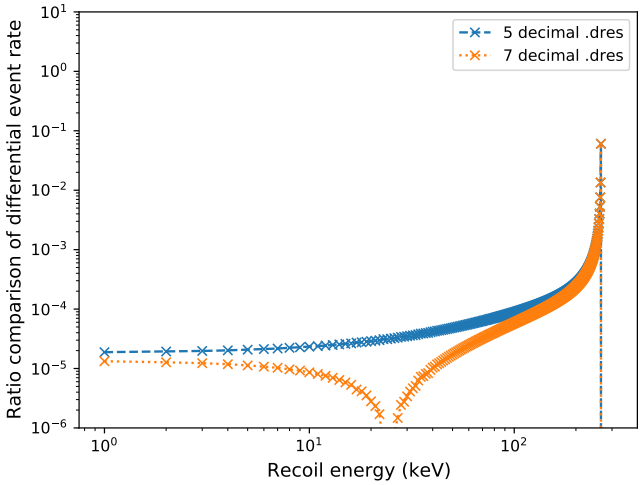

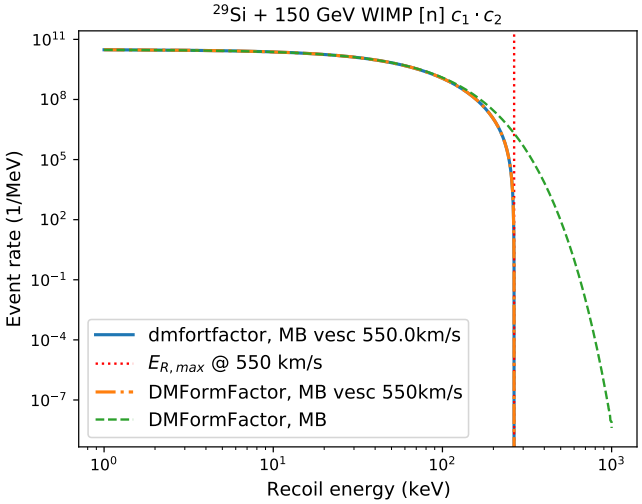

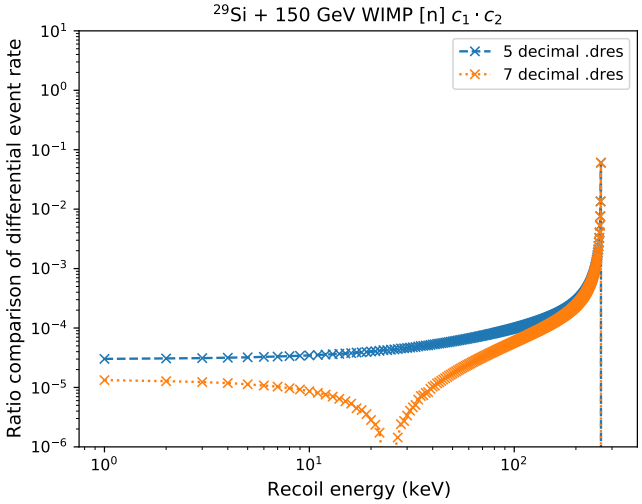

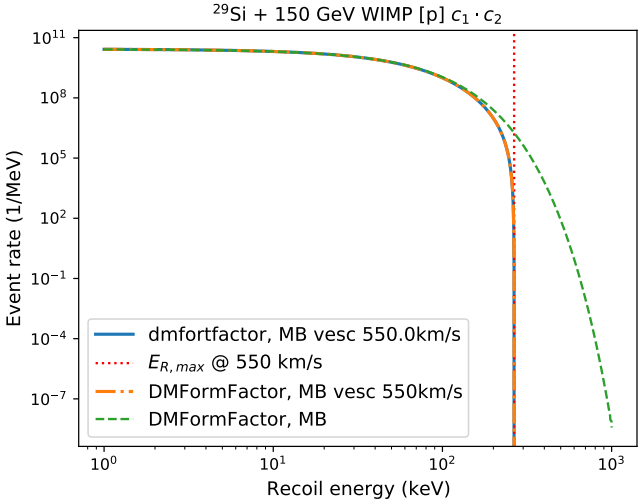
^{29}Si + 150 GeV WIMP [p] $c_1 \cdot c_2$
Event rate (1/MeV)
Recoil energy (keV)
dmfortfactor, MB vesc 550.0km/s
$E_{R,max}$ @ 550 km/s
DMFormFactor, MB vesc 550km/s
DMFormFactor, MB

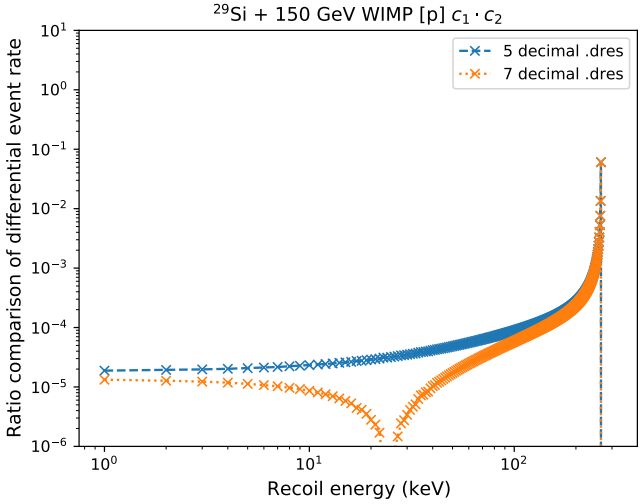
^{29}Si + 150 GeV WIMP [p] $c_1 \cdot c_2$
Ratio comparison of differential event rate
Recoil energy (keV)
5 decimal .dres
7 decimal .dres

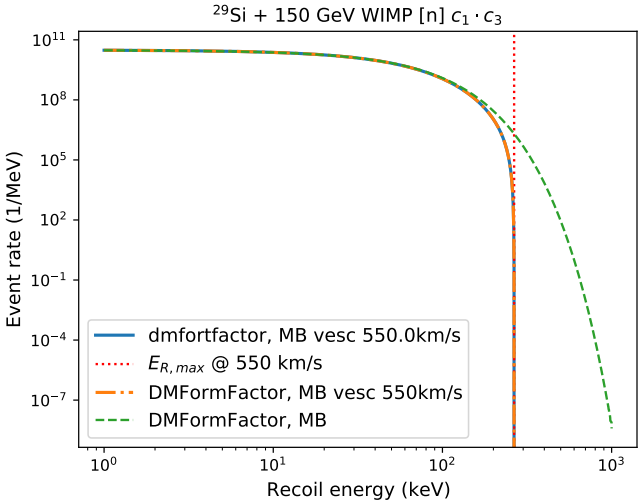
^{29}Si + 150 GeV WIMP [n] $c_1 \cdot c_3$
Event rate (1/MeV)
Recoil energy (keV)
dmfortfactor, MB vesc 550.0km/s
$E_{R,max}$ @ 550 km/s
DMFormFactor, MB vesc 550km/s
DMFormFactor, MB

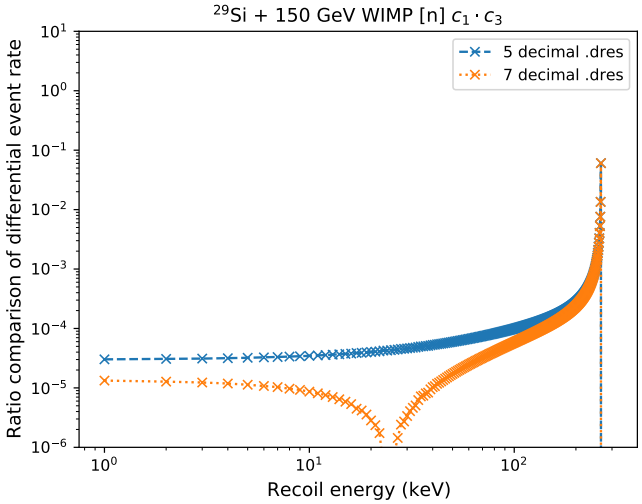
^{29}Si + 150 GeV WIMP [n] $c_1 \cdot c_3$
Ratio comparison of differential event rate
Recoil energy (keV)
5 decimal .dres
7 decimal .dres

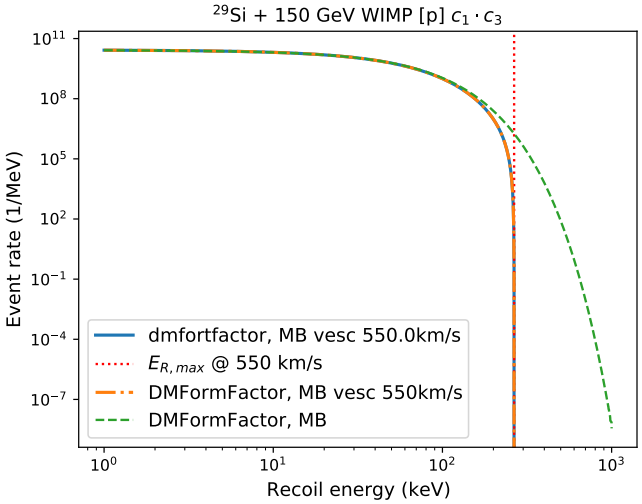
^{29}Si + 150 GeV WIMP [p] $c_1 \cdot c_3$
Event rate (1/MeV)
Recoil energy (keV)
dmfortfactor, MB vesc 550.0km/s
$E_{R,max}$ @ 550 km/s
DMFormFactor, MB vesc 550km/s
DMFormFactor, MB

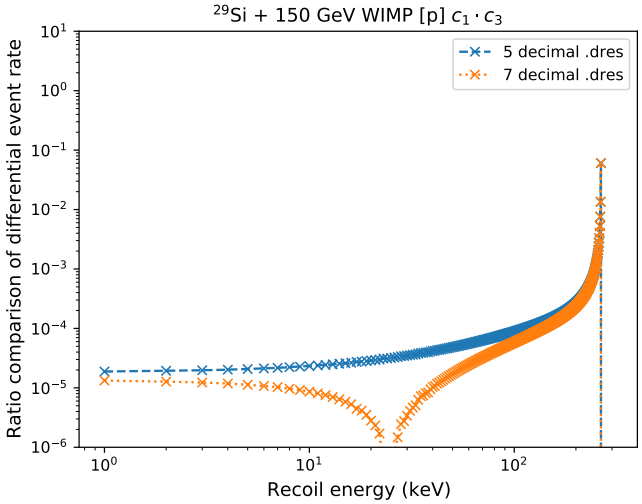
^{29}Si + 150 GeV WIMP [p] $c_1 \cdot c_3$
Ratio comparison of differential event rate
Recoil energy (keV)
5 decimal .dres
7 decimal .dres

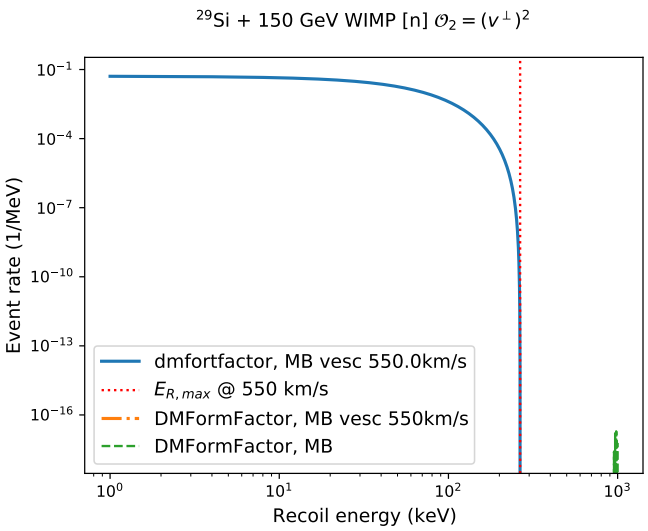
^{29}Si + 150 GeV WIMP [n] $\mathcal{O}_2 = (v^\perp)^2$
Event rate (1/MeV)
Recoil energy (keV)
dmfortfactor, MB vesc 550.0km/s
$E_{R,max}$ @ 550 km/s
DMFormFactor, MB vesc 550km/s
DMFormFactor, MB

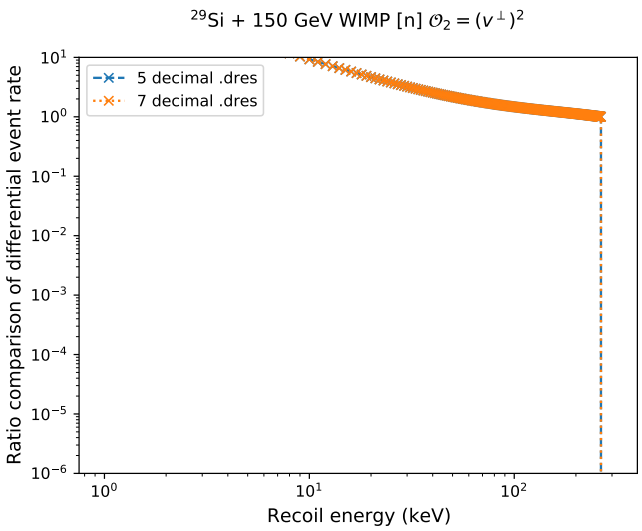
^{29}Si + 150 GeV WIMP [n] $\mathcal{O}_2 = (v^\perp)^2$
Ratio comparison of differential event rate
Recoil energy (keV)
5 decimal .dres
7 decimal .dres

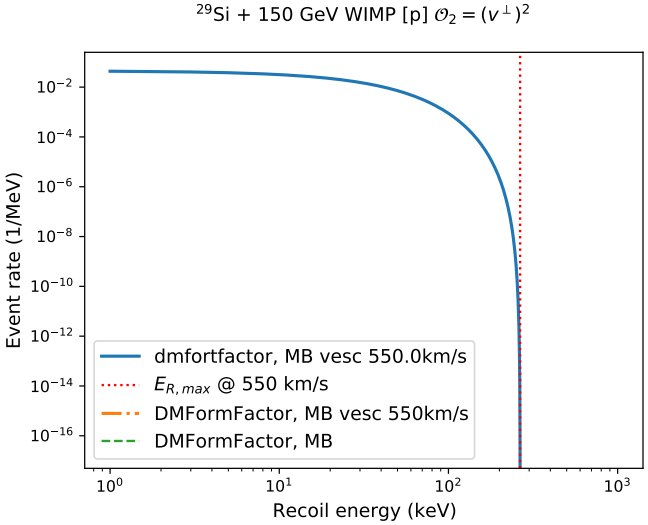
^{29}Si + 150 GeV WIMP [p] $\mathcal{O}_2 = (v^\perp)^2$
Event rate (1/MeV)
Recoil energy (keV)
dmfortfactor, MB vesc 550.0km/s
$E_{R,max}$ @ 550 km/s
DMFormFactor, MB vesc 550km/s
DMFormFactor, MB

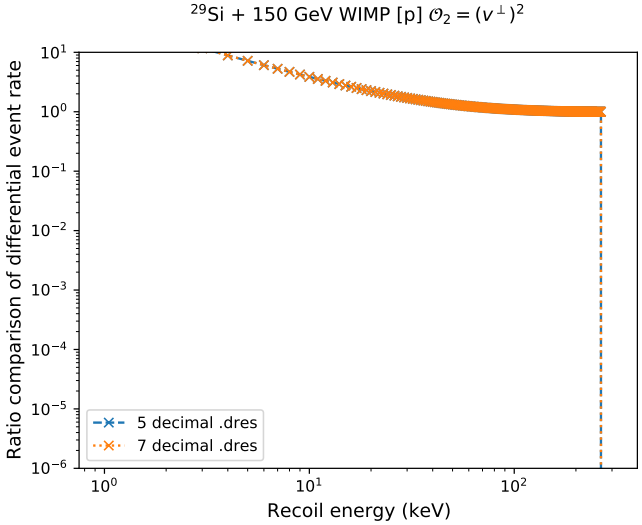
^{29}Si + 150 GeV WIMP [p] $\mathcal{O}_2 = (v^\perp)^2$
Ratio comparison of differential event rate
Recoil energy (keV)
5 decimal .dres
7 decimal .dres

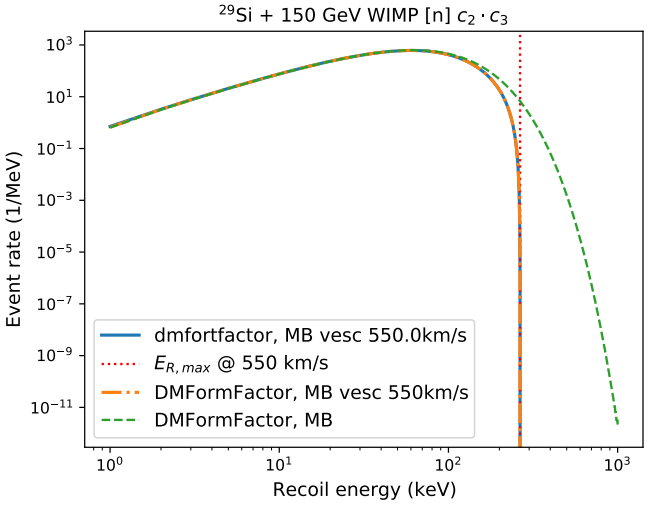
^{29}Si + 150 GeV WIMP [n] $c_2 \cdot c_3$
Event rate (1/MeV)
Recoil energy (keV)
dmfortfactor, MB vesc 550.0km/s
$E_{R,max}$ @ 550 km/s
DMFormFactor, MB vesc 550km/s
DMFormFactor, MB

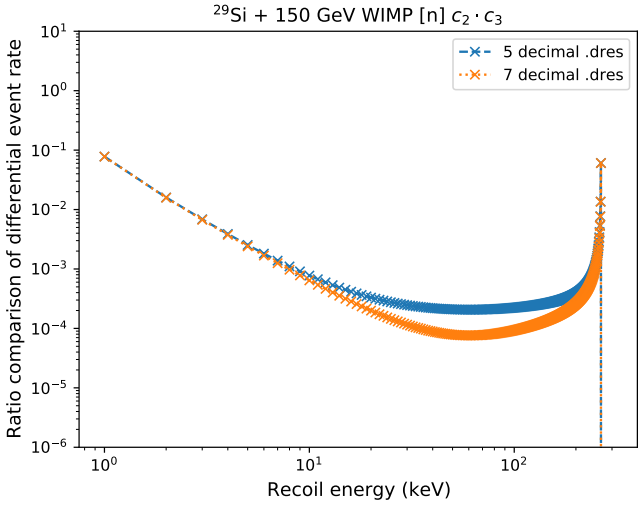
^{29}Si + 150 GeV WIMP [n] $c_2 \cdot c_3$
Ratio comparison of differential event rate
Recoil energy (keV)
5 decimal .dres
7 decimal .dres

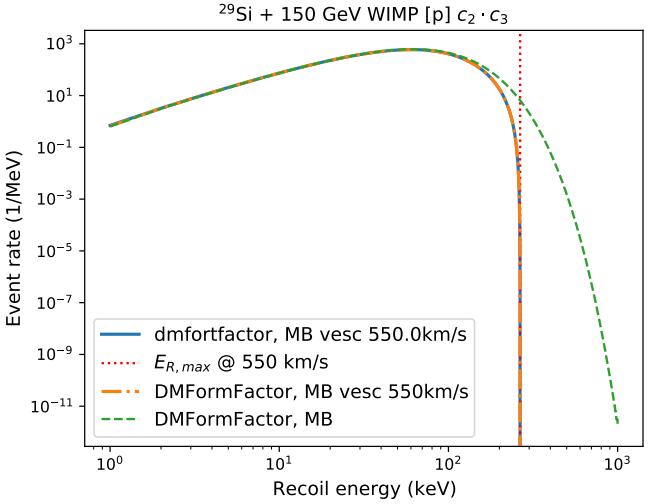
^{29}Si + 150 GeV WIMP [p] $c_2 \cdot c_3$
Event rate (1/MeV)
Recoil energy (keV)
dmfortfactor, MB vesc 550.0km/s
$E_{R,max}$ @ 550 km/s
DMFormFactor, MB vesc 550km/s
DMFormFactor, MB

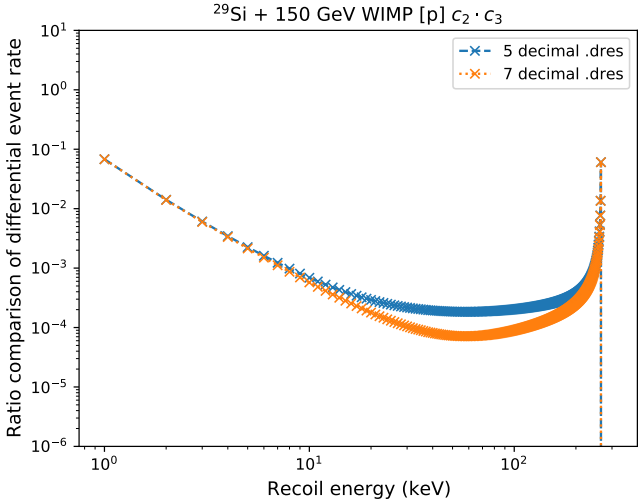
^{29}Si + 150 GeV WIMP [p] $c_2 \cdot c_3$
Ratio comparison of differential event rate
Recoil energy (keV)
5 decimal .dres
7 decimal .dres

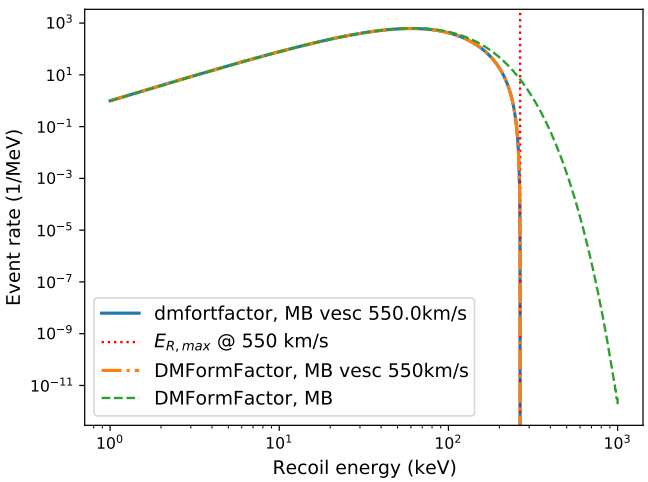
^{29}Si + 150 GeV WIMP [n] $\mathcal{O}_3 = i\vec{S}_N \cdot \left(\frac{\vec{q}}{m_N} \times \vec{v}^{\perp}\right)$
Event rate (1/MeV)
Recoil energy (keV)
dmfortfactor, MB vesc 550.0km/s
$E_{R,max}$ @ 550 km/s
DMFormFactor, MB vesc 550km/s
DMFormFactor, MB

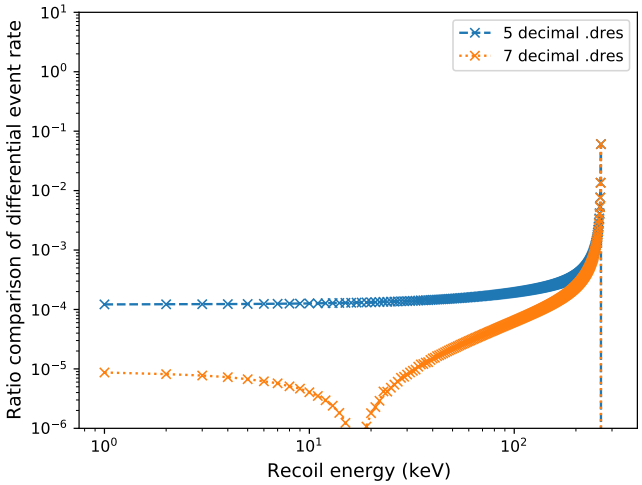
^{29}Si + 150 GeV WIMP [n] $\mathcal{O}_3 = i\vec{S}_N \cdot \left(\frac{\vec{q}}{m_N} \times \vec{v}^{\perp}\right)$
Ratio comparison of differential event rate
Recoil energy (keV)
5 decimal .dres
7 decimal .dres

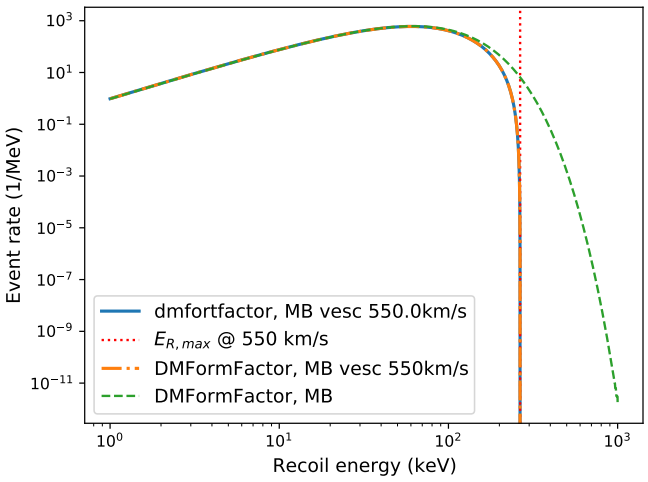
^{29}Si + 150 GeV WIMP [p] $\mathcal{O}_3 = i\vec{S}_N \cdot \left(\frac{\vec{q}}{m_N} \times \vec{v}^{\perp}\right)$
Event rate (1/MeV)
Recoil energy (keV)
dmfortfactor, MB vesc 550.0km/s
$E_{R,max}$ @ 550 km/s
DMFormFactor, MB vesc 550km/s
DMFormFactor, MB

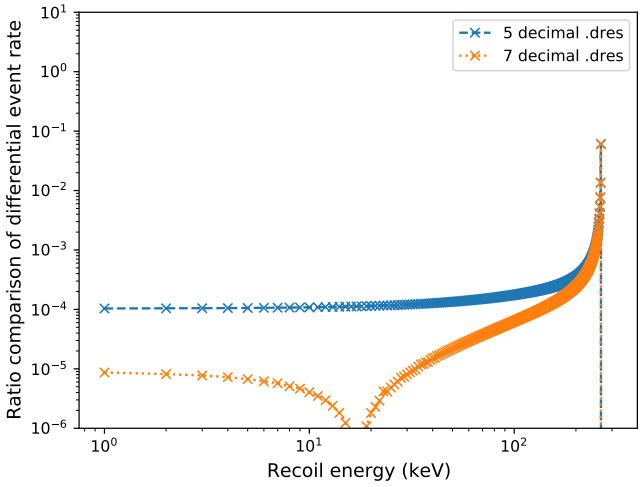
^{29}Si + 150 GeV WIMP [p] $\mathcal{O}_3 = i\vec{S}_N \cdot \left(\frac{\vec{q}}{m_N} \times \vec{v}^{\perp}\right)$
Ratio comparison of differential event rate
Recoil energy (keV)
5 decimal .dres
7 decimal .dres

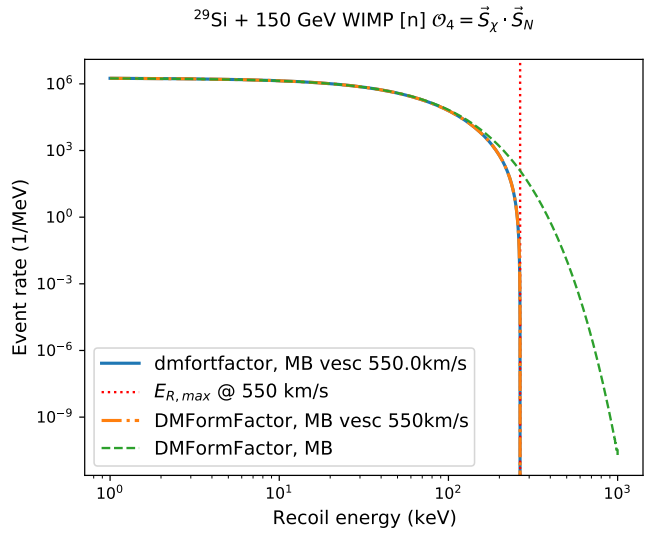
^{29}Si + 150 GeV WIMP [n] $\mathcal{O}_4 = \vec{S}_\chi \cdot \vec{S}_N$
Event rate (1/MeV)
Recoil energy (keV)
dmfortfactor, MB vesc 550.0km/s
$E_{R,max}$ @ 550 km/s
DMFormFactor, MB vesc 550km/s
DMFormFactor, MB

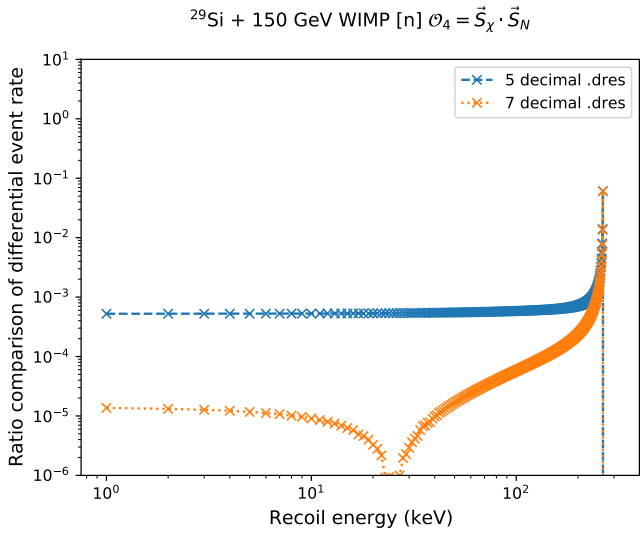
^{29}Si + 150 GeV WIMP [n] $\mathcal{O}_4 = \vec{S}_\chi \cdot \vec{S}_N$
Ratio comparison of differential event rate
Recoil energy (keV)
5 decimal .dres
7 decimal .dres

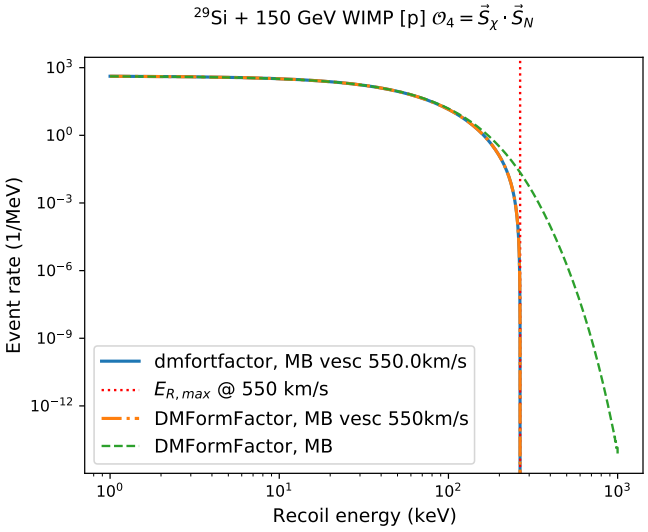
^{29}Si + 150 GeV WIMP [p] $\mathcal{O}_4 = \vec{S}_\chi \cdot \vec{S}_N$
Event rate (1/MeV)
Recoil energy (keV)
dmfortfactor, MB vesc 550.0km/s
$E_{R,max}$ @ 550 km/s
DMFormFactor, MB vesc 550km/s
DMFormFactor, MB

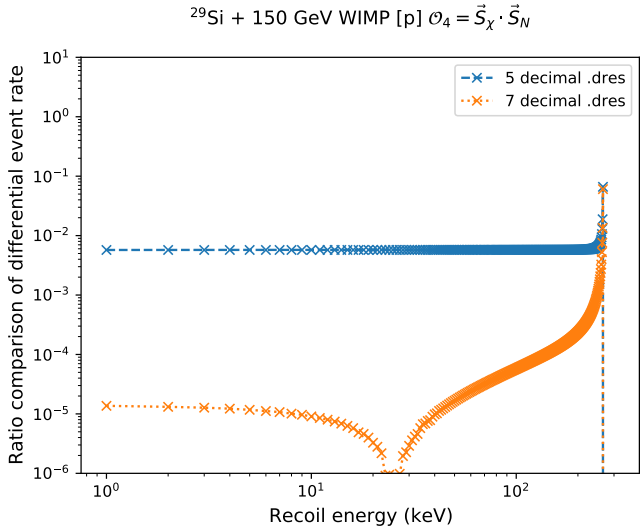
^{29}Si + 150 GeV WIMP [p] $\mathcal{O}_4 = \vec{S}_\chi \cdot \vec{S}_N$
Ratio comparison of differential event rate
Recoil energy (keV)
5 decimal .dres
7 decimal .dres

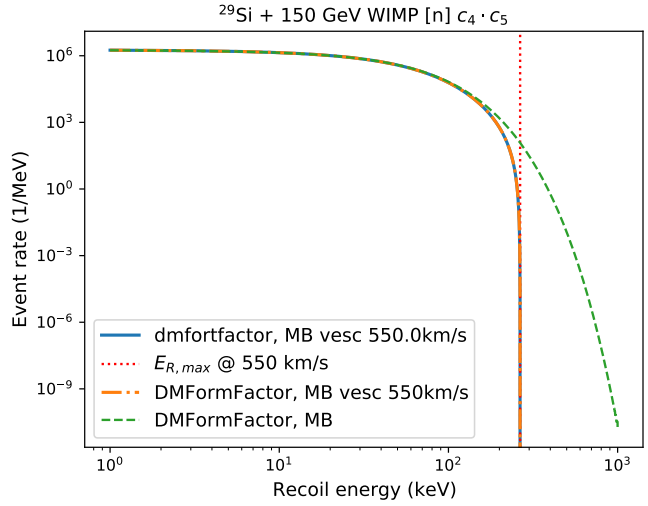
^{29}Si + 150 GeV WIMP [n] $c_4 \cdot c_5$
Event rate (1/MeV)
Recoil energy (keV)
dmfortfactor, MB vesc 550.0km/s
$E_{R,max}$ @ 550 km/s
DMFormFactor, MB vesc 550km/s
DMFormFactor, MB

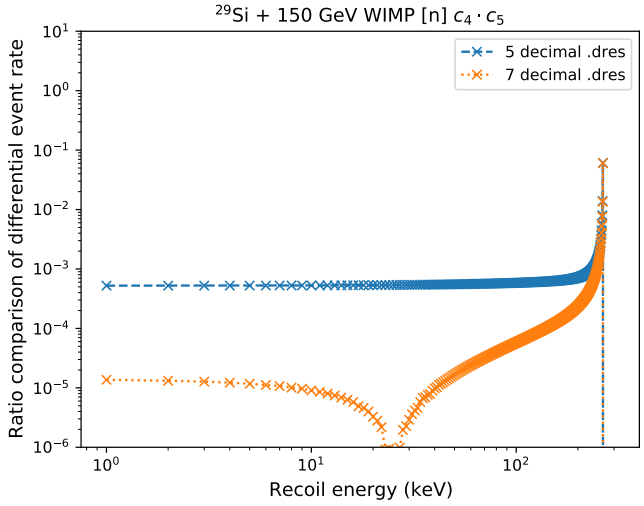
^{29}Si + 150 GeV WIMP [n] $c_4 \cdot c_5$
Ratio comparison of differential event rate
Recoil energy (keV)
5 decimal .dres
7 decimal .dres

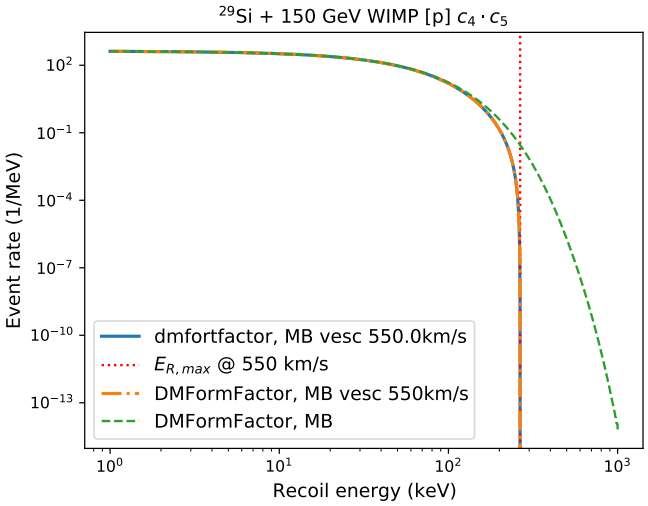
^{29}Si + 150 GeV WIMP [p] $c_4 \cdot c_5$
Event rate (1/MeV)
Recoil energy (keV)
dmfortfactor, MB vesc 550.0km/s
$E_{R,max}$ @ 550 km/s
DMFormFactor, MB vesc 550km/s
DMFormFactor, MB

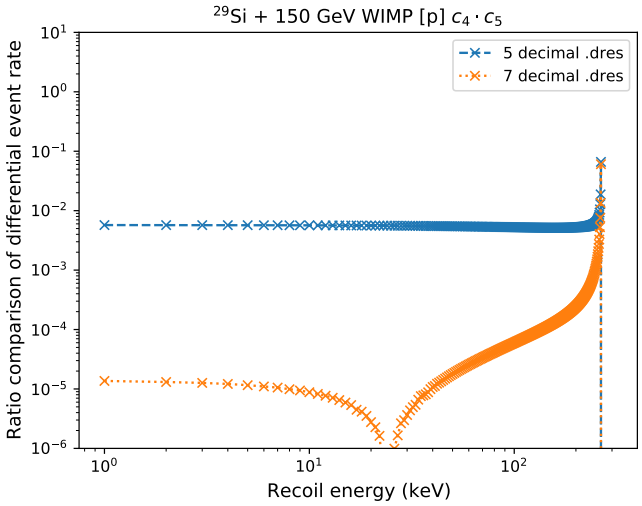
^{29}Si + 150 GeV WIMP [p] $c_4 \cdot c_5$
Ratio comparison of differential event rate
Recoil energy (keV)
5 decimal .dres
7 decimal .dres

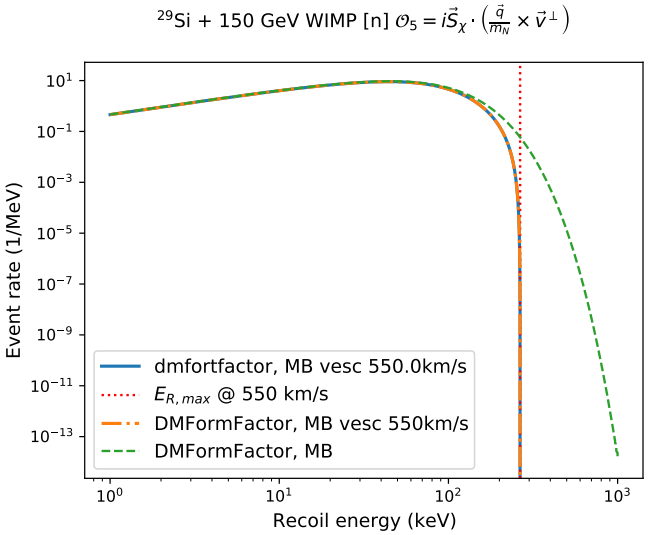
^{29}Si + 150 GeV WIMP [n] $\mathcal{O}_5 = i\vec{S}_\chi \cdot \left(\frac{\vec{q}}{m_N} \times \vec{v}^{\perp}\right)$
Event rate (1/MeV)
Recoil energy (keV)
dmfortfactor, MB vesc 550.0km/s
$E_{R,max}$ @ 550 km/s
DMFormFactor, MB vesc 550km/s
DMFormFactor, MB

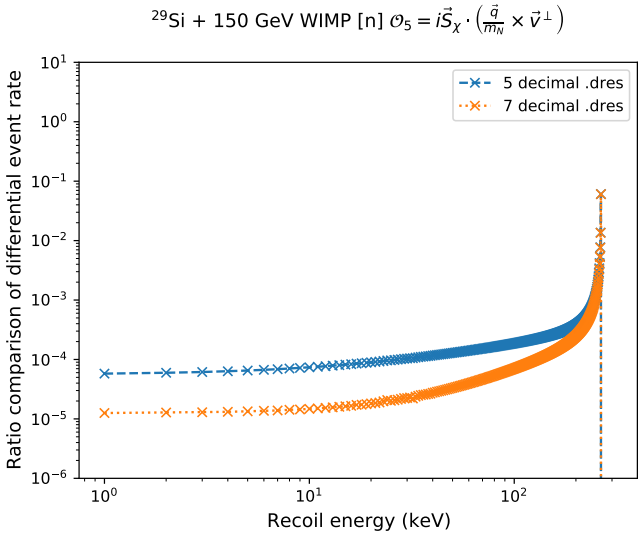
^{29}Si + 150 GeV WIMP [n] $\mathcal{O}_5 = i\vec{S}_\chi \cdot \left(\frac{\vec{q}}{m_N} \times \vec{v}^{\perp}\right)$
Ratio comparison of differential event rate
Recoil energy (keV)
5 decimal .dres
7 decimal .dres

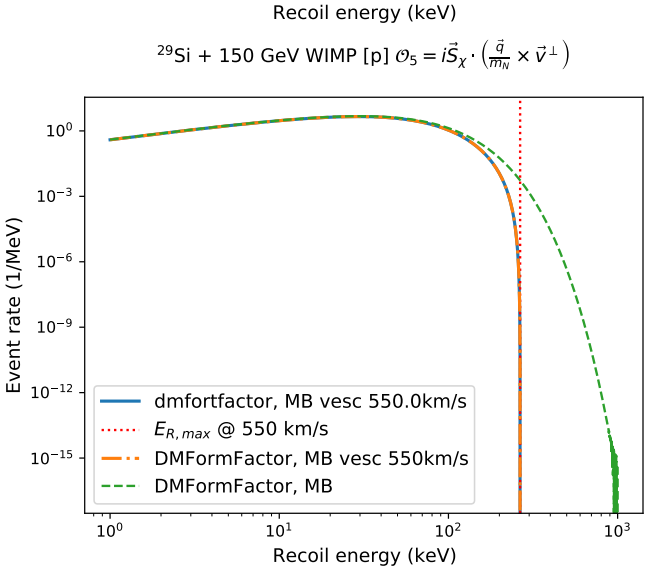
^{29}Si + 150 GeV WIMP [p] $\mathcal{O}_5 = i\vec{S}_\chi \cdot \left(\frac{\vec{q}}{m_N} \times \vec{v}^{\perp}\right)$
Event rate (1/MeV)
Recoil energy (keV)
dmfortfactor, MB vesc 550.0km/s
$E_{R,max}$ @ 550 km/s
DMFormFactor, MB vesc 550km/s
DMFormFactor, MB

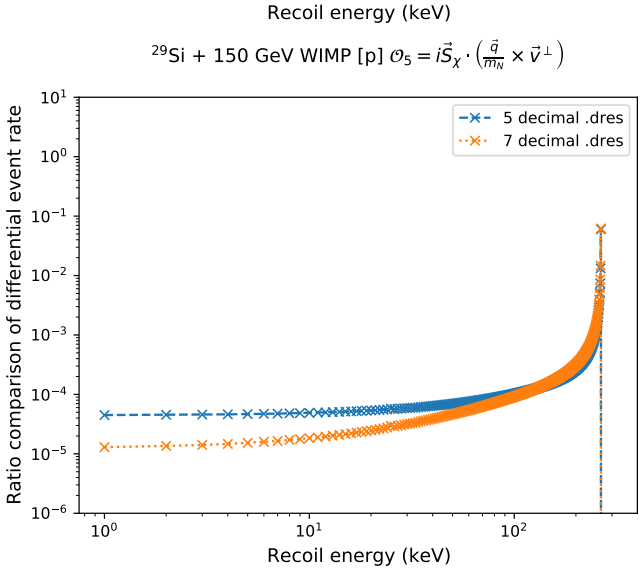
^{29}Si + 150 GeV WIMP [p] $\mathcal{O}_5 = i\vec{S}_\chi \cdot \left(\frac{\vec{q}}{m_N} \times \vec{v}^{\perp}\right)$
Ratio comparison of differential event rate
Recoil energy (keV)
5 decimal .dres
7 decimal .dres

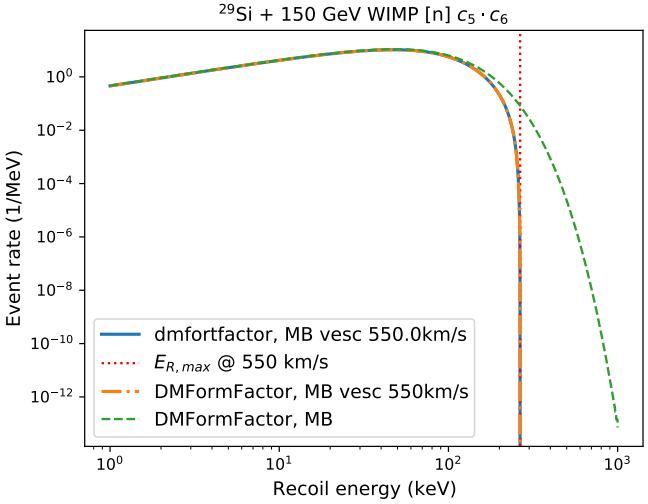
^{29}Si + 150 GeV WIMP [n] $c_5 \cdot c_6$
Event rate (1/MeV)
Recoil energy (keV)
dmfortfactor, MB vesc 550.0km/s
$E_{R,max}$ @ 550 km/s
DMFormFactor, MB vesc 550km/s
DMFormFactor, MB

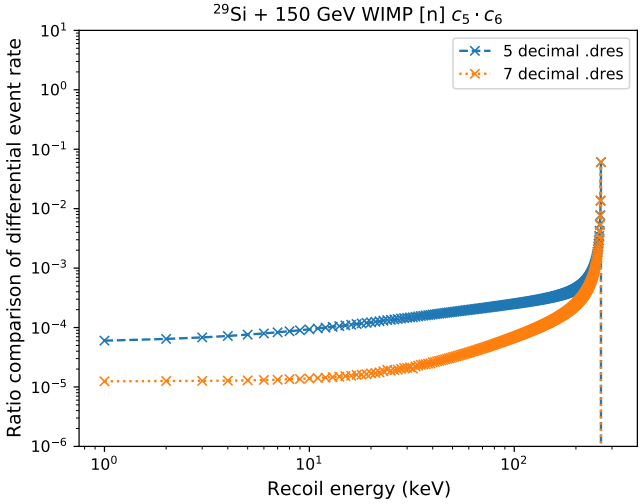
^{29}Si + 150 GeV WIMP [n] $c_5 \cdot c_6$
Ratio comparison of differential event rate
Recoil energy (keV)
5 decimal .dres
7 decimal .dres

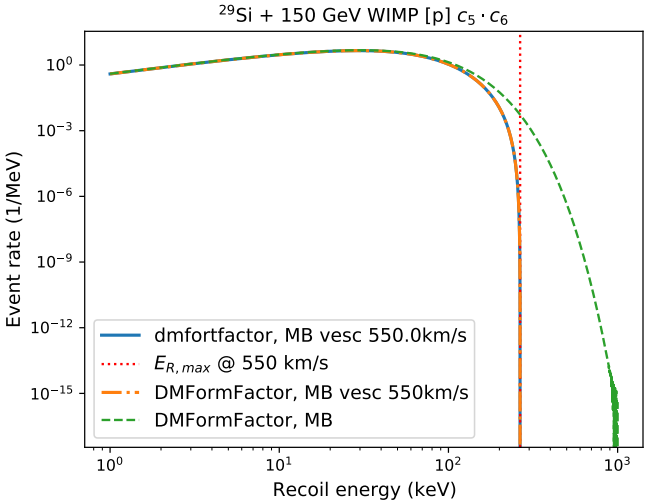
^{29}Si + 150 GeV WIMP [p] $c_5 \cdot c_6$
Event rate (1/MeV)
Recoil energy (keV)
dmfortfactor, MB vesc 550.0km/s
$E_{R,max}$ @ 550 km/s
DMFormFactor, MB vesc 550km/s
DMFormFactor, MB

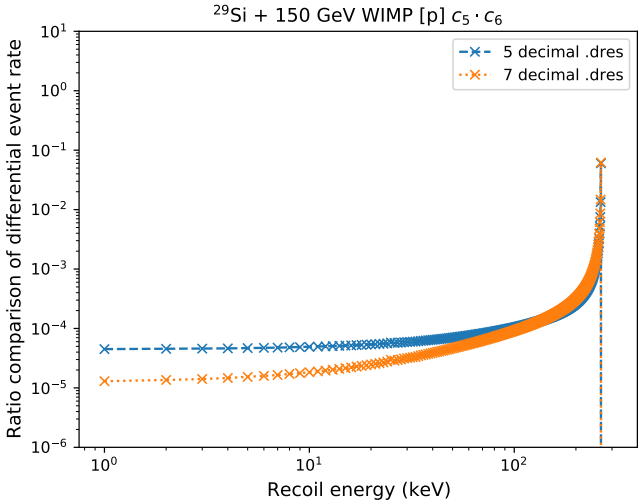
^{29}Si + 150 GeV WIMP [p] $c_5 \cdot c_6$
Ratio comparison of differential event rate
Recoil energy (keV)
5 decimal .dres
7 decimal .dres

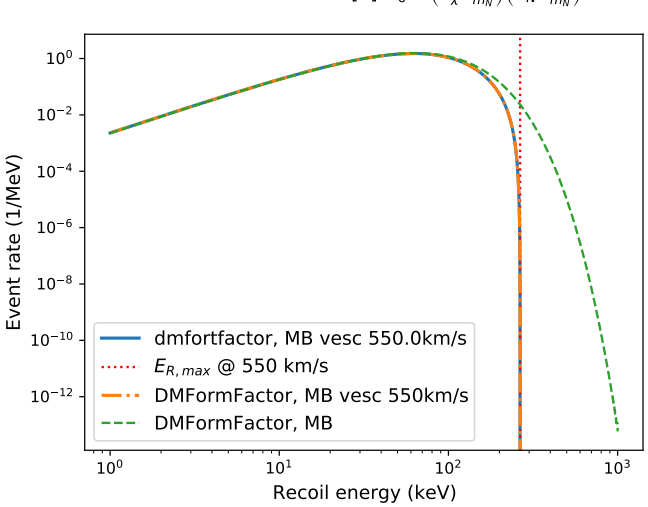
^{29}Si + 150 GeV WIMP [n] $\mathcal{O}_6 = \left(\vec{S}_\chi \cdot \frac{\vec{q}}{m_N}\right)\left(\vec{S}_N \cdot \frac{\vec{q}}{m_N}\right)$
Event rate (1/MeV)
Recoil energy (keV)
dmfortfactor, MB vesc 550.0km/s
$E_{R,max}$ @ 550 km/s
DMFormFactor, MB vesc 550km/s
DMFormFactor, MB

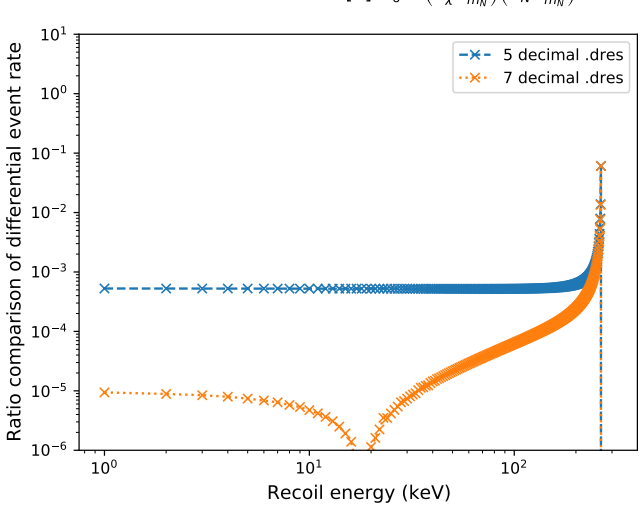
^{29}Si + 150 GeV WIMP [n] $\mathcal{O}_6 = \left(\vec{S}_\chi \cdot \frac{\vec{q}}{m_N}\right)\left(\vec{S}_N \cdot \frac{\vec{q}}{m_N}\right)$
Ratio comparison of differential event rate
Recoil energy (keV)
5 decimal .dres
7 decimal .dres

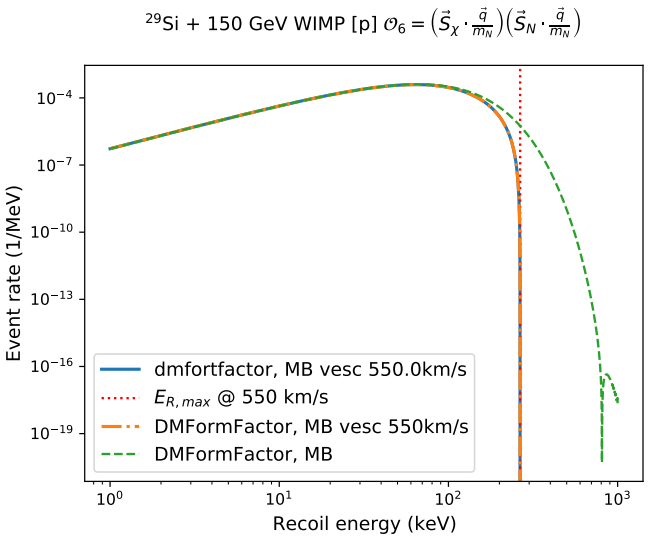
^{29}Si + 150 GeV WIMP [p] $\mathcal{O}_6 = \left(\vec{S}_\chi \cdot \frac{\vec{q}}{m_N}\right)\left(\vec{S}_N \cdot \frac{\vec{q}}{m_N}\right)$
Event rate (1/MeV)
Recoil energy (keV)
dmfortfactor, MB vesc 550.0km/s
$E_{R,max}$ @ 550 km/s
DMFormFactor, MB vesc 550km/s
DMFormFactor, MB

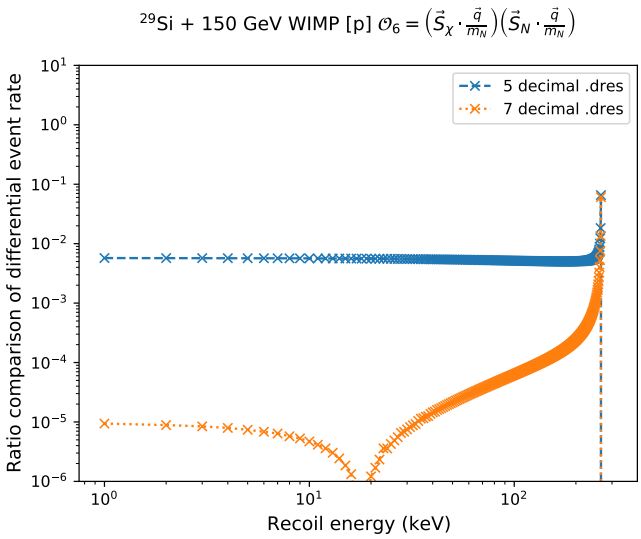
^{29}Si + 150 GeV WIMP [p] $\mathcal{O}_6 = \left(\vec{S}_\chi \cdot \frac{\vec{q}}{m_N}\right)\left(\vec{S}_N \cdot \frac{\vec{q}}{m_N}\right)$
Ratio comparison of differential event rate
Recoil energy (keV)
5 decimal .dres
7 decimal .dres

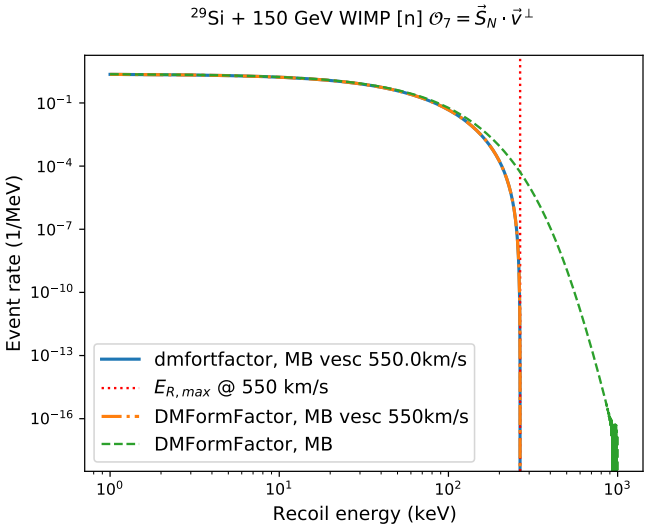
^{29}Si + 150 GeV WIMP [n] $\mathcal{O}_7 = \vec{S}_N \cdot \vec{v}^\perp$
Event rate (1/MeV)
Recoil energy (keV)
dmfortfactor, MB vesc 550.0km/s
$E_{R,max}$ @ 550 km/s
DMFormFactor, MB vesc 550km/s
DMFormFactor, MB

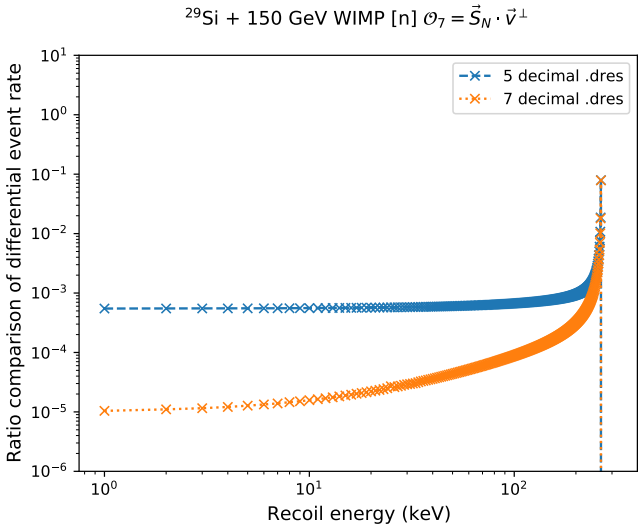
^{29}Si + 150 GeV WIMP [n] $\mathcal{O}_7 = \vec{S}_N \cdot \vec{v}^\perp$
Ratio comparison of differential event rate
Recoil energy (keV)
5 decimal .dres
7 decimal .dres

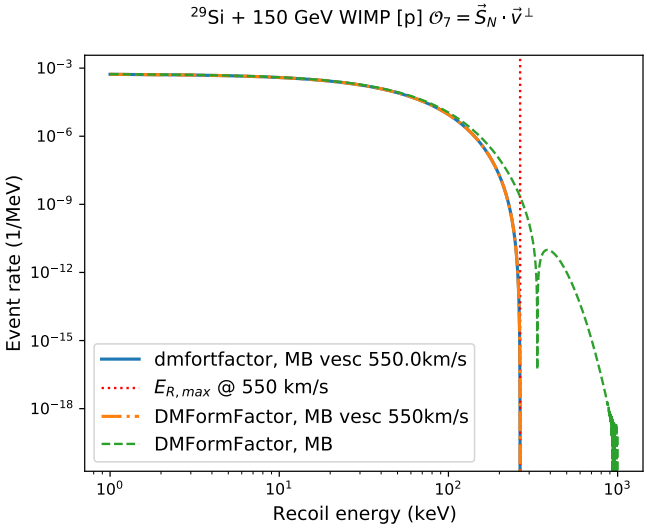
^{29}Si + 150 GeV WIMP [p] $\mathcal{O}_7 = \vec{S}_N \cdot \vec{v}^\perp$
Event rate (1/MeV)
Recoil energy (keV)
dmfortfactor, MB vesc 550.0km/s
$E_{R,max}$ @ 550 km/s
DMFormFactor, MB vesc 550km/s
DMFormFactor, MB

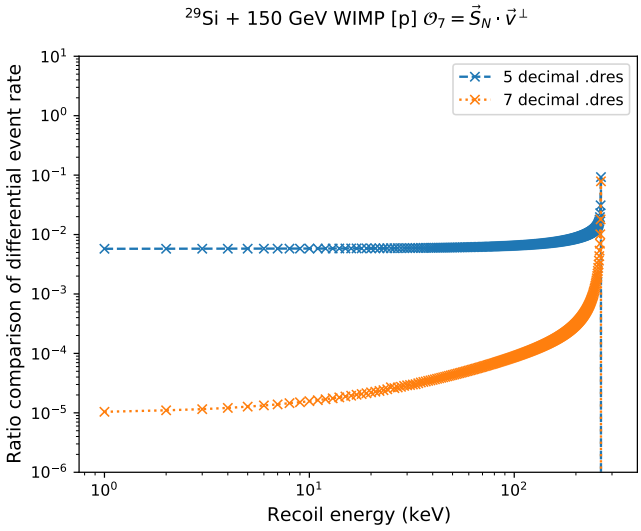
^{29}Si + 150 GeV WIMP [p] $\mathcal{O}_7 = \vec{S}_N \cdot \vec{v}^\perp$
Ratio comparison of differential event rate
Recoil energy (keV)
5 decimal .dres
7 decimal .dres

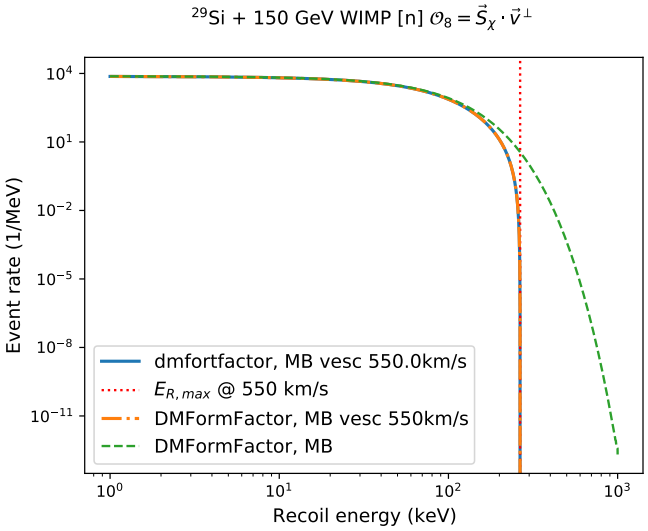
^{29}Si + 150 GeV WIMP [n] $\mathcal{O}_8 = \vec{S}_\chi \cdot \vec{v}^\perp$
Event rate (1/MeV)
Recoil energy (keV)
dmfortfactor, MB vesc 550.0km/s
$E_{R,max}$ @ 550 km/s
DMFormFactor, MB vesc 550km/s
DMFormFactor, MB

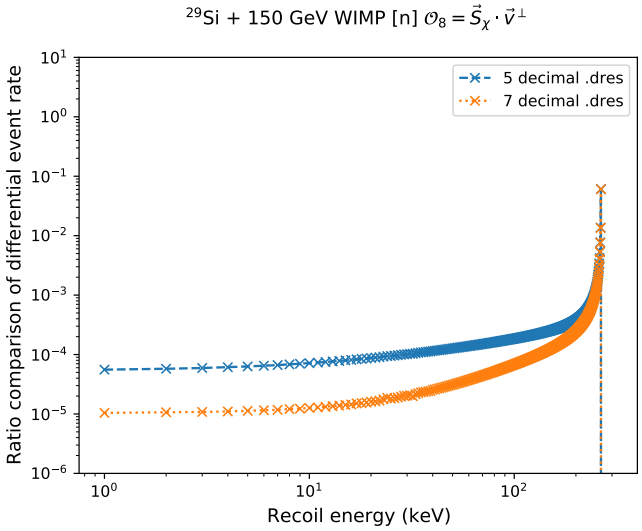
^{29}Si + 150 GeV WIMP [n] $\mathcal{O}_8 = \vec{S}_\chi \cdot \vec{v}^\perp$
Ratio comparison of differential event rate
Recoil energy (keV)
5 decimal .dres
7 decimal .dres

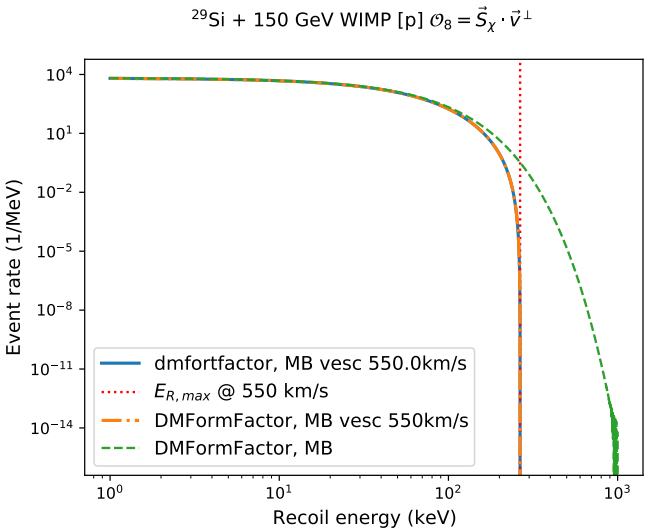
^{29}Si + 150 GeV WIMP [p] $\mathcal{O}_8 = \vec{S}_\chi \cdot \vec{v}^\perp$
Event rate (1/MeV)
Recoil energy (keV)
dmfortfactor, MB vesc 550.0km/s
$E_{R,max}$ @ 550 km/s
DMFormFactor, MB vesc 550km/s
DMFormFactor, MB

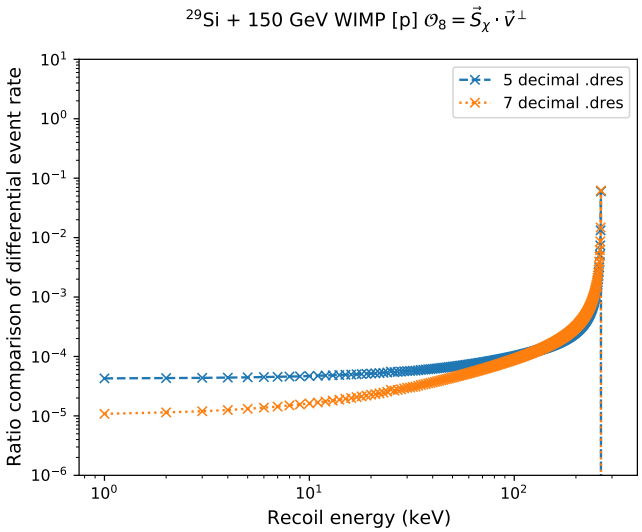
^{29}Si + 150 GeV WIMP [p] $\mathcal{O}_8 = \vec{S}_\chi \cdot \vec{v}^\perp$
Ratio comparison of differential event rate
Recoil energy (keV)
5 decimal .dres
7 decimal .dres

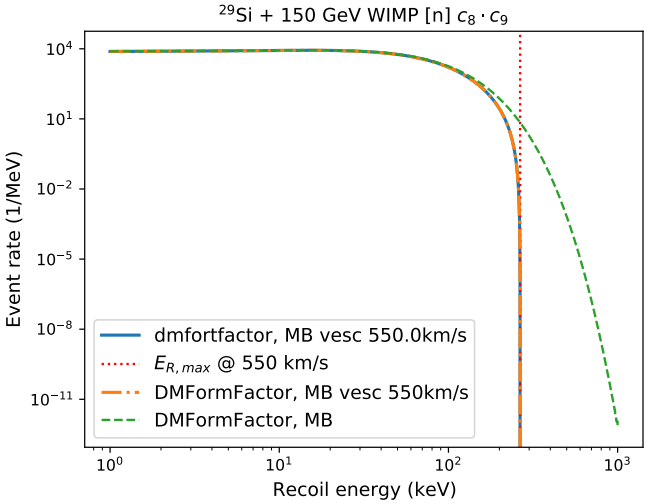
^{29}Si + 150 GeV WIMP [n] $c_8 \cdot c_9$
Event rate (1/MeV)
Recoil energy (keV)
dmfortfactor, MB vesc 550.0km/s
$E_{R,max}$ @ 550 km/s
DMFormFactor, MB vesc 550km/s
DMFormFactor, MB

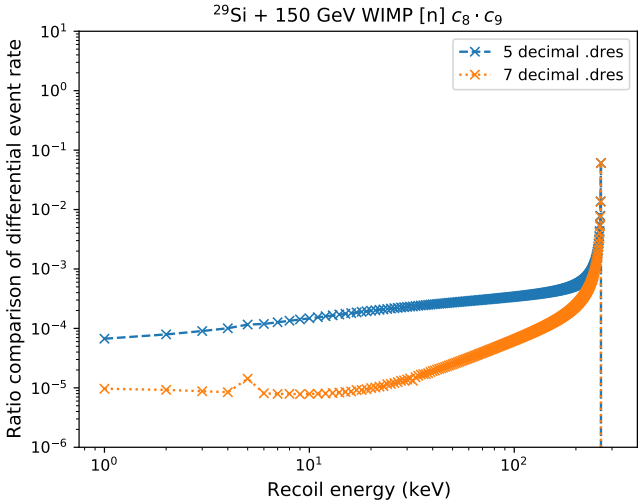
^{29}Si + 150 GeV WIMP [n] $c_8 \cdot c_9$
Ratio comparison of differential event rate
Recoil energy (keV)
5 decimal .dres
7 decimal .dres

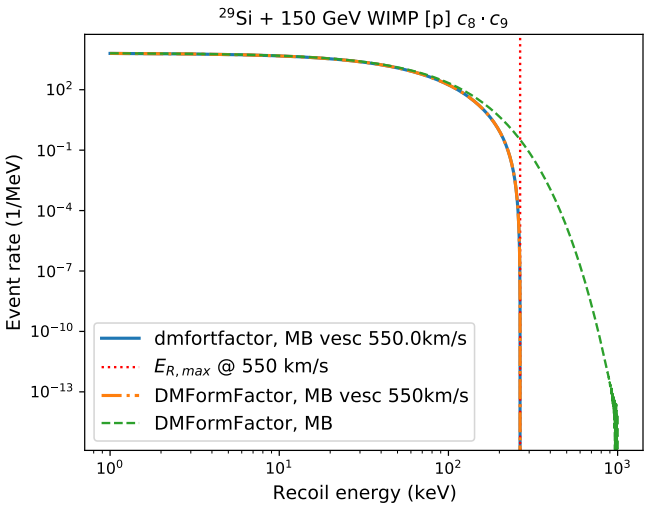
^{29}Si + 150 GeV WIMP [p] $c_8 \cdot c_9$
Event rate (1/MeV)
Recoil energy (keV)
dmfortfactor, MB vesc 550.0km/s
$E_{R,max}$ @ 550 km/s
DMFormFactor, MB vesc 550km/s
DMFormFactor, MB

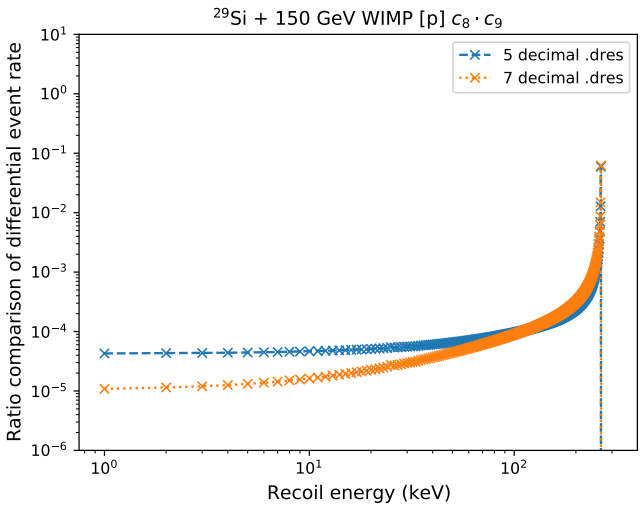
^{29}Si + 150 GeV WIMP [p] $c_8 \cdot c_9$
Ratio comparison of differential event rate
Recoil energy (keV)
5 decimal .dres
7 decimal .dres

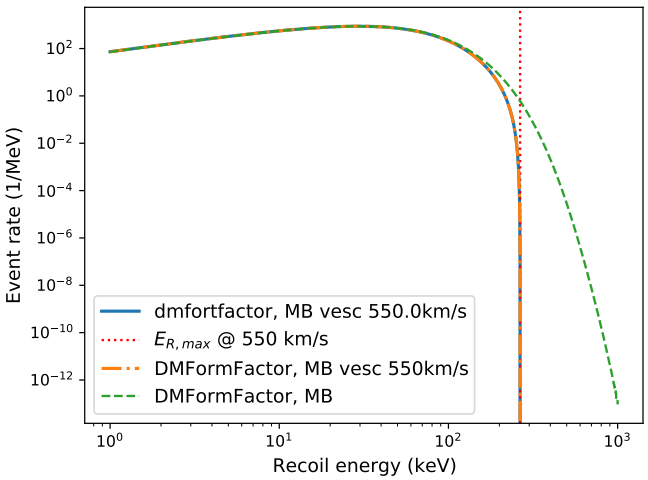
^{29}Si + 150 GeV WIMP [n] $\mathcal{O}_9 = i\vec{S}_\chi \cdot \left(\vec{S}_N \times \frac{\vec{q}}{m_N}\right)$
Event rate (1/MeV)
Recoil energy (keV)
dmfortfactor, MB vesc 550.0km/s
$E_{R,max}$ @ 550 km/s
DMFormFactor, MB vesc 550km/s
DMFormFactor, MB

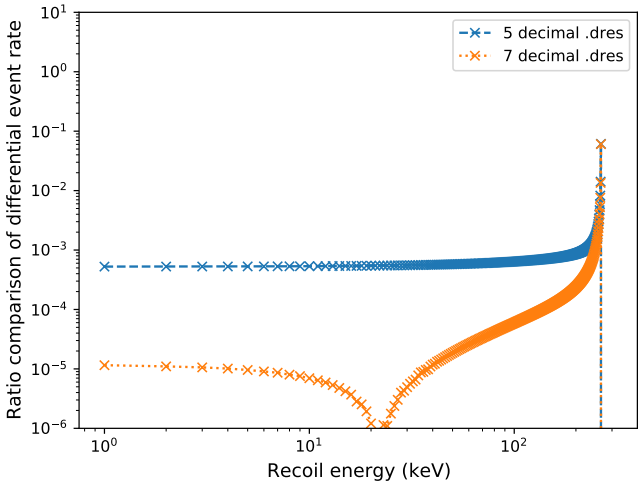
^{29}Si + 150 GeV WIMP [n] $\mathcal{O}_9 = i\vec{S}_\chi \cdot \left(\vec{S}_N \times \frac{\vec{q}}{m_N}\right)$
Ratio comparison of differential event rate
Recoil energy (keV)
5 decimal .dres
7 decimal .dres

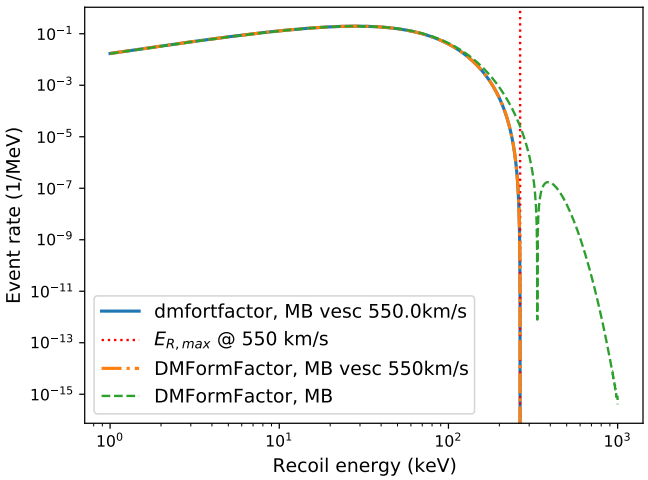
^{29}Si + 150 GeV WIMP [p] $\mathcal{O}_9 = i\vec{S}_\chi \cdot \left(\vec{S}_N \times \frac{\vec{q}}{m_N}\right)$
Event rate (1/MeV)
Recoil energy (keV)
dmfortfactor, MB vesc 550.0km/s
$E_{R,max}$ @ 550 km/s
DMFormFactor, MB vesc 550km/s
DMFormFactor, MB

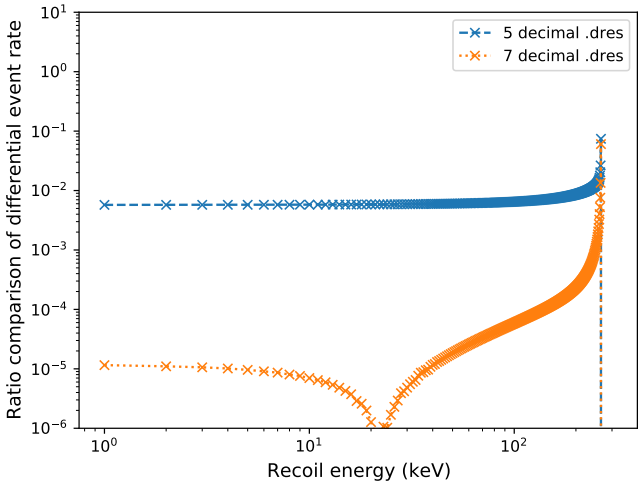
^{29}Si + 150 GeV WIMP [p] $\mathcal{O}_9 = i\vec{S}_\chi \cdot \left(\vec{S}_N \times \frac{\vec{q}}{m_N}\right)$
Ratio comparison of differential event rate
Recoil energy (keV)
5 decimal .dres
7 decimal .dres

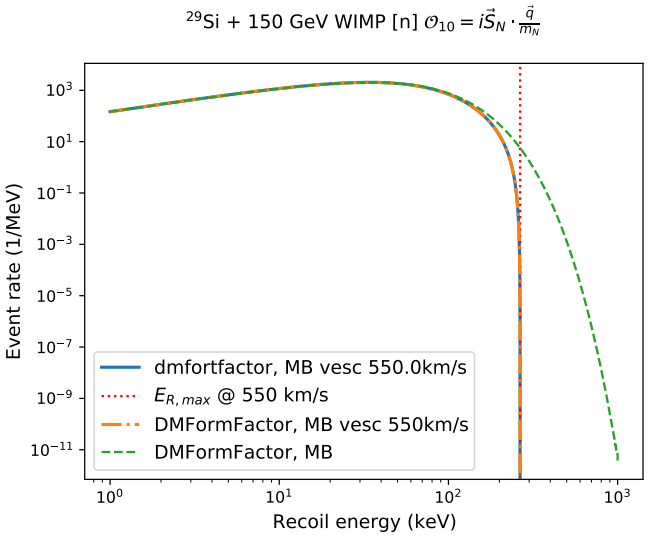
^{29}Si + 150 GeV WIMP [n] $\mathcal{O}_{10} = i\vec{S}_N \cdot \frac{\vec{q}}{m_N}$
Event rate (1/MeV)
Recoil energy (keV)
dmfortfactor, MB vesc 550.0km/s
$E_{R,max}$ @ 550 km/s
DMFormFactor, MB vesc 550km/s
DMFormFactor, MB

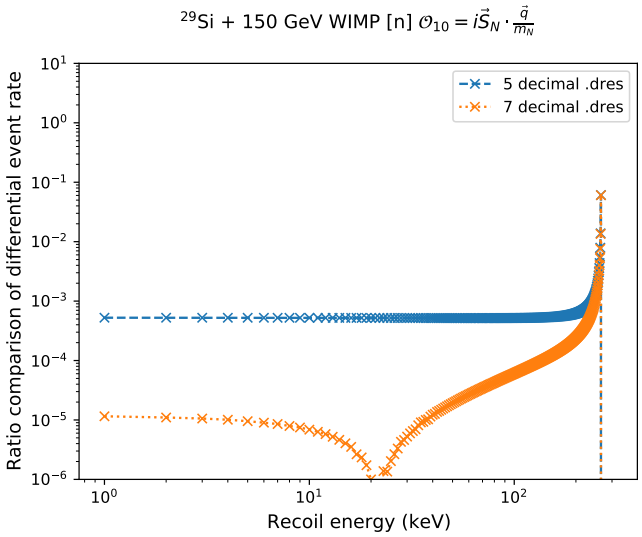
^{29}Si + 150 GeV WIMP [n] $\mathcal{O}_{10} = i\vec{S}_N \cdot \frac{\vec{q}}{m_N}$
Ratio comparison of differential event rate
Recoil energy (keV)
5 decimal .dres
7 decimal .dres

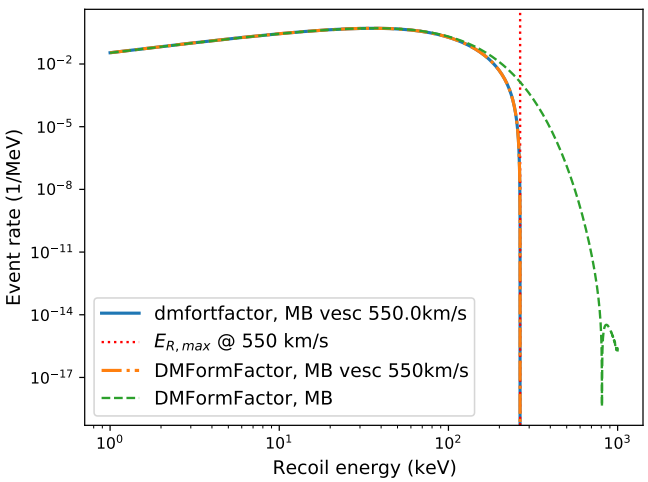
^{29}Si + 150 GeV WIMP [p] $\mathcal{O}_{10} = i\vec{S}_N \cdot \frac{\vec{q}}{m_N}$
Event rate (1/MeV)
Recoil energy (keV)
dmfortfactor, MB vesc 550.0km/s
$E_{R,max}$ @ 550 km/s
DMFormFactor, MB vesc 550km/s
DMFormFactor, MB

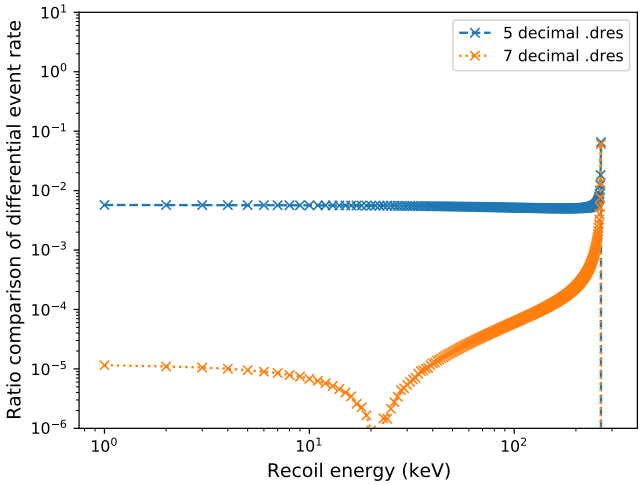
^{29}Si + 150 GeV WIMP [p] $\mathcal{O}_{10} = i\vec{S}_N \cdot \frac{\vec{q}}{m_N}$
Ratio comparison of differential event rate
Recoil energy (keV)
5 decimal .dres
7 decimal .dres

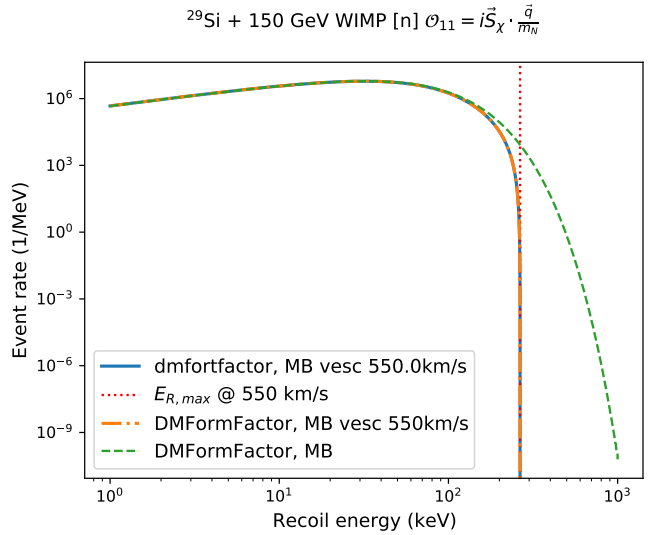
^{29}Si + 150 GeV WIMP [n] $\mathcal{O}_{11} = i\vec{S}_\chi \cdot \frac{\vec{q}}{m_N}$
Event rate (1/MeV)
Recoil energy (keV)
dmfortfactor, MB vesc 550.0km/s
$E_{R,max}$ @ 550 km/s
DMFormFactor, MB vesc 550km/s
DMFormFactor, MB

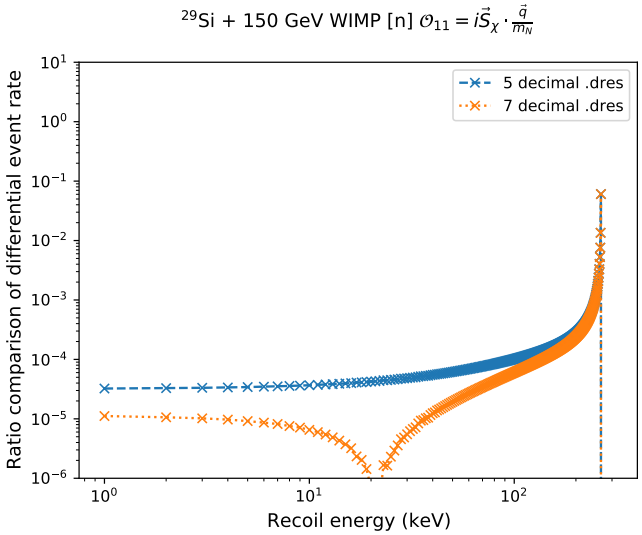
^{29}Si + 150 GeV WIMP [n] $\mathcal{O}_{11} = i\vec{S}_\chi \cdot \frac{\vec{q}}{m_N}$
Ratio comparison of differential event rate
Recoil energy (keV)
5 decimal .dres
7 decimal .dres

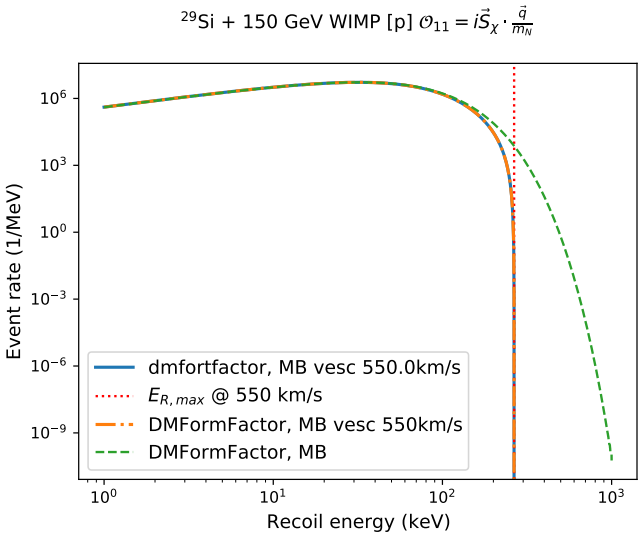
^{29}Si + 150 GeV WIMP [p] $\mathcal{O}_{11} = i\vec{S}_\chi \cdot \frac{\vec{q}}{m_N}$
Event rate (1/MeV)
Recoil energy (keV)
dmfortfactor, MB vesc 550.0km/s
$E_{R,max}$ @ 550 km/s
DMFormFactor, MB vesc 550km/s
DMFormFactor, MB

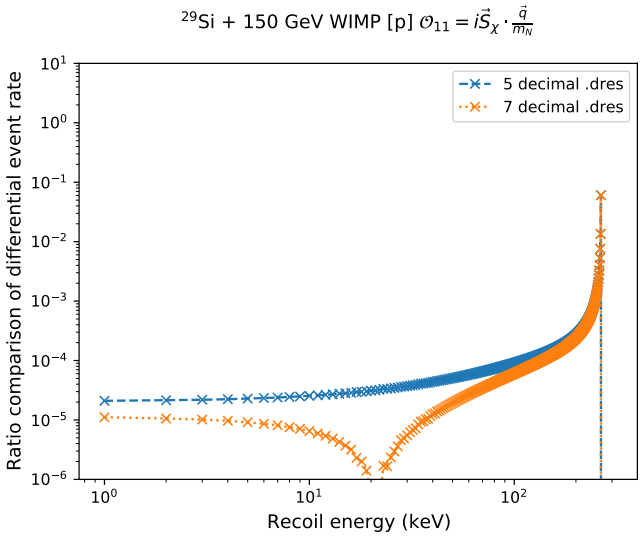
^{29}Si + 150 GeV WIMP [p] $\mathcal{O}_{11} = i\vec{S}_\chi \cdot \frac{\vec{q}}{m_N}$
Ratio comparison of differential event rate
Recoil energy (keV)
5 decimal .dres
7 decimal .dres

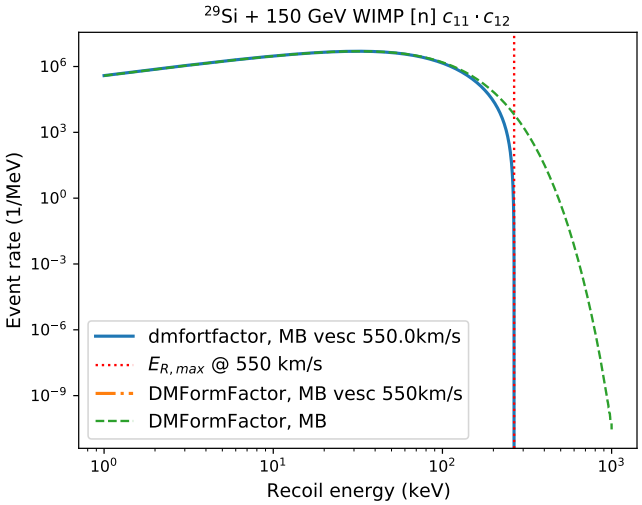
^{29}Si + 150 GeV WIMP [n] $c_{11} \cdot c_{12}$
Event rate (1/MeV)
Recoil energy (keV)
dmfortfactor, MB vesc 550.0km/s
$E_{R,max}$ @ 550 km/s
DMFormFactor, MB vesc 550km/s
DMFormFactor, MB

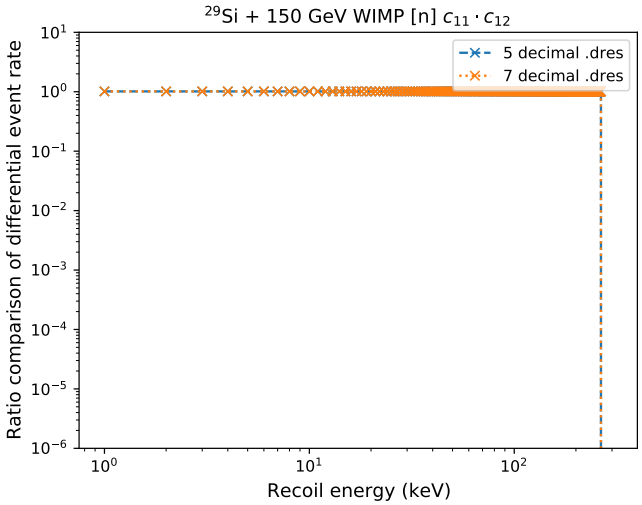
^{29}Si + 150 GeV WIMP [n] $c_{11} \cdot c_{12}$
Ratio comparison of differential event rate
Recoil energy (keV)
5 decimal .dres
7 decimal .dres

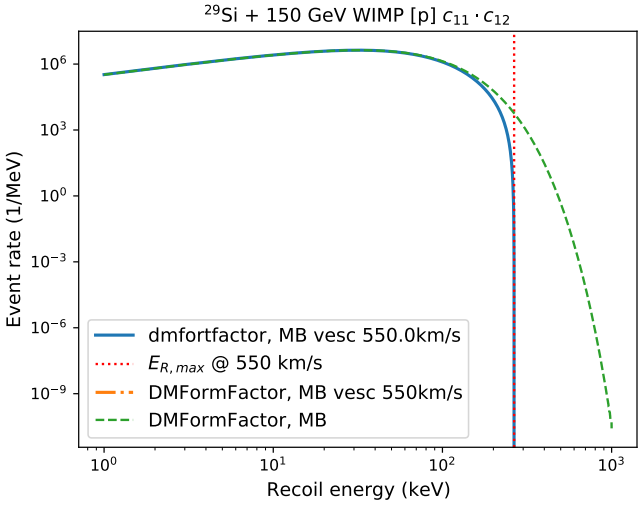
^{29}Si + 150 GeV WIMP [p] $c_{11} \cdot c_{12}$
Event rate (1/MeV)
Recoil energy (keV)
dmfortfactor, MB vesc 550.0km/s
$E_{R,max}$ @ 550 km/s
DMFormFactor, MB vesc 550km/s
DMFormFactor, MB

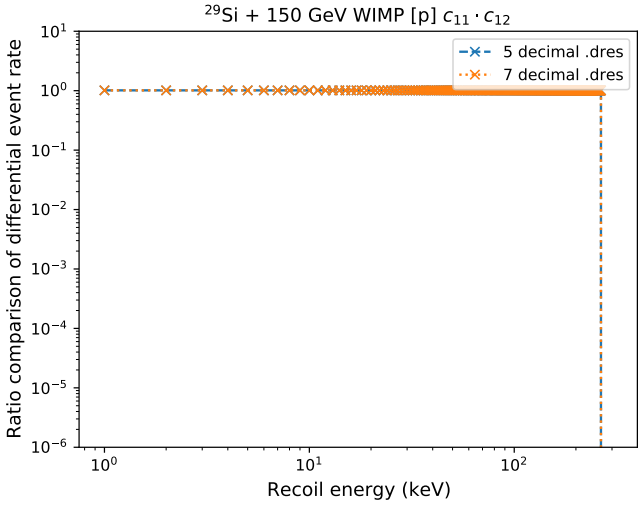
^{29}Si + 150 GeV WIMP [p] $c_{11} \cdot c_{12}$
Ratio comparison of differential event rate
Recoil energy (keV)
5 decimal .dres
7 decimal .dres

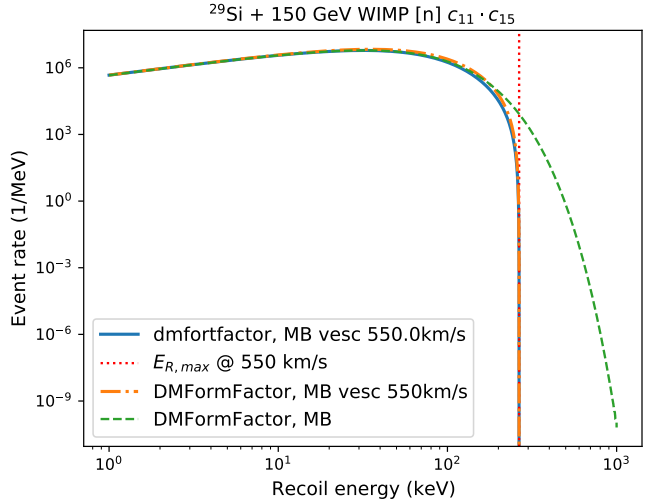
^{29}Si + 150 GeV WIMP [n] $c_{11} \cdot c_{15}$
Event rate (1/MeV)
Recoil energy (keV)
dmfortfactor, MB vesc 550.0km/s
$E_{R,max}$ @ 550 km/s
DMFormFactor, MB vesc 550km/s
DMFormFactor, MB

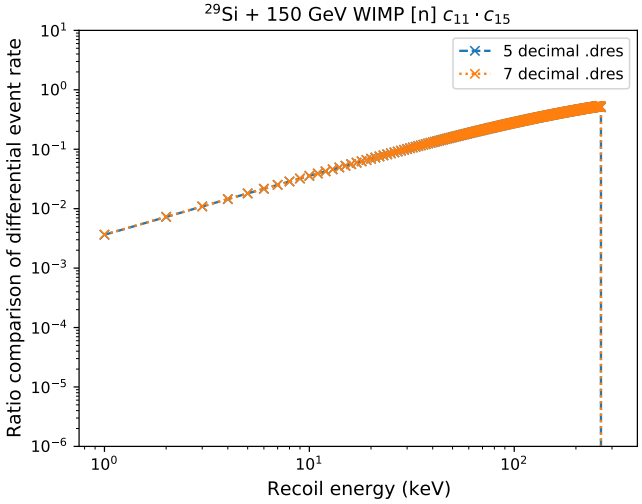
^{29}Si + 150 GeV WIMP [n] $c_{11} \cdot c_{15}$
Ratio comparison of differential event rate
Recoil energy (keV)
5 decimal .dres
7 decimal .dres

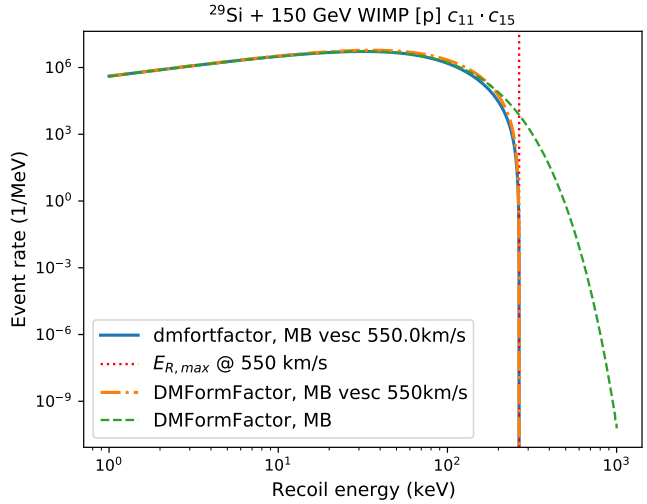
^{29}Si + 150 GeV WIMP [p] $c_{11} \cdot c_{15}$
Event rate (1/MeV)
Recoil energy (keV)
dmfortfactor, MB vesc 550.0km/s
$E_{R,max}$ @ 550 km/s
DMFormFactor, MB vesc 550km/s
DMFormFactor, MB

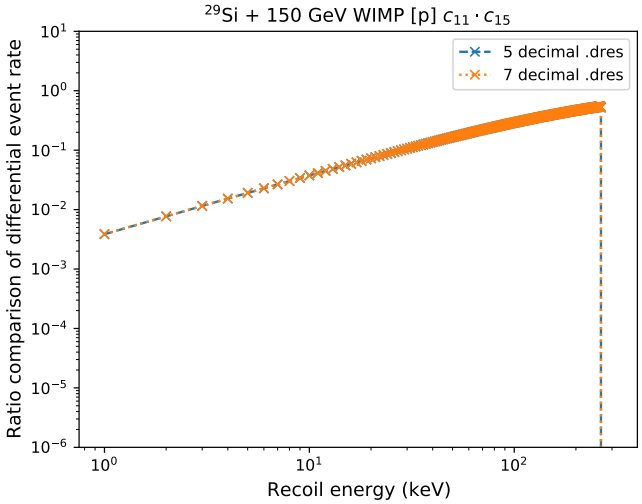
^{29}Si + 150 GeV WIMP [p] $c_{11} \cdot c_{15}$
Ratio comparison of differential event rate
Recoil energy (keV)
5 decimal .dres
7 decimal .dres

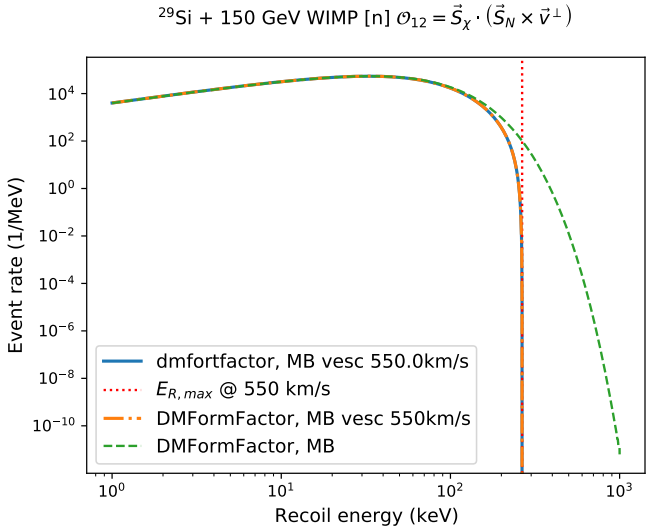
^{29}Si + 150 GeV WIMP [n] $\mathcal{O}_{12} = \vec{S}_\chi \cdot (\vec{S}_N \times \vec{v}^\perp)$
Event rate (1/MeV)
Recoil energy (keV)
dmfortfactor, MB vesc 550.0km/s
$E_{R,max}$ @ 550 km/s
DMFormFactor, MB vesc 550km/s
DMFormFactor, MB

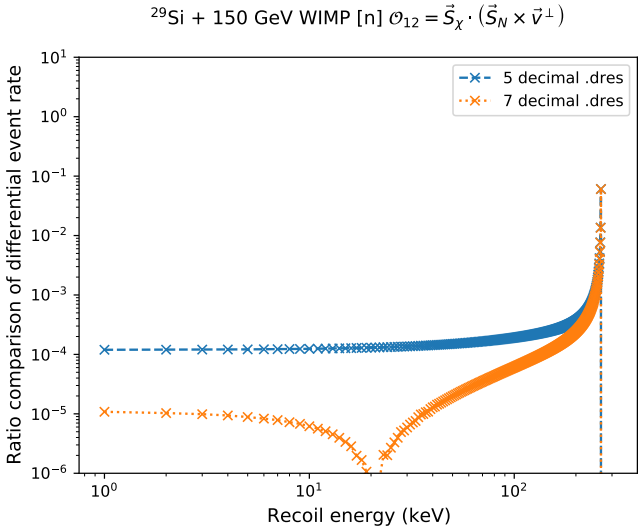
^{29}Si + 150 GeV WIMP [n] $\mathcal{O}_{12} = \vec{S}_\chi \cdot (\vec{S}_N \times \vec{v}^\perp)$
Ratio comparison of differential event rate
Recoil energy (keV)
5 decimal .dres
7 decimal .dres

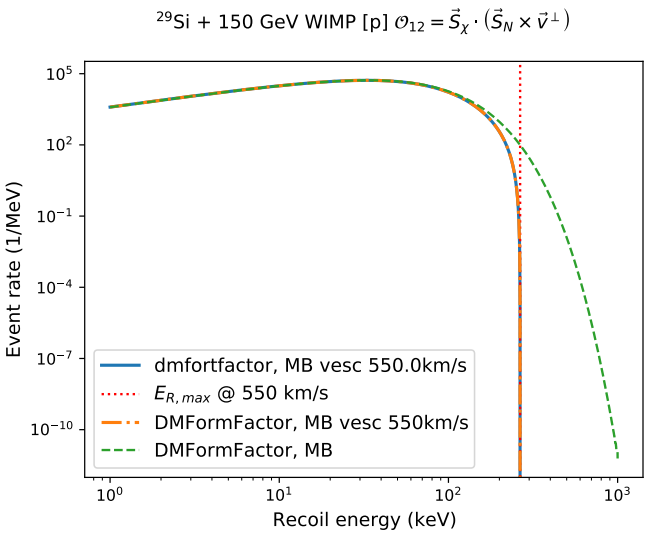
^{29}Si + 150 GeV WIMP [p] $\mathcal{O}_{12} = \vec{S}_\chi \cdot (\vec{S}_N \times \vec{v}^{\perp})$
Event rate (1/MeV)
Recoil energy (keV)
dmfortfactor, MB vesc 550.0km/s
$E_{R,max}$ @ 550 km/s
DMFormFactor, MB vesc 550km/s
DMFormFactor, MB

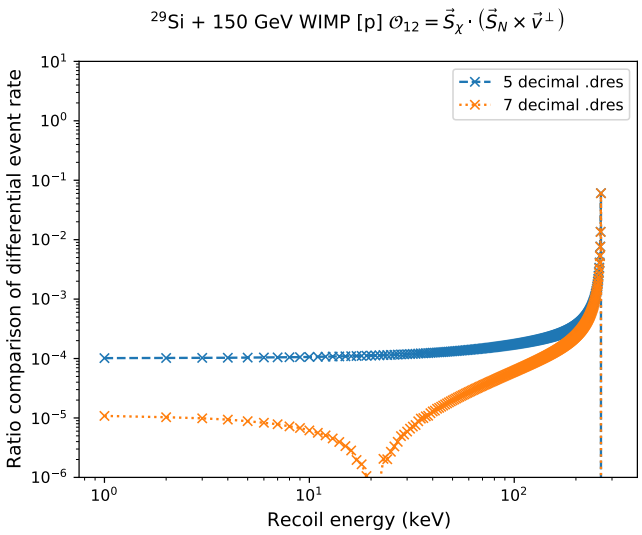
^{29}Si + 150 GeV WIMP [p] $\mathcal{O}_{12} = \vec{S}_\chi \cdot (\vec{S}_N \times \vec{v}^{\perp})$
Ratio comparison of differential event rate
Recoil energy (keV)
5 decimal .dres
7 decimal .dres

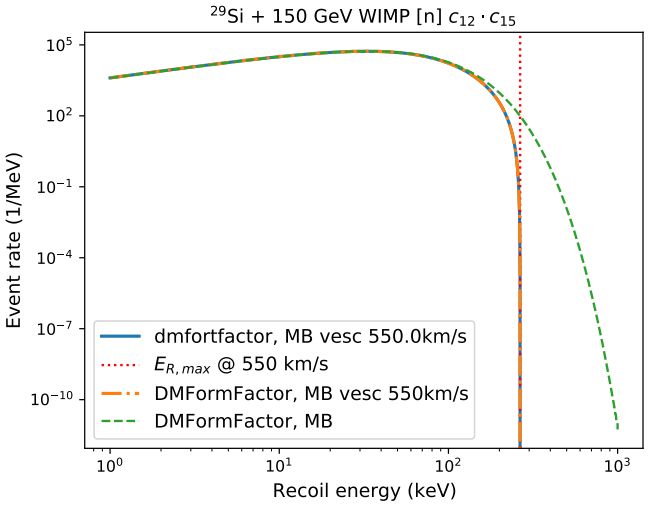
^{29}Si + 150 GeV WIMP [n] $c_{12} \cdot c_{15}$
Event rate (1/MeV)
Recoil energy (keV)
dmfortfactor, MB vesc 550.0km/s
$E_{R,max}$ @ 550 km/s
DMFormFactor, MB vesc 550km/s
DMFormFactor, MB

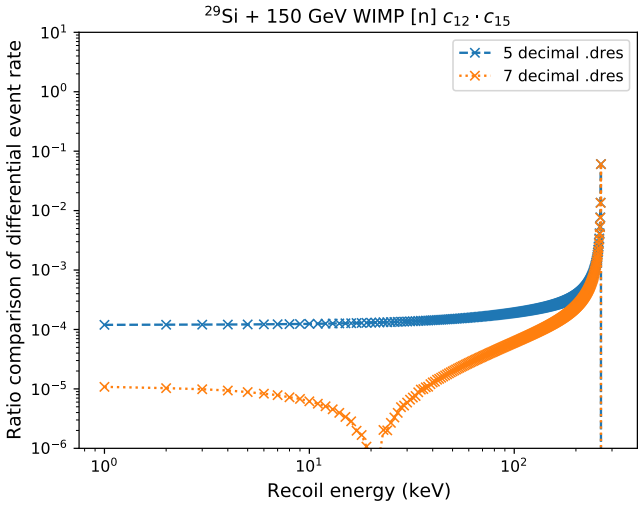
^{29}Si + 150 GeV WIMP [n] $c_{12} \cdot c_{15}$
Ratio comparison of differential event rate
Recoil energy (keV)
5 decimal .dres
7 decimal .dres

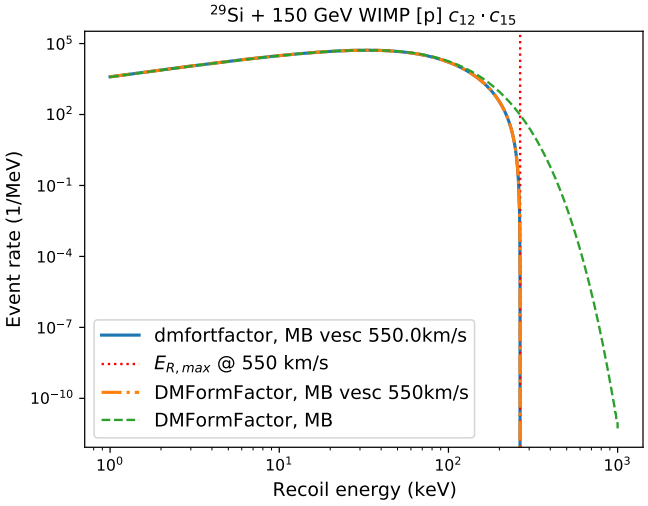
^{29}Si + 150 GeV WIMP [p] $c_{12} \cdot c_{15}$
Event rate (1/MeV)
Recoil energy (keV)
dmfortfactor, MB vesc 550.0km/s
$E_{R,max}$ @ 550 km/s
DMFormFactor, MB vesc 550km/s
DMFormFactor, MB

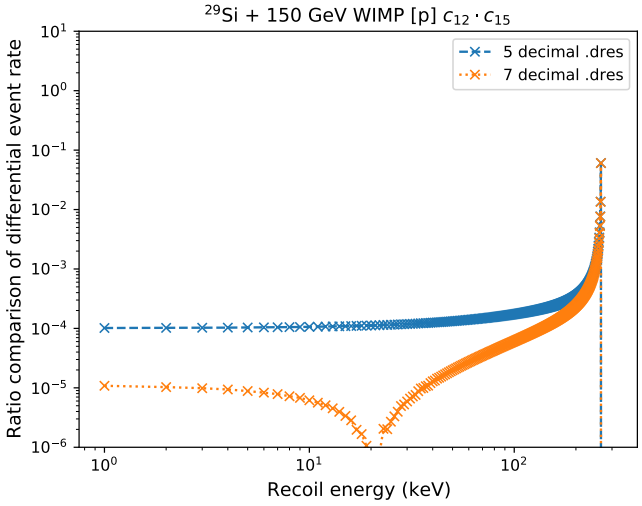
^{29}Si + 150 GeV WIMP [p] $c_{12} \cdot c_{15}$
Ratio comparison of differential event rate
Recoil energy (keV)
5 decimal .dres
7 decimal .dres

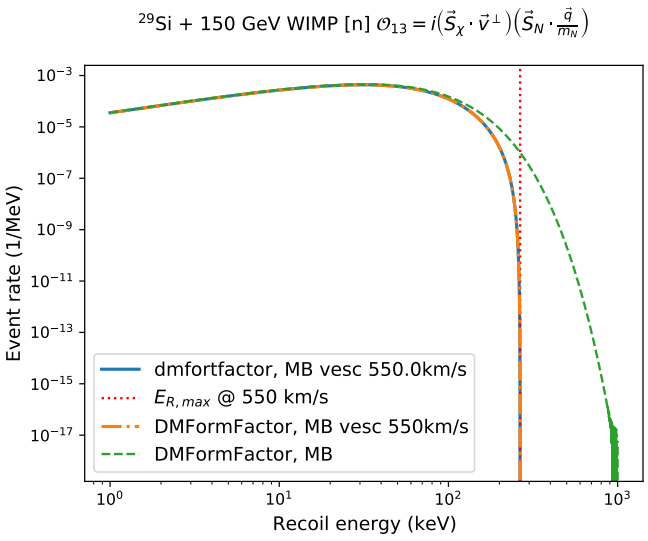
^{29}Si + 150 GeV WIMP [n] $\mathcal{O}_{13} = i(\vec{S}_\chi \cdot \vec{v}^\perp)(\vec{S}_N \cdot \frac{\vec{q}}{m_N})$
Event rate (1/MeV)
Recoil energy (keV)
dmfortfactor, MB vesc 550.0km/s
$E_{R,max}$ @ 550 km/s
DMFormFactor, MB vesc 550km/s
DMFormFactor, MB

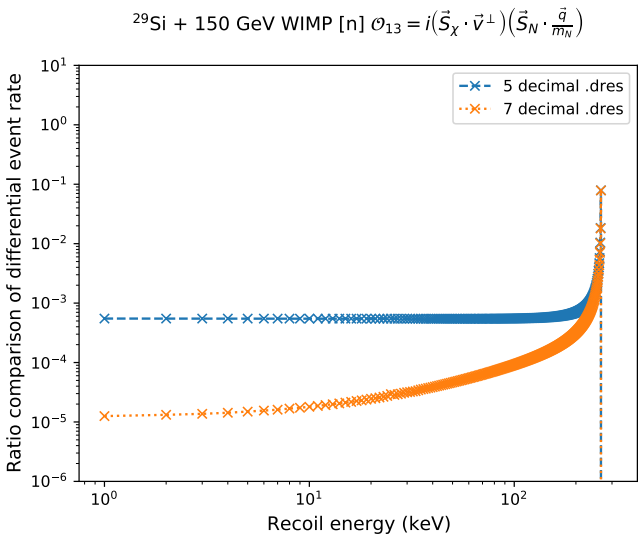
^{29}Si + 150 GeV WIMP [n] $\mathcal{O}_{13} = i(\vec{S}_\chi \cdot \vec{v}^\perp)(\vec{S}_N \cdot \frac{\vec{q}}{m_N})$
Ratio comparison of differential event rate
Recoil energy (keV)
5 decimal .dres
7 decimal .dres

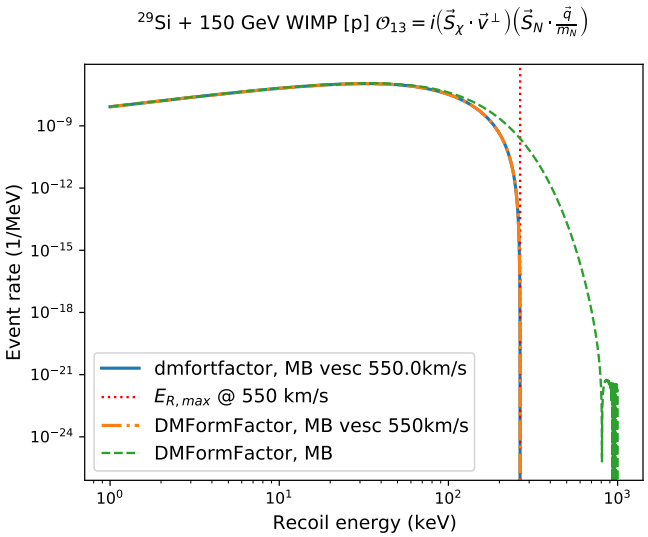
^{29}Si + 150 GeV WIMP [p] $\mathcal{O}_{13} = i(\vec{S}_\chi \cdot \vec{v}^\perp)(\vec{S}_N \cdot \frac{\vec{q}}{m_N})$
Event rate (1/MeV)
Recoil energy (keV)
dmfortfactor, MB vesc 550.0km/s
$E_{R,max}$ @ 550 km/s
DMFormFactor, MB vesc 550km/s
DMFormFactor, MB

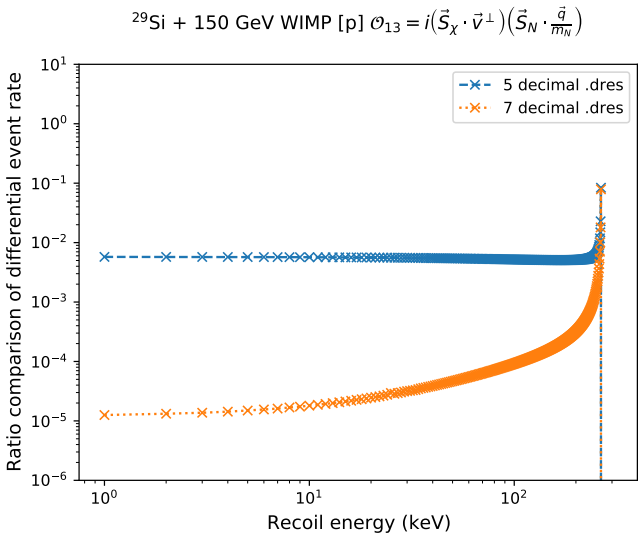
^{29}Si + 150 GeV WIMP [p] $\mathcal{O}_{13} = i(\vec{S}_\chi \cdot \vec{v}^\perp)(\vec{S}_N \cdot \frac{\vec{q}}{m_N})$
Ratio comparison of differential event rate
Recoil energy (keV)
5 decimal .dres
7 decimal .dres

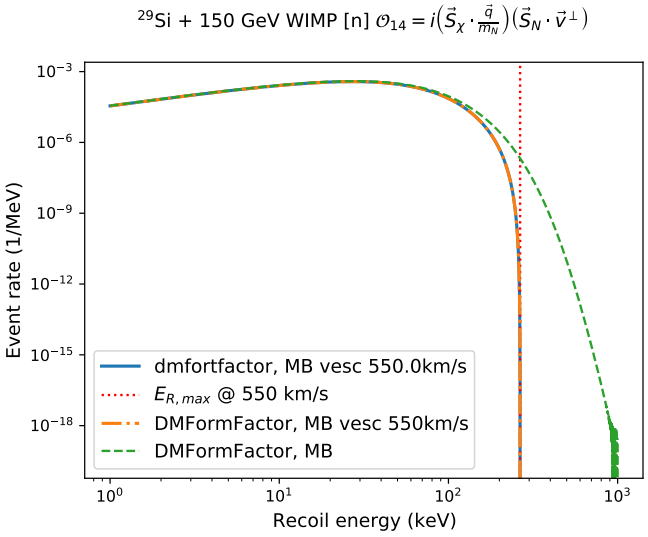
^{29}Si + 150 GeV WIMP [n] $\mathcal{O}_{14} = i(\vec{S}_\chi \cdot \frac{\vec{q}}{m_N})(\vec{S}_N \cdot \vec{v}^\perp)$
Event rate (1/MeV)
Recoil energy (keV)
dmfortfactor, MB vesc 550.0km/s
$E_{R,max}$ @ 550 km/s
DMFormFactor, MB vesc 550km/s
DMFormFactor, MB

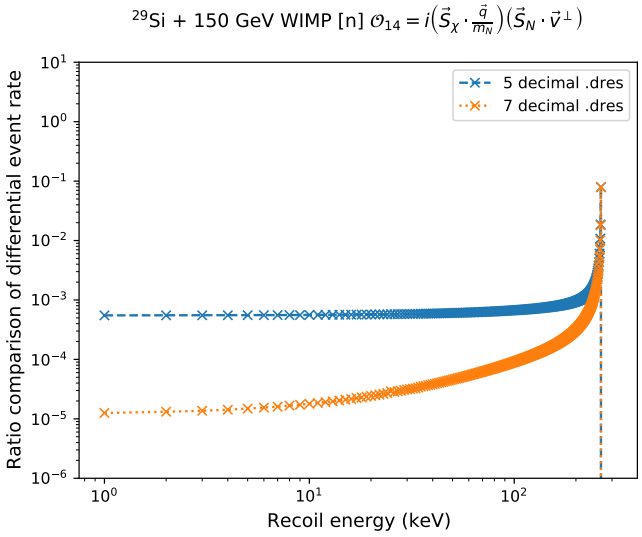
^{29}Si + 150 GeV WIMP [n] $\mathcal{O}_{14} = i(\vec{S}_\chi \cdot \frac{\vec{q}}{m_N})(\vec{S}_N \cdot \vec{v}^\perp)$
Ratio comparison of differential event rate
Recoil energy (keV)
5 decimal .dres
7 decimal .dres

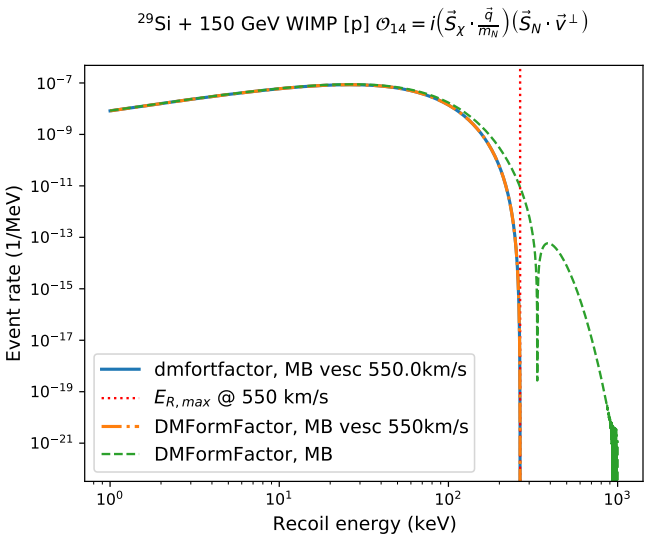
^{29}Si + 150 GeV WIMP [p] $\mathcal{O}_{14} = i\left(\vec{S}_\chi \cdot \frac{\vec{q}}{m_N}\right)(\vec{S}_N \cdot \vec{v}^\perp)$
Event rate (1/MeV)
Recoil energy (keV)
dmfortfactor, MB vesc 550.0km/s
$E_{R,max}$ @ 550 km/s
DMFormFactor, MB vesc 550km/s
DMFormFactor, MB

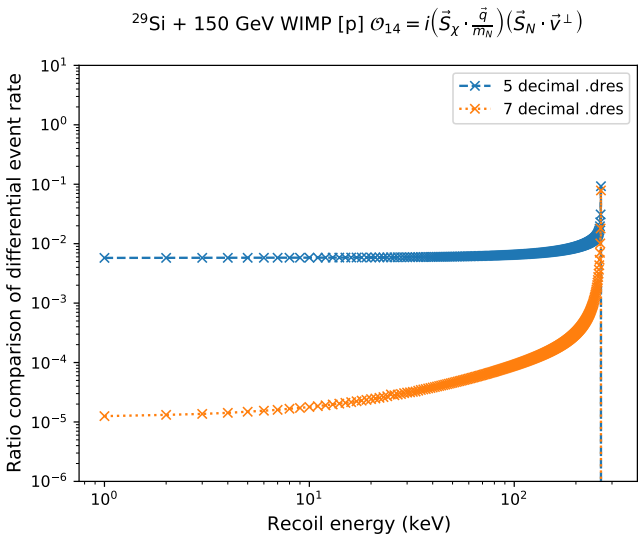
^{29}Si + 150 GeV WIMP [p] $\mathcal{O}_{14} = i\left(\vec{S}_\chi \cdot \frac{\vec{q}}{m_N}\right)(\vec{S}_N \cdot \vec{v}^\perp)$
Ratio comparison of differential event rate
Recoil energy (keV)
5 decimal .dres
7 decimal .dres

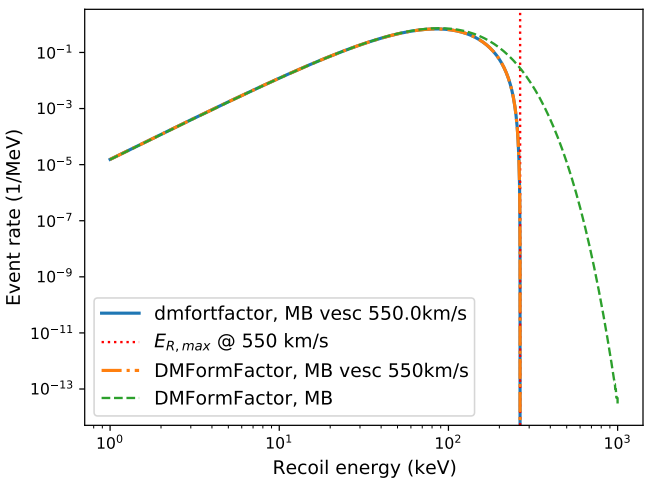
^{29}Si + 150 GeV WIMP [n] $\mathcal{O}_{15} = -\left(\vec{S}_\chi \cdot \frac{\vec{q}}{m_N}\right)\left((\vec{S}_N \times \vec{v}^\perp) \cdot \frac{\vec{q}}{m_N}\right)$
Event rate (1/MeV)
Recoil energy (keV)
dmfortfactor, MB vesc 550.0km/s
$E_{R,max}$ @ 550 km/s
DMFormFactor, MB vesc 550km/s
DMFormFactor, MB

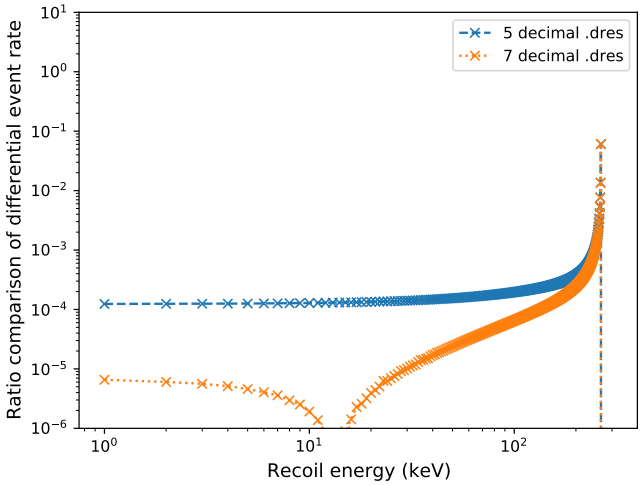
^{29}Si + 150 GeV WIMP [n] $\mathcal{O}_{15} = -\left(\vec{S}_\chi \cdot \frac{\vec{q}}{m_N}\right)\left((\vec{S}_N \times \vec{v}^\perp) \cdot \frac{\vec{q}}{m_N}\right)$
Ratio comparison of differential event rate
Recoil energy (keV)
5 decimal .dres
7 decimal .dres

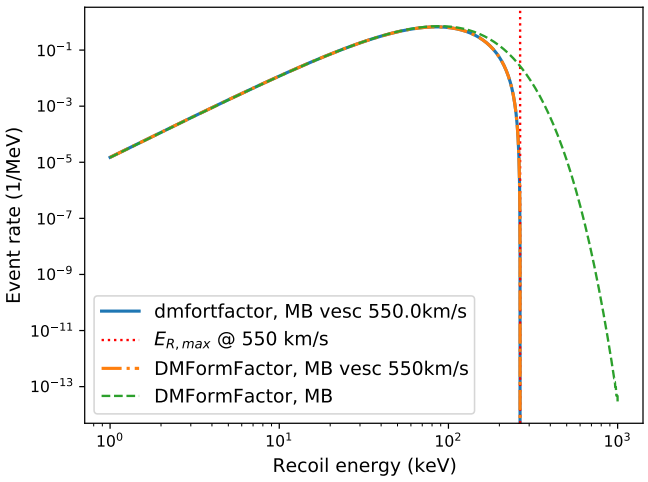
^{29}Si + 150 GeV WIMP [p] $\mathcal{O}_{15} = -\left(\vec{S}_\chi \cdot \frac{\vec{q}}{m_N}\right)\left((\vec{S}_N \times \vec{v}^\perp) \cdot \frac{\vec{q}}{m_N}\right)$
Event rate (1/MeV)
Recoil energy (keV)
dmfortfactor, MB vesc 550.0km/s
$E_{R,max}$ @ 550 km/s
DMFormFactor, MB vesc 550km/s
DMFormFactor, MB

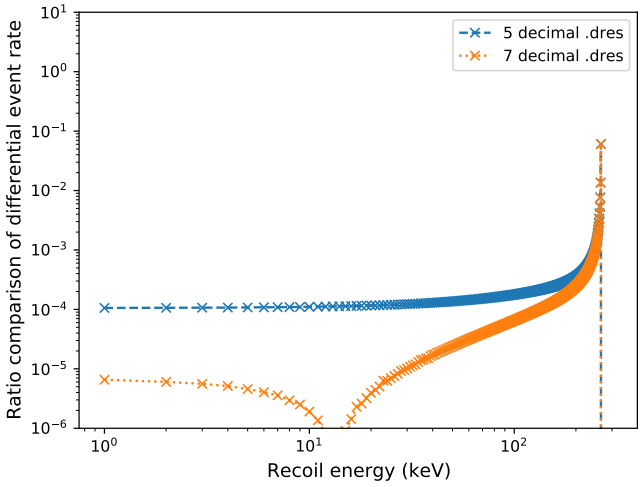
^{29}Si + 150 GeV WIMP [p] $\mathcal{O}_{15} = -\left(\vec{S}_\chi \cdot \frac{\vec{q}}{m_N}\right)\left((\vec{S}_N \times \vec{v}^\perp) \cdot \frac{\vec{q}}{m_N}\right)$
Ratio comparison of differential event rate
Recoil energy (keV)
5 decimal .dres
7 decimal .dres